A STUDY OF THE EFFECT OF STRUCTURE AND CONFORMATION ON THE TRANSPORT PROPERTIES OF IONOPHORES USING NMR

Stephen James Tompsett

A Thesis Submitted for the Degree of PhD
at the
University of St Andrews

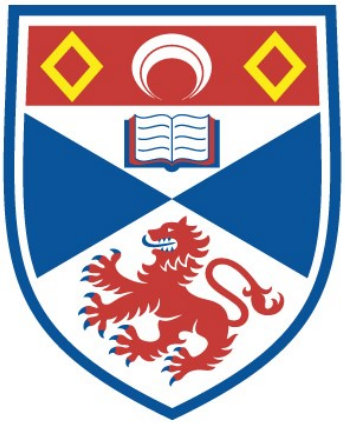

1992

ΑΙΕΝ ΑΡΙΣΤΕΥΕΙΝ

A Study of the Effect of Structure and Conformation on the Transport Properties of Ionophores using NMR

Being a thesis by

Stephen James Tompsett.

Submitted for the degree of
Doctor of Philosophy
in the Faculty of Science of the
University of St Andrews.

October 1991.

United College of St Salvators
and St Leonards College.

Th B43

DECLARATION

I, Stephen J. Tompsett, hereby certify that this thesis has been composed by myself, that it is a record of my own work and that it has not been accepted in partial or complete fulfilment of any other degree or professional qualification.

I was admitted to the Faculty of Science of the University of St. Andrews under Ordinance General Nº. 12 in October 1988 and as a candidate for the degree of PhD. in October 1989.

Signed. ..... October 1991.

CERTIFICATION

I hereby certify that the candidate has fulfilled the conditions of the Resolution and Regulations appropriate to the degree of PhD.

Signed. ..... October 1991.

Acknowledgements.

Firstly, I would like to thank Dr. Frank Riddell for all his help, ideas and enthusiasm over the last three years. Thanks are also due to Dr. S. Arumugam for his help with the transport studies and for maintaining the MSL500 in working order.

I would also like to thank various members of the technical staff for their help in producing this thesis. These are: Mrs. M. Smith for nmr spectra, Mrs S. Smith for microanalyses and atomic absorption measurements and Mr J. Bews for his help on how to use the computers.

I acknowledge my debt to the SERC for providing the funding to enable me to carry out this work.

Finally, thanks are due to my parents for their help and support over the last 25 years.

Publications.

Riddell, F.G. and Tompsett, S.J. (1990), The transport of Na^+ and K^+ through phospholipid bilayers mediated by the antibiotics salinomycin and narasin studied by ^{23}Na and ^{39}K-NMR spectroscopy. *Biochim. Biophys. Acta*, **1024**, 193-197.

Riddell, F.G. and Tompsett, S.J., (1991), The total assignment of the ^{1}H and ^{13}C nmr spectra of the polyether antibiotics salinomycin and narasin. *Tetrahedron*, In press.

Contents.

Abstract.

The first part of this work is a study of cation transport mediated by salinomycin and narasin, two polyether antibiotics. The transport rates were measured in phosphatidylcholine vesicles using ^{7}Li, ^{23}Na and ^{39}K nmr. The results showed that salinomycin and narasin both transport potassium more rapidly than sodium. Lithium is transported two orders of magnitude slower still. Thermodynamically, salinomycin prefers potassium to sodium, while narasin shows little preference for either cation. A brief study on dihydrosalinomycin shows that this transports sodium at rates an order of magnitude slower than seen for salinomycin itself.

The second section is concerned with the total assignment of the ^{1}H and ^{13}C nmr spectra of the alkali metal salts of narasin and salinomycin. This was achieved by the use of two dimensional nmr techniques, including COSY, NOESY and XHCORD spectra. The chemical shifts of certain sites were seen to be dependent on the cation present. These sites were mostly situated near the "hinge" regions of the molecules where conformational changes can occur during the complexation process. This showed that these sites are also important in the accommodation of different sized cations. The basic conformation of the molecule remains the same, it is only at certain sites that there is flexibility.

The final portion of this work is a brief study of transport mediated by synthetic ionophores. This involved synthesising materials expected to be carriers for both cations and anions and testing them for transport properties. It was also necessary to

develop a contrast reagent for halide ions, to enable their transport to be observed and measured by nmr. It was found that nitroxyl radicals and dextran magnetite were both ineffective as contrast reagents. Manganous ions were found to be good relaxation agents but were seen to destroy the vesicles, except at low pH. Alternative methods of stabilising the vesicles using hydroxymethyl substituted pyridinium salts were unsuccessful. The anion carriers attempted were hydroxylated tetra-alkylammonium and pyridinium salts. The transport studies carried out showed that these were only slightly more effective ion carriers than their non-hydroxylated homologues.

In a study of cation transport it was tried, unsuccessfully, to synthesise various proton ionisable crown ethers.

CHAPTER 1

Chapter 1 General introduction.

1.1 Cell Membrane Structure.

Cell Membranes are very important and highly complex structures. If it were not for the compartmentalisation of biological systems the huge complexity of life could not exist.

1.1.1 A brief history of cell membranes.

It was in 1665 that the microscopist Robert Hooke first described the box like structures seen in cork as cells. Over the next 10 years Antoni van Leeuwenhoek produced drawings of a wide range of bacteria, protozoa and red blood cells. It was however over 100 years before it was realised that cells were the basis of all tissues. The various components of cells eg. mitochondria and vacuoles were identified but it was not until 1855 that Carl Nageli discovered what he called the 'Plasma Membrane'. He suggested that it was this structure that produced the observed osmotic sensitivity of the cells, making them swell and contract with differing ionic strength in the extracellular medium.[1]

The next major breakthrough in the understanding of cell membrane structure was made in 1899 by Charles Overton. He published figures which showed that the less polar a substance was the more readily it could penetrate the membrane. This led to the conclusion that the cell membrane was in fact lipoidal in nature. Work done in 1925 by Gorter and Grendel using surface area calculations produced the theory, later to be proven using electron microscopy, that the cell membrane consists of lipid bilayers.

Further work in 1935 by Danielli proposed that the membrane also included proteins.

The currently accepted model of membrane structure is the "fluid mosaic" structure put forward by Singer and Nicholson in 1972.[2] This proposes that the membrane is a dynamic and motile system with proteins imbedded in and penetrating through the lipid bilayer. This structure is held together by the hydrophobic effect, which is the tendency of non-polar groups to interact with each other rather than with the water.

1.1.2 Lipid structure

Biological membranes consist of mainly lipid, protein and carbohydrate with about 20% water. The proportions of the organic components vary from 80% lipid in myelin to 25% lipid in inner mitochondrial membranes but the lipid bilayer is still the basis of the structure. Therefore an understanding of lipid structure is necessary before a discussion of membrane properties is started.

Lipids are water insoluble organic substances extractable by non-polar organic solvents such as ether or chloroform. There is no single universally accepted classification of lipids. However there are a number of different systems, the one followed here is on the basis of hydrolysis product. There are three basic classes of lipids

1) Simple eg. fatty acids and waxes. These give fatty acids and glycerol on hydrolysis

2) Compound eg. phospholipids. These give a fatty acid, glycerol,phosphoric acid and a nitrogenous moiety on hydrolysis.

3) Steroids eg Cholesterol. These are based on the carbon skeleton shown in figure 1-1.

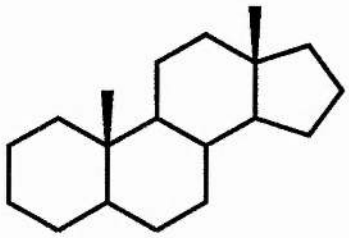

Figure 1-1. Steroid skeleton.

The lipids found in membranes are all polar and mostly fall into the latter two categories. These can be amphipathic which have an ionic or polar headgroup attached to long hydrocarbon tails or they may be sterols with a polar hydroxyl at one end of the molecule. The common feature of these molecules is a dichotomy with a hydrophilic group at one end and a hydrophobic group at the other.

Most of the lipids in biological systems are esters of glycerol with long chain carboxylic acids. These are usually triacyl glycerols or phospholipids which consist of one glycerol moiety with fatty acids esterified at carbons 1 and 2 (see figure 1-2). The remaining hydroxyl of the glycerol has a phosphate attached which is usually also esterified, eg. phosphatidylcholine (PC), phosphatidylserine (PS) and phosphatidylethanolamine (PE) (see figure 1-3). Glycerol has a prochiral centre at carbon 2, the numbering system used is such that the pro-S carbon is C_1. As well as the phosphoglycerides

there are also another important group of lipids called the sphingolipids, which are derivatives of the long chain amino-alcohol sphingosine, $CH_3(CH)_{12}CH{:}CHCH(OH)CH(NH)CH_2OH$. These sphingolipids consist of a sphingosine molecule with a fatty acid attached by an amide linkage and a polar headgroup, eg. a phosphate ester, on the terminal hydroxyl.

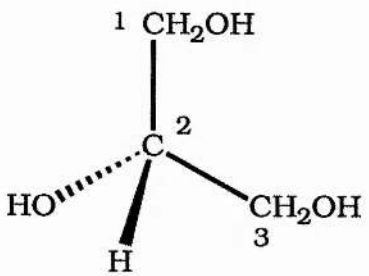

Glycerol

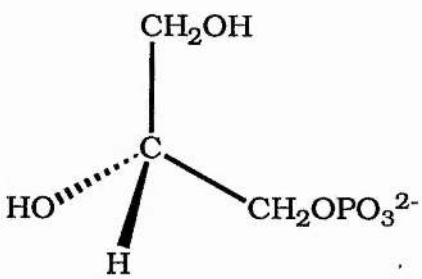

sn glycerol 3-phosphate
(L-α-glycerol phosphate)

Figure 1-2. The numbering system used for phosphoglycerides.

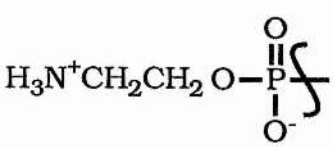

Phosphatidylethanolamine

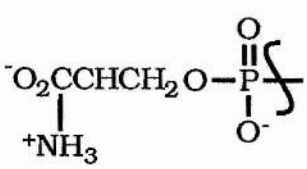

Phosphatidylserine

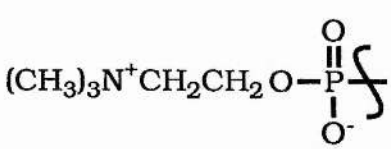

Phosphatidylcholine

Figure 1-3. Three of the commonly encountered phospholipid headgroups.

A wide range of carboxylic acids can be esterified in lipids with both saturated and unsaturated chains found. The unsaturated acids are often the Z-isomers which prevents close

packing of the chains, leading to membranes with lower melting points and higher fluidity than those with saturated or E-unsaturated hydrocarbon chains. It is found that the percentage of unsaturated lipid in a membrane is inversely proportional to the temperature of the growth medium.[1]

The carboxylic acids found in lipids usually have an even number of carbon atoms between 12 and 26, 80% have chains of 16 to 20 carbon atoms. There may be up to six carbon-carbon double bonds mostly *cis* and usually methylene interrupted so there is no conjugation. The usual organisation is to have a saturated fatty acyl group at carbon 1 and an unsaturated fatty acyl group on carbon 2. In animals the most abundant phosphatidylcholine has a saturated 16 carbon fatty acyl group on carbon 1 and a mono- or di- unsaturated 22 carbon chain on carbon 2. Phosphatidylethanolamine generally has longer chains and more unsaturation than phosphatidylcholine.[1]

1.1.3 Membrane structure.

Lipids form bilayers with the exposed head groups perpendicular to the axis of the chains forming a barrier to prevent interaction between the hydrophobic interior of the membrane and the water. It is found that the interior of the membrane is fluid and deformable as there are no strong attractive forces. This fluidity reflects the membrane's viscocity, which is due to both inter-molecular and intra-molecular motion.

The intra-molecular motion is of three types:

1) Segmental motion, rotation and vibration about carbon-carbon bonds.

2) Rotation about an axis perpendicular to the plane of the membrane.

3) A pendulum motion of the hydrocarbon chains.[3]

The inter-molecular motion is the lateral diffusion by exchange of the lipid molecules.

The fluidity of a membrane is very important to its activity. The fluidity is dependent on a number of factors, such as the proportion of saturated and unsaturated lipids and the amount of cholesterol present. The mobility gradient across the bilayer is not uniform, there is an abrupt increase in the mobility at the centre of the membrane. The overall viscocity within a cell membrane is roughly comparable to that of light engine oil with a lateral diffusion rate of about $10^{-8}\,cm^2s^{-1}$.

Biological membranes consist of a mixture of lipids as well as containing proteins. Each different tissue has its own different and generally closely defined mixture of lipids, see Table 1.1.

In mixed bilayers the phospholipids are distributed asymmetrically between the inner and outer halves of the membrane (see table 1.2). This is believed to be due to steric and electrostatic effects caused by the curvature of the bilayer. This imbalance shows that whilst the lateral diffusion of lipids may be facile, the "flip-flop" motion of a lipid from one face to the other is slow. The rates seen vary from several days to several minutes in rapidly growing bacterial membranes.[4] It is possible that this "flip-flop" motion is accelerated by proteins penetrating the bilayer.

Table 1.1. The lipid constituents of some cell membranes.

% w/w	Rat liver mitochondria inner	Rat liver mitochondria outer	Rat erythrocytes	Human erythrocytes
Chol	<3	<5	24	24
PC	45	50	31	23
SPH	3	5	9	18
PE	25	23	15	20
PS	1	2	7	8
PI	6	13	2	3
PG	2	3	0	0
DPG	18	3	0	0

Chol; cholesterol, PC; phosphatidylcholine, SPH; sphingomyelin, PE; phosphatidylethanolamine, PS; phosphatidylserine, PI; phosphatidylinositol, PG; phosphatidylglycerol, DPG; diphosphatidylglycerol.

Table 1.2. The distribution of phospholipids between the internal and external faces of the cell membrane of human erythrocytes.

	In	Out
Total Phospholipid	50%	50%
Sphingomyelin	2%	24%
Phosphatidylcholine	5%	25%
Phosphatidylserine	18%	1%
Phosphatidylethanolamine	10%	0%

In their active state membranes consist of lipids in a liquid crystalline state, which provides mobility in an organised framework. For a pure phospholipid there is a well defined phase transition between a rigid gel and liquid crystal at a specific temperature, which is easily found using differential scanning calorimetry. The phase transition increases the disorder and mobility of the membrane and is affected by a number of factors.

1	Chain length	In general the longer the chain, the higher the transition temperature. The position of the carbon on which the chain is substituted is very important.
2	Unsaturation	*cis* unsaturated bonds reduce the transition temperature.
3	Head Group	e.g. Phosphatidylcholine may have a transition temperature 20°C lower than the same phosphatidylethanolamine.
4	Divalent ions	In charged membranes the transition temperature may be increased by the presence of Ca^{2+} or Mg^{2+} by more than 50°C.

In real membranes there is a wide range of miscibility. If one mixes two lipids with widely different phase transition temperatures there may be two independent phase transitions. Between these two temperatures the lipid is present as both gel and liquid crystals. In more complex mixtures eg. egg yolk phosphatidylcholine the lipids are all completely miscible but a lateral phase separation may be induced by divalent ions.[5]

Phospholipid phase transitions have mostly been studied in the membranes of bacteria and mycoplasmas. They tend to show a broad peak in differential scanning calorimetry studies[6] and the bacteria will not grow below the phase transition temperature. This broadening of the differential scanning calorimetry peak is also seen when cholesterol is added to a pure phospholipid. Cholesterol is often called a fluidity regulator as it increases the membrane fluidity below the phase transition temperature but decreases it when above the phase transition temperature. This behaviour of cholesterol is part of the reason there is no overall phase transition seen in the differential scanning calorimetry trace of mammalian membranes. It is certain however that the majority of such membranes are in a liquid crystalline state.

Some biological membranes seem to include areas of lipid with restricted motion for example in red blood cells.[7] This could be due to phospholipid associated with cholesterol rich regions, proteins or both.[8,9,10] Lipid molecules are required by many membrane-bound enzymes to produce activity eg Na^+/K^+ ATPase. In these cases the lipid must be in a liquid crystalline phase,[11] this may be the reason for the discontinuity seen in the Arrhenius plots of some membrane bound enzymes. It is seen that below a localised phase transition temperature the reaction rate falls off sharply.[12]

Biological membranes also contain proteins, which can account for up to 75% of the dry weight of the membrane. There are two types of protein associated with the cell membrane.

1)	Peripheral or Extrinsic	Washed away from a membrane using a buffer of different pH or ionic strength or by chelating agents.
2)	Integral or Intrinsic	Only removable by the disruption of the membrane.

The latter group of proteins are much more difficult to study as they are hard to extract and purify, modern techniques rely on monoclonal antibodies[13] after the membrane has been disrupted by organic solvents and detergents. The proteins are also asymmetrically distributed across the membrane and this compartmentalisation is often the reason for their efficacity.

1.2 Membrane Transport

The transport of material across cell membranes is very important. In resting humans 30-40% of the energy consumed is spent in maintaining the ion gradients across cell membranes. There are three types of transport across cell membranes.[1]

1	Passive diffusion	Simple diffusion along the concentration gradient
2	Facilitated diffusion	Diffusion along the concentration gradient mediated by a membrane component.
3	Active Transport	Mediated by a specific transport protein working against the concentration gradient, requires the input of energy.

1.2.1 Passive Diffusion.

Passive diffusion is the leak of ions across intact cell membranes without any outside assistance. Biological membranes are good barriers for ions and polar molecules under normal circumstances. As can be seen from the following data, table 1.4.

Table 1.4. Diffusion coefficients of a range of species through phospholipid bilayers.[1]

Ion/Molecule	H_2O	Cl^-	K^+	Na^+
Diffusion Coefficient	$5x10^{-3}$	$7x10^{-10}$	$5x10^{-12}$	$1x10^{-12}$

1.2.2 Facilitated diffusion.

This is similar to passive diffusion in that it proceeds along the diffusion gradient and involves no input of energy. The difference lies in the activation energy of the process. So facilitated diffusion is in fact catalysed passive diffusion. The catalysts in biological systems tend to be pore forming materials such as gramicidin and amphotericin. These open up an ion channel through the membrane enabling the rapid exchange of ions between the intracellular and extracellular solutions. An example of this type of transport in living systems is the Band 3 protein which mediates chloride transport. This enables the chloride ions to pass through a lipid membrane at a rate much higher than that given above.

1.2.3 Active transport.

The third type of transport seen is active transport. This involves the input of energy but unlike the previous two types enables ions to be transported against the diffusion gradient. This is very important in living systems, one example of this type of transport is the enzyme Na^+/K^+ ATPase. This transports three sodium ions out of a cell while two potassium ions move in the opposite direction consuming one molecule of ATP in the process. In resting humans roughly 30% of the ATP consumed is by this process.

1.3 Ionophores.

1.3.1 History of ionophores.

The name ionophores or ionophorous agents was first coined by Pressman et al in 1967[14] to describe antibiotics in the valinomycin and nigericin classes. These ionophorous agents are all efficient transporters of ions across cell membranes. They exhibit a number of different strategies to achieve this. There are three main classes, of which two consist of neutral ionophores and the third are weakly acidic. One type of neutral ionophore is the complexation agents. These render a cation soluble in non-polar solvents by forming a charged complex. These materials include naturally occuring species such as valinomycin (see figure 1-4) and synthetic species like crown ethers and cryptands. The second class of neutral ionophores function by pore formation. This class includes materials such as gramicidin (see figure 1-5) and amphotericin, which enable an ion channel to be opened through

the membrane. The third class of ionophores are those with an ionisable acid group such as the polyether antibiotics of interest here. The advantage of this type of material is that it forms a neutral complex so it does not require the transport of a counter ion. The advantage of this has led to synthetic crown ethers containing acidic groups being synthesised.[15]

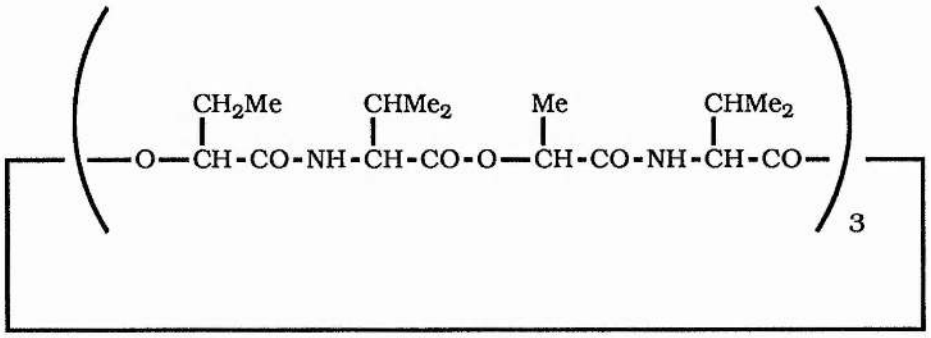

Figure 1-4. The structure of valinomycin.

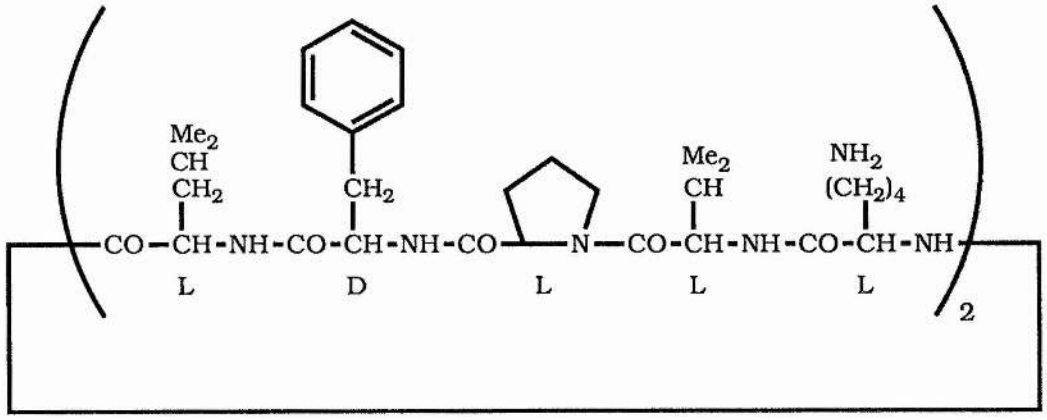

Figure 1-5. The structure of gramicidin

The acid ionophores or polyether antibiotics have played a major role in the development of these meterials which work by forming a lipid soluble complex with a cation which enables it to pass through biological membranes.[16] Over the 30 years from 1950 to 1980 the number of novel antibiotics in this class increased from 0 to 72 the number is now nearer 100. There

were two reasons behind this growth one was the use of ionophores in the study of cation transport but the more important factor was the discovery of their efficacity as coccidiostats and as agents to improve the feed efficiency of ruminants.

1.3.2 Polyether antibiotics.

In 1951 three novel antibiotics were reported as X-206, X-464 (nigericin) and X-537A (lasalocid A).[17] No attempt was made at the time to discover their structure but common properties suggested that they were part of a new class of antibiotics. It was found that they were slightly acidic, but when they were exposed to aqueous sodium carbonate they extracted sodium ions into the organic layer. These materials were found to have relatively high toxicity so little interest was shown in them. It was not until the discovery of monensin in 1967 by Agtarap et al,[18] and the identification of its anticoccidial activity, that ionophores really took off. This paper was also the first to present the structure of a polyether antibiotic. It was found that monensin's anticoccidial activity was shared by all the other four known ionophores nigericin, dianemycin, X-206 and lasalocid.[19] It was proposed at the same time that these antibiotics were effective due to direct interaction with alkali metal cations and the carrier mechanism which regulates potassium transport across mitochondrial membranes.

1.3.3 Structure

The polyether antibiotics all have certain structural features in common. These include a terminal carboxyl group with a tertiary hydroxyl at the other terminus. A hydrogen bond between

these enables the molecules to take up their characteristic cyclic structure.[20] There are also many alkyl groups (methyl and ethyl) branched along the carbon backbone. Biosynthetic studies [20,21,22,23] were consistent with a similar polyketide biosynthetic pathway for all the polyether antibiotics. This meant that a universal numbering system based on their biosynthetic origins could be used, in fact such a system was proposed by Westley in 1976.[24] This system starts numbering from the carboxylic acid C1 and proceeds to the far terminus along the backbone and then back along the methyl and ethyl substituents. The oxygens are numbered sequentially from the carboxylic acid O1 and O2, the rings are denoted A, B, C... also starting from the carboxyl end of the molecule. (see figure 1-6).

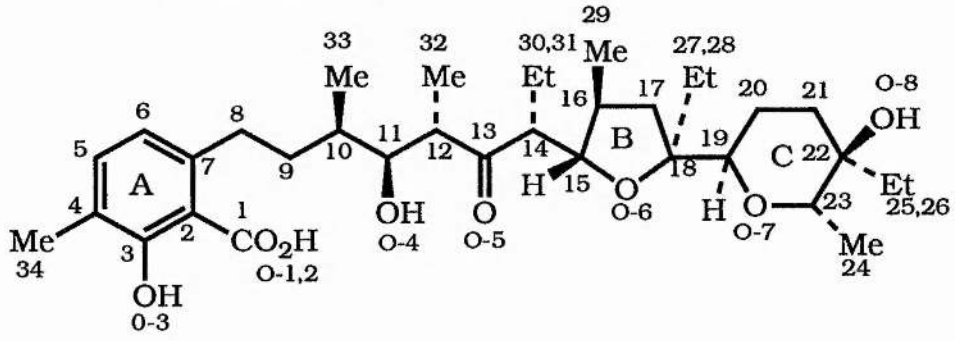

Figure 1-6. The numbering system shown for Lasalocid A.[24]

The polyether antibiotics, when in their cyclic configuration, have all the oxygens on the inside able to complex with a cation and all the alkyl chains on the exterior surface to increase the lipid solubility. Thus they can transport cations across cell membranes by the process of facilitated diffusion. There is no energy required and the transport is down the concentration gradient across the membrane. All of the acidic ionophores known are able to transport monovalent cations but only a few, like lasalocid are able

to complex with divalent cations with binding constants of the same order as with alkali metal ions.[25]

The ionophores are all molecules with many chiral centres, the geometry of which is crucial to their activity. In general the more constrained a molecule is the more more stable its complexes are.[26] This is why crown ethers are much better at complexing with alkali metal ions than the corresponding linear polyethers. The polyether antibiotics generally contain rigid sections of structure and are designed to wrap themselves around the ion to which they are complexed. Such rigid sections are seen best in the spiro-tricyclic groups in narasin and salinomycin.

1.3.4 Origins.

All of the polyether antibiotics known so far are produced by micro-organisms in the Actinomycetales order, an order of filamentous, branching bacteria. All but three of the microbes known to produce polyether antibiotics belong to the genus Streptomyces, by 1981 half of the known polyether antibiotics had been isolated from different strains of two species, S. albus and S. hygroscopicus.

The bacteria used in the production of ionophoric antibiotics are isolated from soil and around 3% of the actinomyces cultures screened are found to produce polyether antibiotics.[27] The most commonly produced ionophore is nigericin which is found in fermentations of strains of both S. albus and S. hygroscopicus. The cell cultures used to produce the ionophores are often found to give a complex mixture of several closely related compounds, for example salinomycin is the major component of a nine-membered

complex produced by S. albus. The minor components of these mixtures are usually homologues of the main material and as the isolated yields increase they will almost certainly add to the collection of known ionophores. Other classes of antibiotics and even antifungal agents are often produced along with the polyether antibiotics in these fermentations.

1.3.5 Biosynthesis

As has been stated earlier the polyether antibiotics are produced by fermentation. The conditions required for a particular microbe vary greatly. The media commonly used include carbon and nitrogen, from plant and animal sources, and minerals. It is important to have the correct qualitative and quantitative supply of nutrients but there are other variables which are often critical. These include the innoculation preparation, temperature, pH, aeration and agitation. Optimisation of these variables is usually done in an empirical manner and studies have been made on only a few of the known ionophores including monensin, narasin and salinomycin. The media vary from an oil rich mixture for salinomycin and monensin to a casein and starch based mixture for narasin. Unexpectedly the presence of traces of inorganic materials can have a large effect on the yield. In monensin the addition of $0.3g/dm^3$ iron (III) sulphate or manganese (II) chloride was found to give a three-fold increase in the yields.[27] This enhancement was not seen in narasin but the presence of calcium carbonate and molasses was found to be effective.[28] In salinomycin the presence of ammonium ions is claimed to produce a 200-fold increase in the yield.[29]

The polyether antibiotics are found in both the broth filtrate and mycelium fraction. In high yield fermentations they are concentrated in the latter. They are usually extracted from the mycelium with a suitable solvent such as acetone or methanol. Alternatively the extraction can be performed on the whole broth using a water-immiscible solvent like ethyl acetate. Extraction may occur as either the free acid or salt but care must be taken to avoid acid degradation especially in those ionophores with ketal groupings.

The biosynthesis of polyether antibiotics has been studied by the use of isotopically labelled substrates to establish the nature and positions of the precursors. The resulting materials were then studied by ^{13}C nmr, or degradation to radioactive particles. The route of preference was found to be the polyketide pathway but the synthase enzymes and the conversion of polyketide are not yet fully understood.

The polyketide pathway is the route used in the production of fatty acids, flavonoids and quinones.[30] The starting materials are the acetic, propionic and butyric thio esters of Coenzyme A (Figure 1-7). The reaction consists of repeated Claisen condensations between acetyl CoA and malonyl CoA with one of the malonyl carboxyls acting as a leaving group. This results in a β-keto ester which may cyclise to give an aromatic ring or be reduced to an alcohol. The alcohol may cyclise to a pyran or furan ring, typical of ionophores, or dehydrate to the alkene which can

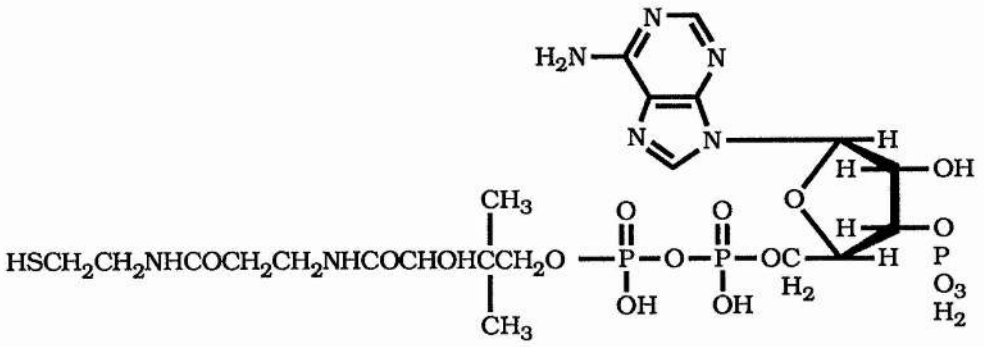

Figure 1-7. The structure of Coenzyme A

be further reduced. Branching can be introduced by using propionyl or butyryl CoA as the starter or using methylene substituted malonyl CoA, derived from propionate or butyrate. The starting acid is the end remote from the carboxylic function in the final product.

1.3.6 Veterinary Applications

Polyether antibiotics are highly effective against gram positive bacteria, Eimeria and a number of anaerobic bacteria. This activity is at the root of large interest in such materials, as it enables their use as both anticoccidial agents and to improve the feed efficiency in ruminants. Coccidiosis is a disease found in poultry caused by microorganisms of the Eimeria family. These are parasites akin to amoebic dysentery which have a similar effect on infected poultry leading to death by dehydration and malnutrition.[31] The ionophores can be seen to act on one of the stages of the life cycle of the Eimeria causing them to burst due to an increase in the osmotic pressure on the cell. This increase in osmotic pressure is due to the disruption of the cell's ion transport system by the ionophore mediated transport across the membrane.[31]

Ionophores have proved to be very useful in the control of coccidiosis as they are efficient and arrived on the scene at a time when a resistance was building to existing anticoccidial agents.[16] The dosage is administered orally in the feed and is typically in 80 mg/kg amounts. Although many ionophores are known the only ones used in chicken are monensin, lasalocid, salinomycin and narasin.[16] Recently it has been noticed that strains of Eimeria resistant to ionophoric antibiotics are appearing. It is observed that if resistance is found to one polyether antibiotic the strain will also be resistant to others.[32]

1.4 Salinomycin and Narasin.

1.4.1 Discovery, structure and properties.

In 1971 Miyazaki et al at the Kaken Chemical Company in Japan discovered a new polyether antibiotic, salinomycin.[33] 8.5g of this material was extracted from 100 litres of a broth of S. albus N°.80614 fermented for 84 hours at 27°C. The sodium salt of salinomycin was produced by a similar method two years later.[34] This salt was characterised and found to have anticoccidial potential.

The mass spectrum and ^{1}H nmr data with the melting point and elemental analysis showed that this was a novel material of unknown structure. The structure was elucidated in 1973 by the use of X-ray crystallography.[35] This preliminary communication was followed by a full paper in 1975.[36] It was found that suitable crystals for study could not be prepared for any of the alkali metal salts. Therefore the p-iodophenacyl derivative was used for these studies, enabling the structure and absolute configuration of

salinomycin to be determined. However, this did not give the crystal structure of an alkali metal complex, so no information on the complexation process could be elucidated.

The structure of salinomycin did reveal some unusual features of this molecule. These concerned the tricyclic spiroketal (dispiroketal) group in the centre of the molecule. This was the first polyether antibiotic seen to contain such a feature. The vinylic group in ring C of the compound was also an unusual feature in this type of material (figure 1-8).

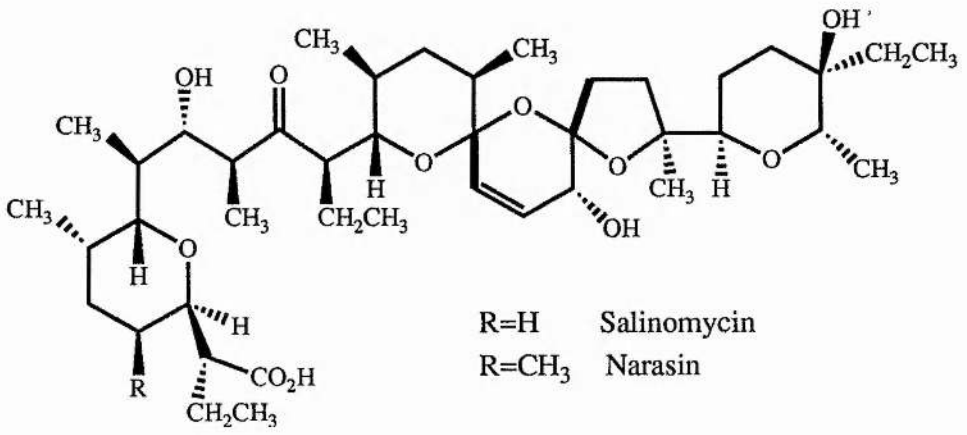

Figure 1-8. The structure of salinomycin and narasin.

The first paper as opposed to patent, on the properties of salinomycin was published in 1974.[37] This was an examination of the properties of salinomycin and the bacterium which produced it. The strain of streptomyces albus was isolated from a soil sample, as is usual for these bacteria. This microorganism was cultured in a variety of media to identify the optimal condition for growth and to discover its taxonomy. For growth to occur it was found that the temperature had to be in the range 21-37°C and the pH between 5.5 and 8.5. It was also seen that starch, gelatin and glucose were all good sources of nutrition for the bacterium.

The physical properties of salinomycin were also studied. It was found to have a pK_a in DMF of 6.4, show an optical rotation of -63° in ethanol, melt between 112.5 and 113.5°C and be soluble in many organic solvents, but insoluble in water. Salinomycin was found to be active against a wide range of gram positive bacteria and also Eimeria in chickens. There was no activity observed against gram negative bacteria and yeasts. Salinomycin was observed to have an LD_{50} (i.p.) in mice of 18mg/kg.

In 1975 a polyether antibiotic was isolated from a broth of S. aureofaciens in the laboratories of Eli Lilly Inc. in America. A patent was applied for the new material under the name of A28086.[38] A follow-up paper was published in 1978 by Berg and Hamill[39] on the properties of the material now known as narasin. This was shown to be a novel polyether antibiotic by its melting point (98-100°C), optical rotation (-54°) and spectral properties. Narasin was also found to be active against gram positive bacteria, anaerobic bacteria and fungi. It was observed that narasin methyl ester, also isolated from the broth, was inactive as an antibiotic. Tests on chicken showed a good degree of protection against E. tenella and there was also evidence of antiviral activity. The LD_{50} (i.p.) in mice was found to be 7mg/kg, less than that seen in salinomycin.

In the period between the publication of the patent and this paper a lot of work on the new material had been carried out. One area of work was on the elucidation of the structure by use of mass spectroscopy[40] and ^{13}C nmr.[41] The fragmentation pattern of narasin was compared to that of salinomycin, which contains a distinctive cleavage in the dispiroketal function.[42] From this it

was seen that the structures differed only in an additional methyl group on ring A in narasin. The position and orientation of this group was identified by ^{13}C nmr, comparing the spectra of salinomycin and narasin.[42] It was seen to be on C(4) in an equatorial position *cis* to the carboxyl containing group. A further paper on the ^{13}C nmr of narasin was published identifying the biosynthetic origins of the carbons in the structure.[43] These two papers, an assignment of the ^{13}C nmr of salinomycin[44] and later papers on the ^{1}H nmr of these materials will be dealt with in greater depth in chapter 3.

1.4.2 Transport and complexation studies.

Salinomycin and narasin were found to be polyether antibiotics, so they function by the mediating cation transport across cell membranes. This means that the complexation and transport properties of these materials have been extensively studied. A wide range of techniques and systems have been used from circular dichroism to cation extraction. These are covered in the introduction to chapter 2.

The following part of this introduction outlines some of the other studies on these materials or which have utilised their special properties. These sections are by no means exhaustive, only a few examples of each application are included. These are really to show the extent of the usefulness of these materials to explain why they should be studied. There is only a tangential relationship to the direction of this thesis, so, any in depth discussion of the the following work would be out of place here.

1.4.3 Veterinary applications.

The greatest volume of work on these two compounds has in the field of medicinal and veterinary applications. Studies of anticoccidial activity have been carried out in chickens,[45] turkeys[46] and pheasants[47] to determine efficacity and required doses. Salinomycin and narasin have also been against legume bloat in pigs[48] and to improve the feed efficiency in ruminants.[49] Salinomycin has also been seen to improve cardiovascular efficiency in dogs with possible extension for use in humans.[50] Another area of human medicine where salinomycin may be of use is in the treatment of malaria. This disease is on the increase in much of the Third World as the resistance to quinine and related compounds builds. Alternative cures are being sought which operate by a different mechanism. In vitro tests have shown that salinomycin causes the destruction of Plasmodium parasites in rat's blood, by a similar method to that seen in the control of Eimeria.[51]

1.4.4 Ion selective electrodes.

A further area where salinomycin has been used is in the production of ion selective electrodes. A number of papers and patents have been issued on these with examples of Ba^{2+} [52] and ammonium[53] selective electrodes being amongst those developed.

1.4.5 Total synthesis.

The total synthesis of salinomycin and narasin has been the subject of several papers and reviews.[54] Due to the complicated structure, and number of chiral centres (~20) these tend to be rather long and inefficient processes. A recent example of such a synthetic route is that of Horita et al[55] there is also a recent review of the work in this area by Yomemitsu et al.[56] Basically though biosynthesis is a much quicker, cheaper and higher yielding approach so synthesised polyether antibiotics are unlikely to go into production.

References to chapter 1.

[1] For a general introduction to lipid biochemistry see, Harrison, R. and Lunt, G.G. (1975), *Biological membranes Their structure and Function*, Blackie, Glasgow. and Sim, E., (1982), *Membrane Biochemistry*, Chapman & Hall, London.

2 Singer, S.J. and Nicholson, G.L. (1972), *Science*, **175**, 720-731

3 Smith, I.C.P., Tulloch, A.P., Stockton, G.W., Schreier, S., Joyce, A., Butler, K.W., Boulanger, Y., Blackwell, B. and Bennet, C.G. (1978) *Ann. NY. Acad. Sci.*, **308**, 8-31.

4 Rothman, J.E., and Kennedy, E.P. (1977), *Proc. Nat. Acad. Sci. USA.*, **74**, 1821-1824.

5 van Djick, P.W.M., Ververgaert, P.H.J.T., Verkleij, A.G., van Deenan, L.L.M., and de Gier, J. (1975), *Biochim. Biophys. Acta*, **406**, 465-478.

6 Mabrey, S. and Sturtevant, J.M. (1978) in *Methods in Membrane Biology*, vol. **9**, Korn, E.D. (Ed), Plenum Press, pp. 237-274.

7 Verma, S.P. and Wallach, D.F.H. (1976), *Biochim. Biophys. Acta*, **436**, 307-318.

8 Bennet, J.P., McGill, K.A. and Warren, G.B. (1980), *Curr. Top. Memb. Transport*, **14**, 207-222.

9 Cable, M.B. and Powell, G.L. (1980), *Biochemistry*, **19**, 5679-5686.

10 Watts, A. (1981), *Nature*, **294**, 512-513.

[11]Grant C.W.M. and McConnell, H.M. (1974), *Proc. Nat. Acad. Science. USA.*, **71**, 4653-4657.

[12] Esfahni, M., Limbrick, A.R., Knutton, S., Oka, T. and Wakil, S.J. (1971), *Proc. Nat. Acad. Science USA.*, **68**, 3180-3184.

[13] Yelton, D.E. and Scharff, M.D. (1981), *Annu. Rev. Biochem.*, **50**, 657-680.

[14]Pressman, B.C., Harris, E.J., Jagger, W.S. and Johnson, J.M. (1967), *Proc. Nat. Acad. Science. USA.*, **58** 1949-1956.

[15]Brown, P.R. and Bartsch, R.A. (1991), in *Inclusion aspects of Membrane Chemistry*, Osa, T. and Atwood, L. (Eds), Kluwer Acad. Pub., Dortrecht.

[16]Westley, J.W. (Ed), (1982), *Polyether Antibiotics. vol 1 & 2.* Marcel Dekker. New York. This is a collection of review articles covering all aspects of the work done on these materials up to 1981.

[17]Berger, J., Rachlin, A.I., Scott, W.E., Stembach, L.H., Goldberg, M.W. (1951), *J. Am. Chem. Soc.*, **73**, 5295-5298.

[18] Agtarap, A. Chamberlin, J.W., Pinkerton, M. and Steinrauf, L. (1967), *J. Amer. Chem. Soc.*, **89,** 5737-5739.

[19]Shumard, R.F. and Callender, M.E. (1968), *Antimicrob. Agents Chemother.*, **1967,** 369-377.

[20]Westley, J.W., Evans, R.H., Pruess, D.L. and Stempel, A. (1970), *Chem. Commun.*, **1970**, 71-72.

[21]Westley, J.W., Pruess, D.L. and Pitcher, R.G. (1972), *Chem. Commun.*, **1972**, 161-162.

[22]Westley, J.W., Evans, R.H., Harvey, C., Pitcher, R.G.,Pruess, D.L., Stempel, A. and Berger, J. (1974), *J. Antibiot.*, **30**, 610-612.

[23] Day, L.E., Chamberlin, J.W., Gordee, E.Z., Chen, S., Gorman, M., Hamill, R.L., Ness, T., Weeks, R.E. and Stroshane, R. (1973), *Antimicrob. Agents Chemother.*, **4**, 410-414.

[24] Westley, J.W. (1976), *J. Antibiot.*, **29**, 584-586.

[25]Taylor, R.W., Kauffman, R.F. and Pfeiffer, D.R., In *Polyether Antibiotics*. **vol 1**, Westley, J.W. (Ed), Marcel Dekker, New York. Ch 4, pp 103-184.

[26]Cram, D.J., (1988), *Angew. Chemie Int. Ed.*, **27**, 1009-1020.

[27] Liu, C-m. (1982), In *Polyether Antibiotics*, Westley, J.W. (Ed), Marcel Dekker, New York. Ch 3, pp. 43-102.

[28]Boeck, L.D., Hoehn, M.N., Kastner, R.E., Wetzel, R.W., Davis, N.E. and Westhead, J.E. (1976 pub. 1977), *Dev. Ind. Microbiol.*, **18**, 471-485.

[29]Hara, M., Hara, K., Yoneta, S., Kasahara, Y. and Nakamura, H. (1978), *Japan Kokai* 78,148,594. 25th. Dec. 1978, *Chem Abs* **90**: 150298a.

[30]Torssell, K.B.G., (1983), *Natural Product Chemistry*, John Wiley and Sons.

[31]Long. P.L. (Ed), (1982), *The Biology of the Coccidia*, University Park Press, Baltimore, Md.

[32]Chapman, H.D. (1986), *Res. Vet. Sci.*, **41**, 281-282.

[33] Miyuzaki, Y., Sugawara, H., Nagatsu, J. and Shibuya, M. (1972), *Japan Kokai*, 72 25,392. 20th. Oct. 1972, *Chem Abs.*, **78**: 41561.

[34] Tanaka, Y., Saito, H., Miyuzaki, Y., Sugawara, H., Nagatsu, J. and Shibuya, M. (1973), *Ger. Offen.* **2,253,031**. 20th Sept. 1973. *Chem. Abs.*, **79**: 144871.

[35] Kinashi, H., Otake, N., Yonehara, H., Saito, S. and Saito, Y. (1973), *Tetrahedron Lett.*, **1973**, (49), 4955-4958.

[36] Kinashi, H., Otake, N., Yonehara, H., Saito, S. and Saito, Y. (1975) *Acta Cystallogr.*, **B31**, 2411-2415.

[37]Miyazaki, Y., Shibuya, M., Sugawara, H., Kawaguchi, O., Hirose, C., Nagatsu, J. and Esumi, S. (1974), *J. Antibiot.*, **27**, 814-821.

[38] Berg, D.H., Hamill, R.L., Hoehn, M.M. and Nakatsukasa, W.M. (1975) *Ger. Offen.* 2,525,095. 18 Dec. 1975. *Chem. Abs.*, **84**: 103844.

[39] Berg, D.H. and Hamill, R.L. (1978), *J. Antibiot.*, **31**, 1-6.

[40] Occolowitz, J.L., Berg, D.H., Debono, M. and Hamill, R.L. (1976), *Biomed. Mass Spect.*, **3**, 272-277

[41]Seto, H., Miyazaki, Y., Fujita, K-i., Otake, N., (1977), *Tetrahedron Lett.*, **28**, 2417-2420.

[42]Kinashi, H. and Otake, N. (1976), *Agric. Biol. Chem.*, **40**, 1625-1632.

[43]Dorman, D.E., Paschal, J.W., Nakatsukasa, W.M., Huckstep, L.L. and Neuss, N., (1976), *Helv. Chim. Acta*, **59**, 2625-2634.

[44]Seto, H., Miyazaki, Y. and Otake, N. (1977), *J. Antibiot.*, **30**, 530-537.

[45] e.g. Jeffers, T.K. (1981), *Avian Dis.*, **25**, 395-408.

[46] e.g. Jeffers, T.K. and Bentley, E.J. (1980), *Poult. Sci.*, **59**, 1722-1730.

[47]e.g. Jurkovic, P., Sevcik, B., Bedrnik, P. and Firmanova, A. (1982), *Arch. Gefluegelkd.*, **46**, 108-110.

[48]eg. Bartley, E.E., Nagaraja, T.G., Pressman, E.S., Dayton, A.D., Katz, M.P. and Finar, L.R. (1983), *J. Anim. Sci.*, **56**, 1400-1406.

[49]eg. Tsuyoshi, K., Abe, M. and Goto, Y. (1979), *Tochigi-ken Rakuno Shikenjo Kenkyu Hokoku.*, **105**, 19-42.

[50]Pressman, B.C. and De Guzman. (1978), NT. US. Pat. no. 4,129,659. 12th. Dec. 1978, *Chem. Abstr.* **90**: P133029.

[51]Mehlhorn, H., Ganster, H.J. and Raether, W. (1984), *Zentralb. Bakteriol. Mikrobiol. Hyg. Ser. A.*, **256**, 305-313.

[52]Suzuki, K., Tohda, K., Sasakura, H. and Shirai, T. (1987) *Anal. Lett.*, **1987**, 533-534.

[53]Davies, O.G., Moody, G.J. and Thomas, J.D.R. (1988), *Analyst (London)*, **113**, 497-500.

[54]eg. Lewis, M.D. (1983), from *Diss. Abstr. Int. B.* 1983, **44**, 1831. *Chem Abs.*, **100**: 85468.

[55]Horita, K., Oikawa, Y., Nagato, S. and Yonemitsu, O. (1988), *Tetrahedron Lett.*, **29**, 5143-5146.

[56]Yonemitsu, O., Horita, K., Noda, I. and Oikawa, Y. (1987), *Lect. Heterocycl. Chem.*, **9**, 105-111.

CHAPTER 2

Chapter 2. Cation transport mediated by naturally occurring polyether antibiotics.

2.1 Introduction.

Ionophores exert their biological action by facilitating the transport of ions across cell membranes along a concentration gradient. Ionophores fall into several classes such as peptides like gramicidin, cyclic depsipeptides like valinomycin and polyether antibiotics such as monensin two of which, salinomycin and narasin have been the subject of this work. Ionophores can produce their effect by either pore formation eg gramicidin or complexation with an ion to form a lipid soluble complex[1] e.g. valinomycin and monensin. As has been stated earlier the polyether antibiotics are active against many micro-organisms and are important in the livestock industry. Therefore an understanding of their mode of action and methods of increasing efficiency and specificity of action are important. The largest problem with these materials for clinical use is their toxicity.[2] This arises from their general ion transport activity, so if they are made more specific for a particular cell type smaller doses could be used thereby reducing toxic side effects.

In the widely accepted model for transport mediated by anionic ionophores the ionophore is totally dissolved in the membrane. All that protrudes from the membrane is the ionised carboxylic acid head group.[1] The first step in the complexation is the approach of a cation to this carboxylate ion exposed by the membrane. After this complexation occurs in a multistep process with the ionophore replacing the bound water molecules

surrounding the solvated cation.[3] The complex formed has the cation centrally situated with the surface composed of non-polar aliphatic and aromatic groups to assist in the lipid solubility. The formation of a lipid soluble complex would facilitate the transport of cations across cell membranes and this solubility effect is believed to be the source of the transport catalysis. Therefore most studies have been on the solution chemistry of the compound to help understand their transport processes.

The solution chemistry for the complexation reaction is not necessarily that seen in the complexation at the lipid surface. Phospholipid bilayers are typically 80-100Å thick,[4] ionophores are large molecules and form complexes about a quarter of this size.[3] The high anisotropy of the interior of a membrane and possible interactions with the lipid headgroups could also affect the reactivities.

2.1.1 Ion complexation studies (Thermodynamic).

The ionophoric antibiotics function by the transport of ions across cell membranes. As they are important in the agricultural industry they have been extensively studied. A large number of systems and methods have been used in the quest for information. The following section contains an overview of the methods used and the results which can be obtained from them.

A good place to start on the trail of information is the measurement of protonation constants (pK_a's) of the ionophores. The complexing species is usually the carboxylate ion so the formation of this species is of interest. Polyether antibiotics are at best sparingly soluble in water so a wide range of different solvents

have been used to perform these experiments. The problem with this is that such data is only applicable to a particular solvent so no comparisons can be made.[5] It has been recommended that a standard solvent system should be adopted. The system put forward is methanol/water as ionophores tend to be methanol soluble and a meaningful pH scale and standard buffers have been developed for this solvent.[6]

The cation complexation constants are of obvious importance enabling predictions to be made about complex stability and ion preference. The low water solubility of the polyether antibiotics is again a problem here but there are two possible approaches. One is to use solvents in which both ion and ionophore are soluble, such as methanol and ethanol. The other is to use a two phase system and to measure the ion extraction from the aqueous phase into an organic layer.[3]

The first method has been successfully used for a number of ionophores including monensin,[7] nigericin[8] and lasalocid A[9] (see Figure 2-1.) but few ionophores have been measured. The formation of the complex can be monitored by a number of methods, including cation-selective electrodes,[10] cation indicating dyes,[3] spectrophotometric[11] and fluorometric[12] methods. The latter two can only be used with ionophores with suitable spectroscopic properties. Lasalocid A, which contains an aromatic group, has been successfully studied in this way.[13]

An alternative solution state method is by use of thallium(I).[12] Tl^+ is complexed by many ionophores with

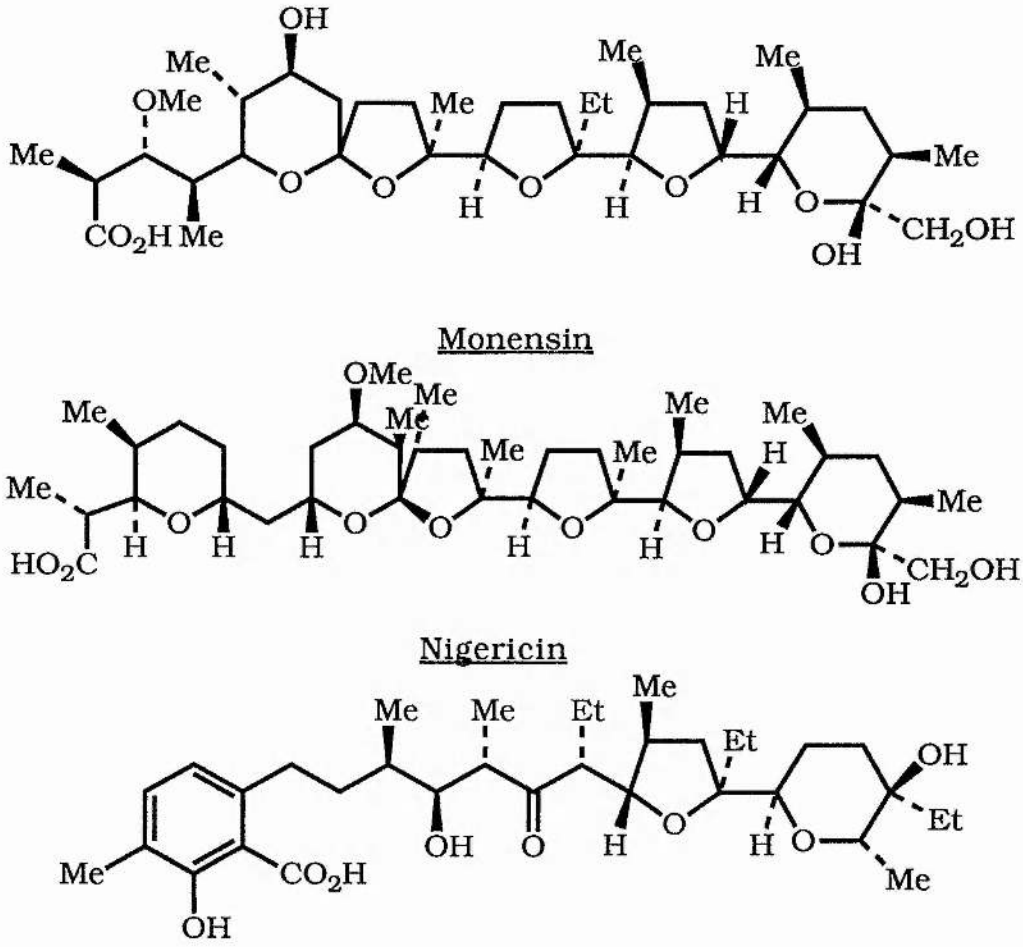

Figure 2-1. The structures of monensin, nigericin and lasalocid A, three common polyether antibiotics.

concomitant quenching of fluorescence. Thus the concentration of the complex can be determined and hence the formation constant can be found. The displacement of Tl^+ by other ions can be measured, thereby obtaining the formation constants of the resulting complex. A similar competetive displacement method follows the replacement of protons with other cations by monitoring the pH.[14]

Instead of measuring the formation constant the extraction

equilibrium constants (K_{ex}) can be determined. These are measured by equilibrating a buffered aqueous solution of cation with an immiscible organic phase containing ionophore. The uptake of cation into the organic phase is followed and assumed to be due to complexation. The known data can then be used to calculate a constant describing the overall equilibrium using the equations.[15]

$$AH_{(org)} + M^{+}_{(aq)} \rightleftharpoons AM_{(org)} + H^{+}_{(aq)}$$

$$K_{ex} = \frac{[AM_{org}][H^{+}_{aq}]}{[AH_{org}][M^{+}_{aq}]} \qquad \text{Eqn 2-1}$$

$$2AH_{(org)} + M^{2+}_{(aq)} \rightleftharpoons A_2M_{(org)} + 2H^{+}_{(aq)}$$

$$K_{ex} = \frac{[A_2M_{org}][H^{+}_{aq}]^2}{[AH_{org}]^2[M^{2+}]} \qquad \text{Eqn 2-2}$$

The numerical values obtained by this method are dependent on the solvent system due to solvation differences, often 70% toluene/30% methanol is used. A simple method which can be used is a competitive displacement of a bound cation in an extraction system.[3] This only gives a relative order of affinities as unfortunately the data is not reliably quantifiable.

2.1.2 Ion Complexation Studies (Kinetic).

The previous section was concerned with the thermodynamic aspects of the complexation process. A complete understanding of this procedure must also include a study of the kinetics. The rate of complexation must necessarily be rapid if a

material is to be an efficient ionophore. Therefore methods such as rapid mixing and transient perturbation must be used.

The complexation reaction occurs *via* the replacement of co-ordinating solvent molecules by the ligand. The polyether antibiotics are all multidentate ligands so the reaction occurs with a number of substitution steps as well as conformational rearrangement. There are two limiting mechanisms:

1 Dissociative The solvent leaves the inner co-ordination sphere prior to the metal-ligand bond formation.

2 Associative The ligand metal bond forms before the solvent molecule is lost.

Most actual reactions fall somewhere between these two extremes. An example could be an S_N2 type reaction where an oxygen atom on the ligand displaces a solvent molecule.

There are a number of problems associated with kinetic studies on ionophores. The reactions are rapid, polyether antibiotics have low water solubility and are generally poor chromophores. Conventional rapid reaction techniques can be used but care must be taken to select the correct method.

The rapid mixing techniques, e.g. stopped flow and pulsed flow, have been used for the study of the kinetics with alkali metal ions. An example of this is a study on the proton/sodium exchange reaction of monensin followed by a stopped flow technique.[16]

The alternative procedures are all relaxation methods. In these the system is rapidly perturbed and the return to equilibrium monitored. The relaxation time related to the concentrations of the species present and the rate constants. Such methods include pressure jump,[17] pressure shock [18] and temperature jump techniques.[19]

2.1.3 Transport studies.

The above methods provide information about the solution state behaviour of polyether antibiotics. It is however their behaviour at solution interfaces which is of most importance as this governs their transport in real systems. Therefore study of ionophore mediated transport across membranes must be carried out. This takes into account the differences between reaction in a solution and a reaction in the highly anisotropic conditions found at the solvent-membrane interface in living cells.

Much work has been carried out on the transport properties of these materials funded by their importance in the livestock industry. They are also widely used as experimental tools, e.g. in ion-selective electrodes, but here only methods which contribute to the understanding of the transport process will be discussed.

The place to start an investigation into ion transport is to decide on a model membrane. The simplest system used is the "Pressman cell" or "U-tube transport". This is a three phase system with two aqueous layers separated at the base of a U tube by a layer of chloroform or carbon tetrachloride (see Figure 2-2.).[14]

One aqueous solution contains the cation under investigation with the ionophore dissolved in the membrane. At the chloroform aqueous interface the ionophore deprotonates and complexes with a cation. The complex then diffuses through the membrane and then disgorges its cation at the other interface, where it is replaced by a proton or another cation. This process will continue until the system reaches equilibrium. The transport can be followed by any suitable method such as atomic absorption or using radiochemical tracer techniques.[3]

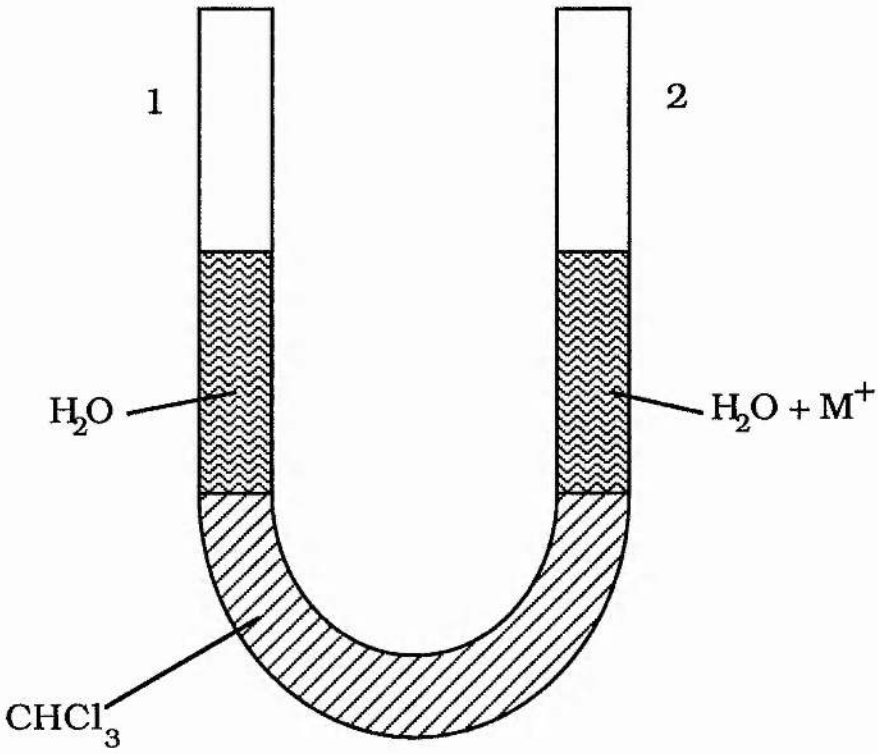

Figure 2-2. A schematic representation of a U-tube system.

An alternative configuration for this system is with the three layers stacked vertically. In practice the density of the organic layer may be decreased by using a mixture of chloroform and alkane, eg decane. The density of the lower aqueous layer being raised by dissolved sucrose (see Figure 2-3).[20] The data obtained

from this system is usually in good agreement with the relative binding affinities found by two phase extraction, as might be expected from the similarity in these techniques. The decomplexation rates are however not always analogous to those obtained from the 2 phase system.[3] In summary this method gives useful information relatively quickly and easily. As might be expected there is a downside to this method. This lies in the high dependence of the final results on the conditions such as stirring rate and vessel geometry.[3]

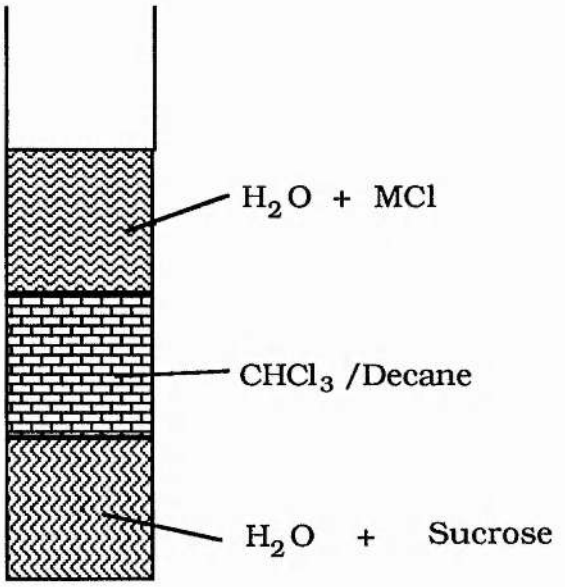

Figure 2-3. A schematic representation of a three layer transport system.

A somewhat similar technique involving diffusion across an organic solvent layer is the use of liquid ion-exchange electrodes.[21] Here the ionophore is dissolved in an organic phase inside an inert matrix with complexation at one face allowing an ion to transport and a charge to pass. This system has been used to produce selectivity sequences which may be equivalent to the binding sequence. The drawback to this process is that ionophore

mediated transport is electrically neutral overall so any charge conductance must alter the transport conditions. This means that any data must be treated with caution when related to membrane transport. A similar system to this are black lipid bilayers. In these two half cells are separated by a phospholipid bilayer, covering a pinhole. The addition of some ionophore allows cations to cross this membrane thereby allowing the transport rates to be measured.

A more accurate picture of *in vivo* transport can be obtained by using phospholipid membranes. These can be as vesicles, multilammellar liposomes or even actual cells. The transport can be followed by a range of techniques from physical methods, to observing the stimulation or depression of a natural activity of the cell. A popular example of the latter case is the use of separated mitochondria which are easily prepared and very versatile.[22] In this case the transport can be followed by:

a) observing the swelling of the mitochondria due to ion uptake,

b) monitoring the release of cations from the mitochondria,

or c) observing one of the functions of the mitochondria, e.g. respiration.

Other cell types can also be used for example erythrocytes,[23] chloroplasts[24] and intact cells where ionophore action generates a cellular response.[25]

The results obtained using these methods must also be treated with caution in comparison to those found using other

systems. The ion binding sequences and the selectivity sequences obtained from liquid membrane electrodes need not match those obtained using other methods. There is usually good qualitative correlation between the transport sequence and binding sequence for isocoulombic ions, although there are exceptions.[26] There is also usually good qualitative agreement between the transport sequences obtained by different methods but there are differences in a few cases, eg. dianemycin [3] (Figure 2-4).

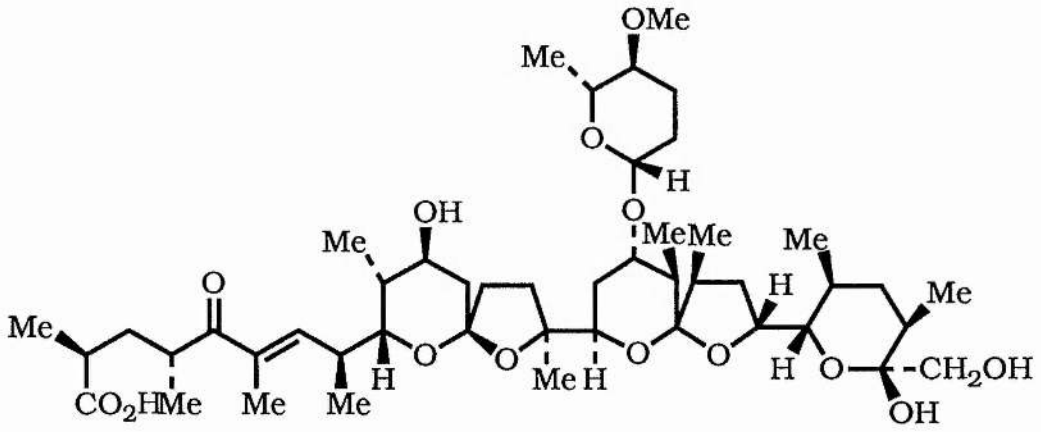

Dianemycin

Figure 2-4. The structure of Dianemycin.

2.2 Transport and Binding Studies on Salinomycin and Narasin.

2.2.1 Discovery and *in vitro* studies.

Salinomycin and narasin, Figure 2-5, are both commercially important polyether antibiotics and as such have been widely studied. Many of the above methods have been used and the results obtained are reviewed below:

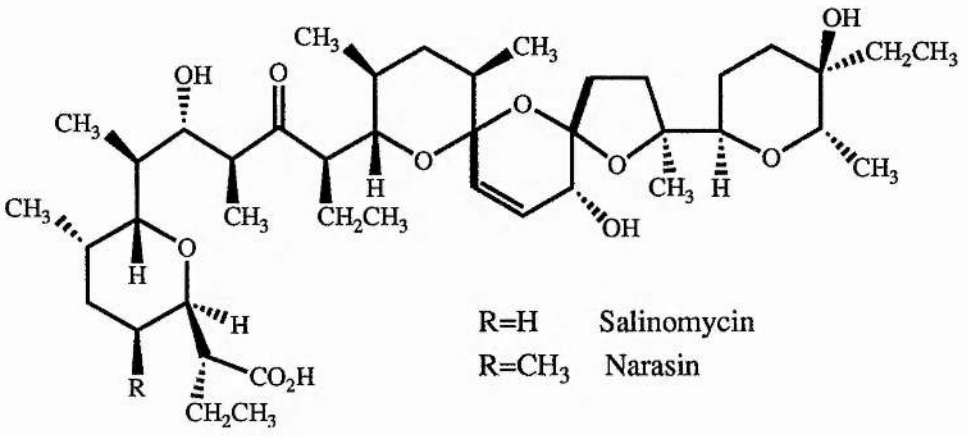

Figure 2-5. The structures of salinomycin and narasin.

Salinomycin was discovered in 1971 by the Kaken Chemical Co. in Japan. The first paper published about the properties of this material followed in 1974.[27] This merely showed that the material was a polyether antibiotic, active against Eimeria and gram positive bacteria. No transport studies were carried out.

The first transport studies on salinomycin and derivatives were published a year later by the same group.[28] Both two phase extraction and transport across a bulk organic membrane were used in the study, the process being followed by the use of radioactive isotopes. The two phase extraction experiments were

carried out using n-butanol/toluene as the organic layer, vigorously mixed with a buffered aqueous layer containing the isotopically labelled cations. The association complexes were calculated using equation 2-1, given above. The results showed a preference for monovalent cations over divalent ones and more specifically a great preference for potassium over all the other cations tested. The derivatives studied were acetyl and propionyl salinomycin and also the methyl and bromophenacyl esters. The site of acylation is unspecified but is probably C(20)-OH. It was observed that the latter pair were unable to complex any cations to any appreciable extent, demonstrating the importance of the carboxylate anion in complexation. The acetyl and propionyl derivatives formed complexes with comparable values of K_A to those exhibited by salinomycin itself. The potassium complexes of these latter compounds had slightly lower K_A values, the sodium slightly higher but there was a ten fold decrease in the values observed for cæsium.

The transport across a bulk organic phase was measured using both a U-tube type system (using a septum to separate two aqueous layers above a carbon tetrachloride layer)[14] and a three layer system. This latter case used a decane/carbon tetrachloride layer with the lower aqueous layer made more dense with dissolved sucrose. The aqueous layers were buffered at pH 9.8. The data obtained from the two systems was comparable. The results showed that for salinomycin in the three phase system the transport sequence was:

Rb^+, $Na^+ > K^+ » Cs^+$, Mg^{2+}, Ca^{2+} and Sr^{2+}

which disagrees with the ion preference data mentioned above. So

the most stable complex is not the most efficient transporter, at least in this experimental system. In transport experiments with the derivatives it was seen that the carboxyl esters were inactive but that the acetyl and propionyl derivatives were of comparable efficiency. Thus the carboxylate ion is crucial for cation complexation and transport but acylating the hydroxyl groups need not be disadvantageous.

In 1976 a further paper on the effect of structural modification on the activity of salinomycin was published by Miyazaki et al.[29] The groups selected for modification were mainly oxygen containing, at C(1), C(11) and C(20) but also included the vinylic sites at C(18) and C(19). The effects on ion complexation abilities and antimicrobial activity on a number of bacteria were studied. The results obtained were very interesting and showed that the ionophoric activity could be enhanced or decreased by the modification of certain sites. It was seen that esterification of the carboxyl group produced complete loss of activity. The acylation of C(20)-OH was found to produce an enhancement of the antimicrobial activity. Hydrogenation of the vinylic double bond and oxidation of C(20)-OH to a ketone were both seen to have a large effect on the activity. The C(18) - C(19) dihydro derivative was seen to have lost most of its potassium and rubidium preference and the C(20)-keto derivative showed even lower values for K_A. Interestingly the C(20)-keto form was generally more active antimicrobially, although this depended on the bacteria being considered. Both however still exhibited considerable antimicrobial activity demonstrating that this site is important but not crucial for complexation. One highly interesting

feature of this experiment was the complete loss of activity caused by reduction of the ketone at C(11) to a hydroxyl. This shows that this β-hydroxy ketone is of crucial importance in the formation of complexes.

Narasin was discovered in 1976 by Eli Lilly in America. The first paper published on this new material [30] showed that it was a new polyether antibiotic and active against gram positive bacteria, anaerobic bacteria and fungi. It was also shown that narasin was active against coccidiosis in chicken, but no transport studies were carried out at this time.

An in vitro study of narasin using a three phase system has also been published[31] but in this case no derivatives were investigated. This work showed a preference for potassium over sodium in a U-tube system with a chloroform membrane. The variation of ion flux with pH of the starting aqueous phase was also measured with the receiving phase maintained at neutral pH. In narasin this showed a roughly parallel increase in the ion flux for both potassium and sodium as the solution became more basic. This increase is attributed to the ease of deprotonation at higher pH which enables the complex to form more readily.

2.2.2 *In vivo* transport studies.

A variety of live cells and glands have been used in the study of the transport properties of salinomycin and narasin. These have included rat liver mitochondria, erythrocytes and submaxillary and parotid glands of rats.

Mitochondria are observed to swell when they are loaded with cations. This can be achieved by stimulating the uptake of alkali metal ions with valinomycin or monazomycin in the presence of ATP and a substrate, usually succinate or glutamate. Any change in the size of mitochondria can be observed by light scattering measurements.[32] Thus, if cations can be removed from preloaded cells the size of the mitochondria will be observed to decrease. This can be used as a method to determine whether or not a particular cation is transported. It also gives some idea of the ion preferences by observing the rates at which the mitochondria decrease in size with a range of cations. The data cannot be relied upon to produce quantitative results but a qualitative preference order can be determined.

The other use for mitochondria in this type of study is the observed inhibition of ATPase activity in the presence of ionophore. In respiring mitochondria certain subtrates e.g. glutamate, α-ketoglutamate, succinate, malate, pyruvate and β-hydroxybutyrates are oxidised.[33] The total sequence involves the hydrolysis of an ATP molecule to ADP and inorganic phosphate which is one way of following the reaction. This ATPase activity has been seen to be inhibited in the presence of a polyether antibiotic.[33] This inhibition is known to be related to the transporting ability of the ionophore with respect to the cation with which the mitochondria are loaded. In this way it is possible to identify an ion preference sequence and certainly elucidate which cations are not transported at a reasonable rate. The loss of ATPase activity is believed to be caused by the lowering of the internal pH of the mitochondria due to the transport of protons

into the mitochondria.[34] This balances the motion of the cations in the opposite direction.

The results of a study of salinomycin with rat liver mitochondria were very clear cut.. This used both mitochondrial swelling and ATPase inhibition measurements to study the transport properties with alkali metal ions. The data suggested that salinomycin transported ions across mitochondrial membranes with a preference sequence of:

$$K^+ > Rb^+ > Na^+ > Li^+, Cs^+.$$

Potassium was found to be easily the most readily transported cation. It was also noted that a high external concentration of alkali metal cations decreased the ATPase inhibition seen and inhibited the antimicrobial activity induced by salinomycin.

A study of the effect of narasin on respiring rat liver mitochondria was published by Wong et al in 1977.[35] In this case the ATPase activity was stimulated by three different agents: a) 2,4-dinitrophenol, b) valinomycin and potassium ions and c) monazomycin. In each case the the addition of narasin inhibited ATP hydrolysis. It was seen that narasin and monensin both preferred to complex with ammonium ions over any alkali metal cation. The observed preference sequence for the alkali metals was:

$$Na^+ > K^+, Rb^+ > Li^+, Cs^+.$$

Thus sodium is preferred over all others with lithium and cæsium only very slowly transported.

Red blood cell are a good medium for studying ion transport. Initially studies on real cells used mitochondria, as in those mentioned above. The problem with these is that they impose their own ion transport mechanisms on the cations making interpretation relatively complex. Erythrocytes however do not give rise to such problems as well as being relatively uniform bags of cations. In the words of Painter and Pressman[23] they are "nature's own liposomes". The problem lies in following the cation transport. In mitochondria this is done by observing the cell activity and seeing how it changes. This approach is not possible in red blood cells. This drawback was overcome by the development of ion selective glass electrodes for sodium and potassium. The studies on salinomycin, narasin and a range of other ionophores have been carried out using such a system [23,36].

The ion preferences can be worked out from the behaviour of the sodium, potassium and hydrogen ion concentrations on addition of the ionophore. Two representative traces, reproduced from reference 36, show the characteristic behaviours of, Figure 2-6. a potassium selective ionophore (nigericin) and, Figure 2-7. a sodium selective ionophore (monensin). It is the initial direction of movement of protons which shows the preferred ion. Erythrocytes have a high potassium concentration inside and high sodium outside, it is the loss of these ion gradients that are watched in these experiments. The transport is electrically neutral, so the total ion fluxes in opposite directions must be the same. Thus the net proton flux is in the same direction as that of the slower moving cation.

Figure 2-6. A plot showing the exchange of internal potassium for external sodium and protons catalysed by nigericin in erythrocytes. Movements of ions from the cells into solution is shown by a downward deflection.[36]

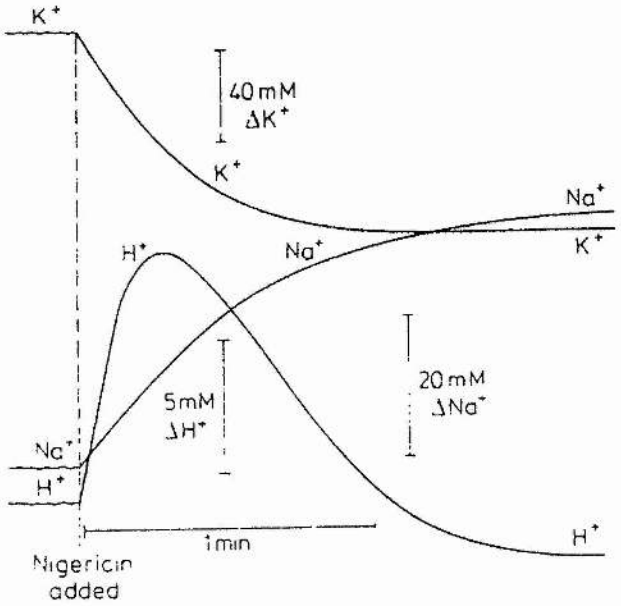

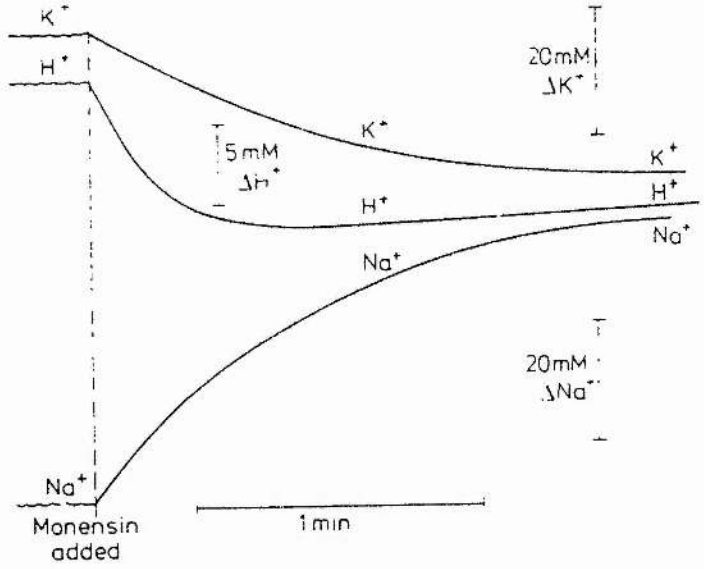

Figure 2-7. A plot showing the exchange of internal potassium and protons for external sodium catalysed by monensin in erythrocytes. Movements of ions from the cells into solution is shown by a downward deflection.[36]

The preference can be quantified by finding the ratio of the initial rates of sodium and potassium transport. With nigericin the potassium ion gradient across the membrane is dissipated much more rapidly than the sodium ion gradient. This gives rise to the observed bidirectional nature of the proton transport. Initially protons are moving into the erythrocytes to balance the loss of potassium, the later efflux is to balance out the much slower influx of sodium ions. The equilibrium values of the concentrations are independent of the ionophore used.

The results of this experiment with salinomycin and narasin showed that both were potassium selective ionophores with narasin demonstrating the greater potassium preference. In the same paper there is a brief note that two artificial ionophores, one an α-carboxyl ω-hydroxyoligoethylene glycol derivative and the other a dinaphthyl 18-crown-6 derivative with two carboxy side arms, failed to show any activity using this method, even at 100 times greater concentrations than those used for the naturally occurring ionophores.

In 1986 Katoh and Tsuda demonstrated that salinomycin transports calcium into the parotid and submaxillary glands of rats.[25,37] This was demonstrated by the stimulation of salivation by the addition of salinomycin to a calcium rich solution containing the glands. If there is no calcium in the external medium then no amylase release is observed. This method shows that transport occurs but cannot give any quantifiable data on rates and preferences.

An alternative method for studying the transport is to use phospholipid vesicles as model membranes. The only published work on salinomycin and narasin is by Riddell and Tompsett, which consists of part of the work in this thesis.[38] The transport rates of the potassium complexes were observed to be faster for both ionophores. Salinomycin also showed a clear thermodynamic preference for potassium with the stability constants of the sodium and potassium complexes of narasin roughly the same.

2.2.3 The binding selectivities of narasin and salinomycin using non-transport methods.

A completely different approach is to calculate the dissociation constants of the complexes in solution which gives information on the stability of the complexes and hence their intrinsic preferences. The problem is how to measure the concentrations of the free anionic and complexed form of the ionophore in solution. One method which has been successfully used is circular dichroism.[39] This is only applicable if there is a suitable chromophore near to a site of major conformational change on complexation. There is such a site present in salinomycin and narasin (the ketone at C(11)) and this approach has been used to obtain useful data.

Plane polarised light can be considered as two components of circularly polarised light with identical amplitude and phase, but rotating in opposite directions. Circular Dichroism (CD) is one of two techniques which rely on the difference in the behaviour of left and right circularly polarised light with optically active materials as the frequency of the light is changed. The other

technique is Optical Rotatory Dispersion (ORD), which is commonly seen as the rotation of monochromatic plane polarised light by an optically active material.

There are two important factors which contribute to the interaction of polarised light with a material. One is the refractive index and the other the extinction coefficient of an absorption. The refractive index contribution arises because light travels at different velocities in different media. It is observed that the different enantiomers of a chiral material show a difference in the refractive index for left and right circularly polarised light. This means that one component of the light will be travelling faster than the other. This leads to a rotation in the plane of polarisation when the light emerges from the other side of the sample. This effect occurs for all wavelengths of light but is at a maximum near the absorption frequency of the chromophore from which it arises. There is a phase change in this effect at the absorption frequency.

The other factor which is different in chiral compounds in their interaction with circularly polarised light is the extinction coefficient. This gives rise to the effect of circular dichroism which is of interest here. This CD absorption is usually at the same wavelength as the UV-visible absorption for that chromophore and occurs as a bell shaped curve with negligible intensity remote from the peak. This makes CD a good method for studying the structure of complex molecules as only groups with absorptions close to each other will interfere. In ORD the effect is seen over the whole spectrum leading to difficulties in interpretation for materials with many chiral centres. Salinomycin and narasin both have nearly 20 chiral centres all of which are enantiomerically pure, so a large

number of superimposed ORD spectra would be seen. There are two types of material which exhibit the properties of CD. The strongest effect arises where there is a chiral chromophore eg hexahelicene, but it is also observed for symmetric chromophores situated adjacent to one or more chiral centres. It is the latter class which are of interest in the following work. An interesting feature of the CD of this class of material is that the observed intensity is not proportional to the absorption of light. Thus the best chromophores for study are those with weak UV absorptions eg. carbonyls, thiones and nitrites. This makes it useful for salinomycin and narasin as these both contain a carbonyl between two chiral centres in a flexible portion of the molecule. It is in fact this absorption which has been used in the studies carried out.[40,41]

The first work published was a study of the conformation of salinomycin as the free acid, anion and sodium and potassium complexed forms.[40] This study used a range of solvents of differing polarities from 50% dioxane/water to 90% dioxane/water. There was a dependence of the conformation on the solvent polarity in some cases. The free acid had the same comformation in all solvents but the anion showed a large step at Z = 80-83 demonstrating that it occurred in two metastable states. Which of these is favoured depends upon the polarity of the solvent being used. There is a similar sharp shift seen in the ratios of the dissociation constants for sodium and potassium, showing that the ability of the ionophore to discriminate between ions depends upon environmental influences on conformation. Values for the dissociation constants were also published. These were obtained by plotting $1/[M^+]$ vs $1/\Delta R_0^T$ where ΔR_0^T is the change in

rotational strength on complexation. The slope of the graphs gave the value of K_s and extrapolation to infinite cation concentration gave R_0^T of the cation-saturated ionophore. ΔR_0^T is the difference between the observed rotational strength and that of the anion and as such is a measure of the concentrations of both the anionic and complexed species. The K_s values obtained show a preference for potassium in all solvents with the selectivity increasing as the Z value increases. This study also demonstrated the importance of conformation in the complexation process.

The previously published reports on narasin had shown a disagreement about the ion preferences exhibited. Caughey and co-workers thought that determining the K_s values for the sodium and potassium complexes in a range of solvents may shed some light on the problem.[41] The K_s values were determined titrimetrically using CD as the tool to assess the degree of complexation. The ionophore in the presence of a large base such as tributylamine will exist as the free anion. If the differential absorption, $\Delta\varepsilon$, of this is found it can be compared to that of a partially complexed mixture. The total absorption seen will be a population weighted average of the two forms:

$$\Delta\varepsilon_x = X_d.\Delta\varepsilon_d + X_b.\Delta\varepsilon_b \qquad \text{Eqn. 2-4.}$$

Where X_b and X_d are the molar fractions of bound and dissociated forms respectively and $\Delta\varepsilon_b$ and $\Delta\varepsilon_d$ are the differential absorptions due to these forms.

The fractional saturation v is given by the equation:

$$v = \frac{(\Delta\varepsilon_x - \Delta\varepsilon_d)}{(\Delta\varepsilon_b - \Delta\varepsilon_d)} \qquad \text{Eqn. 2-5.}$$

Where all the differential absorptions are readily measured. The free cation concentration (L) is calculated as the difference between the the amount added and the amount complexed. K_s is then calculated from a plot of v/L vs v (a Scatchard Plot).

The results obtained showed that in all solvents potassium was preferred over sodium. The solvent polarity affected the dissociation constants and selectivity ratios, both tending to increase with increasing polarity. However, there is no suggestion that a selectivity inversion would occur at extreme polarity as seen for salinomycin.

The basic trend of all these studies is that both salinomycin and narasin prefer potassium to sodium under most conditions. There are however examples of the opposite selectivity seen for both so possibly no large differences between them should be expected. The more systems that are studied with these ionophores the better the understanding of the processes involved in the transport should be. It would be interesting to discover the cause of these differences.

2.3 The Use of NMR to Study Ion Transport.

2.3.1 Kinetics of the transport process.

The transport of alkali metal ions through lipid bilayers mediated by salinomycin and narasin can be studied by nmr. In biological systems the transport is across lipid bilayers[4] so a model containing such a system would be preferable. To this end large unilamellar vesicles made from egg yolk phosphatidylcholine suspended in a dilute aqueous salt solution were used. The vesicles were grown by dialytic detergent removal with the same ionic strength and cation concentration internally and externally. This means that there is no osmotic pressure or ion gradient to complicate further an already complex rate equation. The model used for the transport process is that proposed by Pressman[1] which is shown in Figure 2-8. The formation and dissociation of the complex are both multistep processes but that their representation by an overall constant is valid, has been shown by previous work using the same method.[42,43,44,45,46] These have been the only attempts to apply chemical kinetics in a rigorous way to determine k_f, k_d and K_s for the membrane transport process.

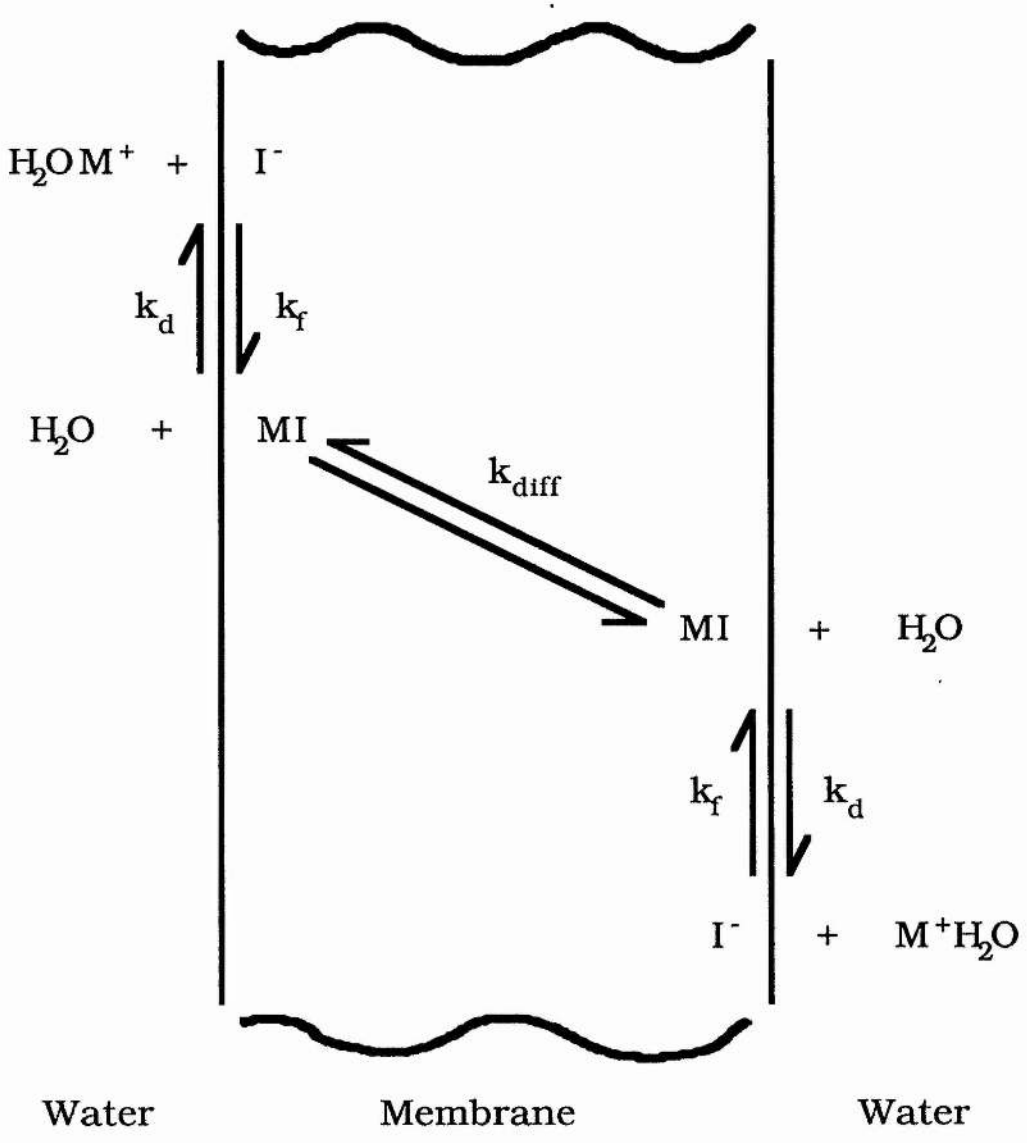

Figure 2-8. Schematic representation of the model used to describe ionophore mediated ion transport through phospholipid bilayers. The rate constants are; k_f formation rate of the complex, k_d dissociation rate of the complex and k_{diff} diffusion coefficient of the complex throughthe membrane.[1]

This model gives rise to the rate equation:

$$\frac{1}{\tau_{M^+in}} = \frac{A.k_{diff}.k_d.[L]_T}{V_{in}.(k_d + 2k_{diff}).([M^+] + k_d/k_f)} \quad \text{Eqn. 2-5.}$$

Where:-

τ_{M^+in}	=	Lifetime of M^+ inside a vesicle.
A	=	Surface area.
V_{in}	=	Internal volume.
$[L]_T$	=	Total concentration of ionophore.
k_f	=	Rate of formation of the complex.
k_d	=	Rate of dissociation of the complex.
k_{diff}	=	Diffusion coefficient of the complex.
$[M^+]$	=	Metal ion concentration.

The terms k_f and k_d are the overall rates for the multistep formation and dissociation reactions. These occur by sequential replacement of the solvating water molecules by the ionophoric oxygens. As each water is replaced the ion can be pictured as sinking further into the membrane progressively surrounded by more of the ionophore molecule.[36]

This equation can be simplified by the introduction of two terms. These are:-

$$K_m = \frac{k_d}{k_f} = K_s^{-1} \quad \text{Eqn.2-6}$$

and $$V_m = \frac{k_{diff}.k_d}{(k_d + 2k_{diff})} \quad \text{Eqn. 2-7}$$

Where K_s is the stability constant of the ionophore : cation complex. Substituting these into equation 2-5 gives the simplified

version:

$$\frac{1}{\tau_{M^+in}} = \frac{A.V_m.[L]_T}{V_{in}.(K_m + [M^+])} \qquad \text{Eqn. 2-8}$$

From this equation it can be seen that the process will be first order in ionophore concentration with a rate constant:

$$k_2 = \frac{A.V_m}{V_{in}.(K_m + [M^+])} \qquad \text{Eqn 2-9}$$

It can also be seen that a plot of $1/k_2$ vs $[M^+]$ will have a gradient of $V_{in}/A.V_m$ and an intercept of $V_{in}.K_m/A.V_m$. Therefore, the ratio of slope to intercept is the stability constant of the membrane bound complex.

There are two limiting conditions of the equation depending on whether the diffusion coefficient is small or large with respect to the rate of dissociation.

If $k_{diff} \gg k_d$ then $V_m = k_d/2$

Therefore the slope is proportional to $1/k_d$ and the intercept to $1/k_f$.

If $k_{diff} \ll k_d$, then $V_m = k_{diff}$.

Therefore, the slope is proportional to $1/k_{diff}$ and the intercept to K_m/k_{diff}. If neither of these conditions hold then V_m cannot be simplified so the slope and intercept have a more complex character. Their ratio, however, is always K_s.

It can be seen from the equations that measurement of the lifetime of an ion inside vesicles at a variety of known ionophore

and alkali metal ion concentrations should enable one to calculate the rate constants associated with the transport process. Such measurements were the aim of this work.

The experiments were carried out by growing phosphatidylcholine vesicles with the same metal ion concentration inside and out. The vesicles were prepared by dialytic detergent removal[47] at constant temperature, in this case 40°C. The temperature of the growth medium had been found to be crucial in determining the size of the vesicles.[43] To ensure the reproducibility of the results and to improve the correlation between experiments on different sets of vesicles it was important to use an identical procedure each time. Small changes in the timing of the solution changes and pH of the growth medium could have a large effect on the end product. The A/V_{in} term in the rate equation makes the results directly dependent on the size of the vesicles. If the vesicles were found to be too small or too large they were unsuitable for study. The vesicles used were all in the size range of 10-15% internal volume.

2.3.2 Contrast reagents.

The transport studies were carried out using ^{23}Na, ^{39}K and ^{7}Li nmr. It had been found that the chemical shift and relaxation times of these cations in aqueous solution are largely independent of the counter-ion.[48] Therefore, to generate the necessary contrast between the intravesicular and extravesicular cations an external agent must be used. In this case the method of choice is to use a paramagnetic shift reagent to induce a chemical shift in the external signal with respect to the internal peak. There are a

number of requisites for such a material it must be:

a) Stable

b) Have a negative charge with rapid exchange of the co-ordinating cations

c) Produce a large shift when present in small concentrations

d) It must not penetrate or destroy the vesicles.

The materials used in this work were bis-triphosphate lanthanide complexes. For lithium and sodium the dysprosium complex was used whilst for potassium the lanthanide of choice was terbium. The proposed structures of these complexes are given in Figure 2-9. These complexes fulfil all of the above requirements, they have 7 negative charges with rapid exchange of the co-ordinating cations and they do not rapidly destroy the vesicles. The large charge and size of these complexes precludes their penetrating the phospholipid bilayer and entering the vesicles.

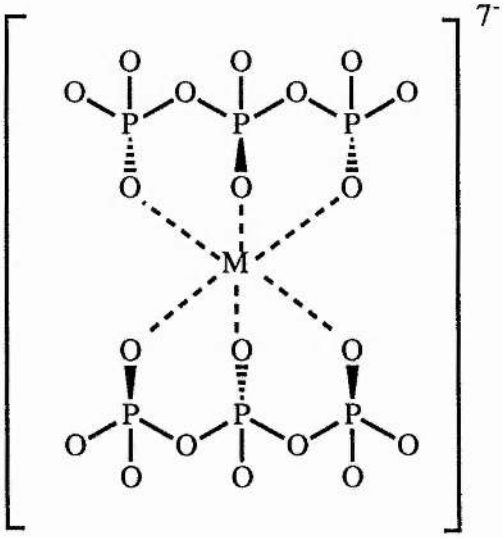

Figure 2-9. The proposed structure of a lanthanide bistriphosphate.

2.3.3 Measurement techniques.

There are a number of ways to measure the rate of exchange across the vesicle membrane using nmr. The three methods used in this work were isotope exchange, magnetisation transfer and dynamic line broadening.

2.3.3.1 Isotope exchange

This method utilises the difference in the resonance frequency of different isotopes of the same element. For this to be possible there must be two stable isotopes of the element in question at least one of which must be nmr active. This is a good method for slow transport rates as the exchange is followed in real time. Therefore, for this method to be effective the transport must be slow with respect to the acquisition time of the spectra. This method was used in the measurement of Li^+ transport using ^7Li nmr with ^6Li as the exchanging species. It is possible to use a different element as the contrasting species, eg Na/Li exchange, but this can affect the result by changing the rate limiting step in the reaction mechanism. The rate is calculated from a plot of $\log(I_t - I_\infty)$ vs t: where I_t is the peak intensity after time t. at constant ionophore concentration. The rate constant k_2 is obtained from a plot of rate vs $[L]_T$. The advantage of this method is that slow rates can be measured so relatively inefficient ionophores can be studied. The disadvantage is that one set of vesicles can only give one point on the rate vs $[L]_T$ plot so it is expensive in both materials and spectrometer time. Typical rates studied by this method fall in the range 10^{-4} to 10^{-5} s^{-1}

2.3.3.2 Dynamic line broadening

This method relies on the coalescence of rapidly exchanging sites into a single peak in the nmr spectrum. This commonly observed phenomenon is schematically represented in Figure 2-10.

Approaching the fast exchange limit the line broadening is proportional to the rate of exchange between the two sites.

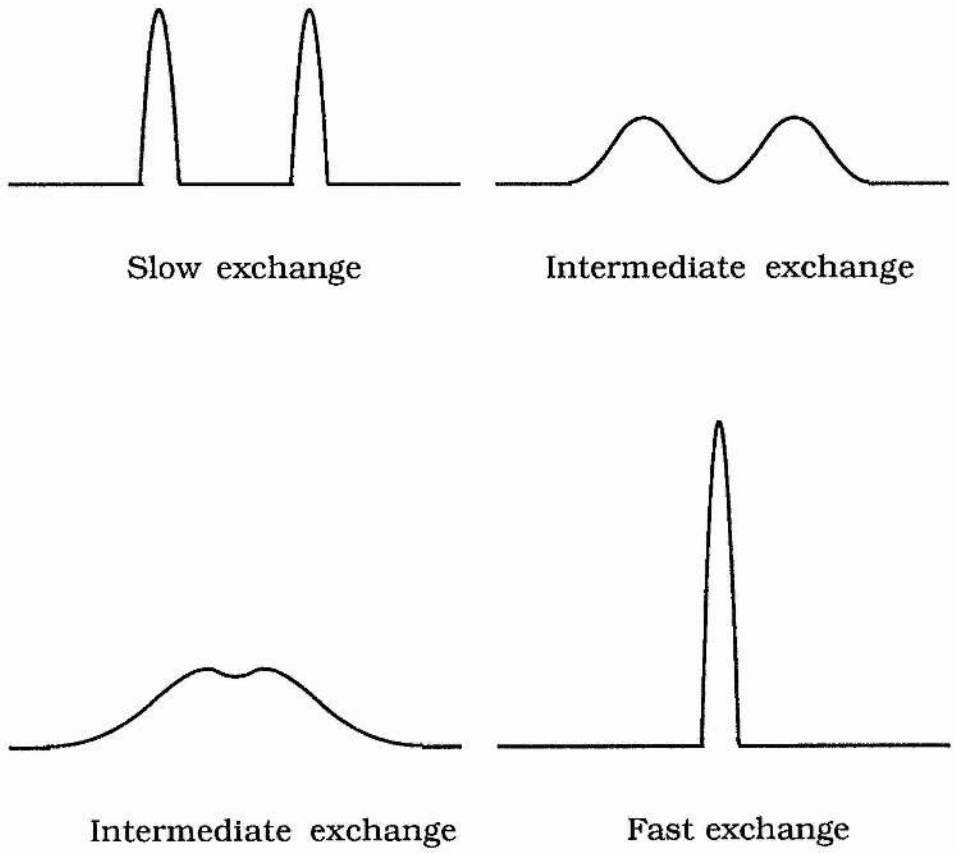

Figure 2-10 a Schematic diagram showing the effect of dynamic line broadening.

Therefore, if one is working under the correct regime then the measurement of line width at different ionophore concentrations enables the graphical calculation of the rate constant. This process requires a good separation of the "in" and "out" signals and can only be used for rapid exchange processes. It is the method of choice for $^{23}Na^+$ and $^{39}K^+$ with the polyether antibiotics. It also has the advantage of being able to calculate k_2 from a single set of vesicles by following the line widths as successive aliquots of ionophore are added. Typical rate constants measured by this method are in the range of 5-100 s^{-1}.[42]

2.3.3.3 Magnetisation transfer

This is a method which uses a three pulse sequence and relies upon inverting the spins at one site, thereby placing a magnetic label there. Chemical exchange then interchanges the two pools of spin of opposite labels (see Figure 2-11).

The rates one is able to measure by this process are dependent on the T_1 of the nucleus in question. To work in a sensible regime this means that nuclei with large T_1's are best. This enables fairly slow rates to be measured before the competing relaxation processes prevent the measurements from being taken. If the relaxation is too rapid there is not enough time for exchange to take place before the peaks have relaxed. This requirement for a long T_1 makes ^7Li an ideal nucleus to study by this method since T_1 in aqueous solution is of the order of 0.5s to 20s depending on the counter-ions, shift reagents, etc. ^6Li has an even longer

relaxation time, up to many minutes in appropriate circumstances, so could, in principle, be used to measure slower rates. In this case one falls foul of the other limitation of this method namely if T_1 is too large the required relaxation time is too long for the spectra to be accumulated at a reasonable rate. The rate constant is worked out by feeding the intensities at different evolution

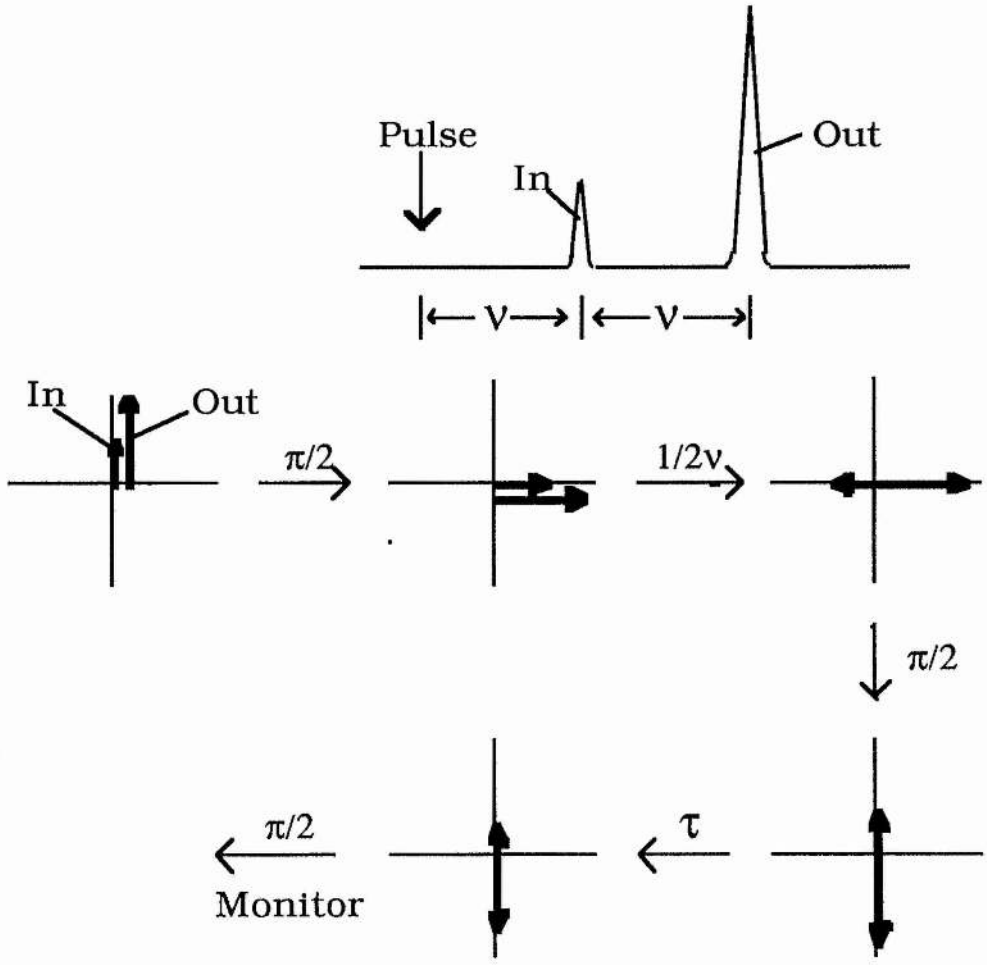

Figure 2-11 The pulse sequence used for magnetisation transfer experiments.

delays (τ) into a curve fitting program which incorporates both the intravesicular and extravesicular relaxation times into the calculation. This means that accurate T_1 values for both sites must be obtained as must the 90° pulse width. There is again the possibility of multiple measurements on the same sample so one set of vesicles is sufficient to calculate k_2 at one cation concentration, although more time is required than for dynamic line broadening. Typical rate constants obtained by this method for the alkali metals ^{7}Li and ^{133}Cs with ionophoric antibiotics are in the range of 10^{-2} to 1 s^{-1}.[45]

2.4. Results and Discussion.

2.4.1 Experimental procedures.

2.4.1.1 Sample preparation.

The methods detailed above all give information about ionophore mediated transport. It has been shown that nmr can be used to study this process in phospholipid vesicles.[42-46] The work in this thesis is a continuation of this to investigate the effect of structure on the transport process. The polyether antibiotics narasin and salinomycin were chosen because they are structurally very similar and are also two of the most widely used and efficient polyether antibiotics in veterinary medicine, see chapter 1 for examples. The system used in these studies was large unilamellar egg yolk-phosphatidylcholine vesicles. These were grown by dialytic detergent removal with the same cation concentration inside and outside the vesicles.

It has been shown[42] that the transport rate is dependent on the average size of the vesicles, which one would expect from the contribution of the surface area and volume components to the rate equation. Direct measurement of the vesicle size is somewhat difficult necessitating the use of electron microscopy. This could not be carried out routinely but previous work using this method[43] had shown that the percentage internal volume of the vesicles is a good indication of the size. This value is easily obtained from the integration of the two peaks in the nmr spectrum. Such measurements were carried out routinely on each set of vesicles before the addition of any ionophore. It was assumed that the size

of the vesicles was accurately reflected by the internal volume. If the vesicles are prepared in the same volume of solution and with the same amount of phospholipid, as was the case here, then this should be a valid assumption. Any set of vesicles with internal volumes falling outside the range of 10-15% were discarded. This measurement is not possible at the start of an isotope exchange experiment, here it is the I_∞ value which gives an indication of the vesicle size.

A typical experiment started with $2cm^3$ of an aqueous suspension containing phosphatidylcholine vesicles which were placed in a 10mm nmr tube. The vesicles were prepared with metal chloride solution inside and usually metal chloride and metal tripolyphosphate outside (for the experiments with potassium pure tripolyphosphate solution was used as the external medium). The metal ion concentration was the same on both sides of the membrane as was the ionic strength, this latter being maintained by the addition of choline chloride. Sufficient dysprosium chloride (Na, Li) or terbium nitrate (K), was added to produce a ca 10 ppm shift for sodium and potassium (only 2-3ppm was required for lithium) which gave a clear area of baseline between the "in" and "out" peaks. It is at this point that the procedure being followed diverges dependent on the method of measurement being used.

2.4.1.2 Dynamic line broadening.

In a dynamic line broadening experiment, which was the quickest and most frequently used technique, the internal volume and width at half height of the internal peak were measured. Then aliquots of the ionophore as a solution in methanol were added and

the line width measured with each addition. The line broadening obtained was then used to calculate a value for the rate of efflux. A typical example of the spectra obtained from such an experiment is given in Figure 2-12. This is plot of the data obtained for salinomycin mediated transport with 100mM potassium chloride.

2.4.1.3 Magnetisation transfer.

The procedure for a magnetisation transfer experiment is a little more complex as the T_1 for both internal and external signals must be measured. This is achieved using the inversion recovery technique which requires an accurate knowledge of the 90° pulse width which often needed measuring anew. An accurate 90° pulse is also required for use in the magnetisation transfer experiments themselves. Once the T_1 and internal volumes have been determined aliquots of an ionophore solution, also in methanol, were added. The pulse sequence detailed above is used and once all the spectra have been collected the internal peak heights at different time delays were measured. These values along with T_1(in) and T_1(out) were fed into a curve fitting programme on the computer which minimises the data using a least squares technique to produce a value of k. Further aliquots of ionophore solution were then added and the experiment repeated for each. An example of the spectra obtained is given in Figure 2-13. This shows clearly the change in intensity of the "in" peak with different relaxation delays. These spectra are those obtained for a salinomycin/phosphatidylcholine ratio of 5.7×10^{-3} in vesicles with 75mM lithium chloride.

Figure 2-12. ^{39}K spectra taken during a dynamic line broadening experiment. These spectra were obtained at 100mM [K^+].

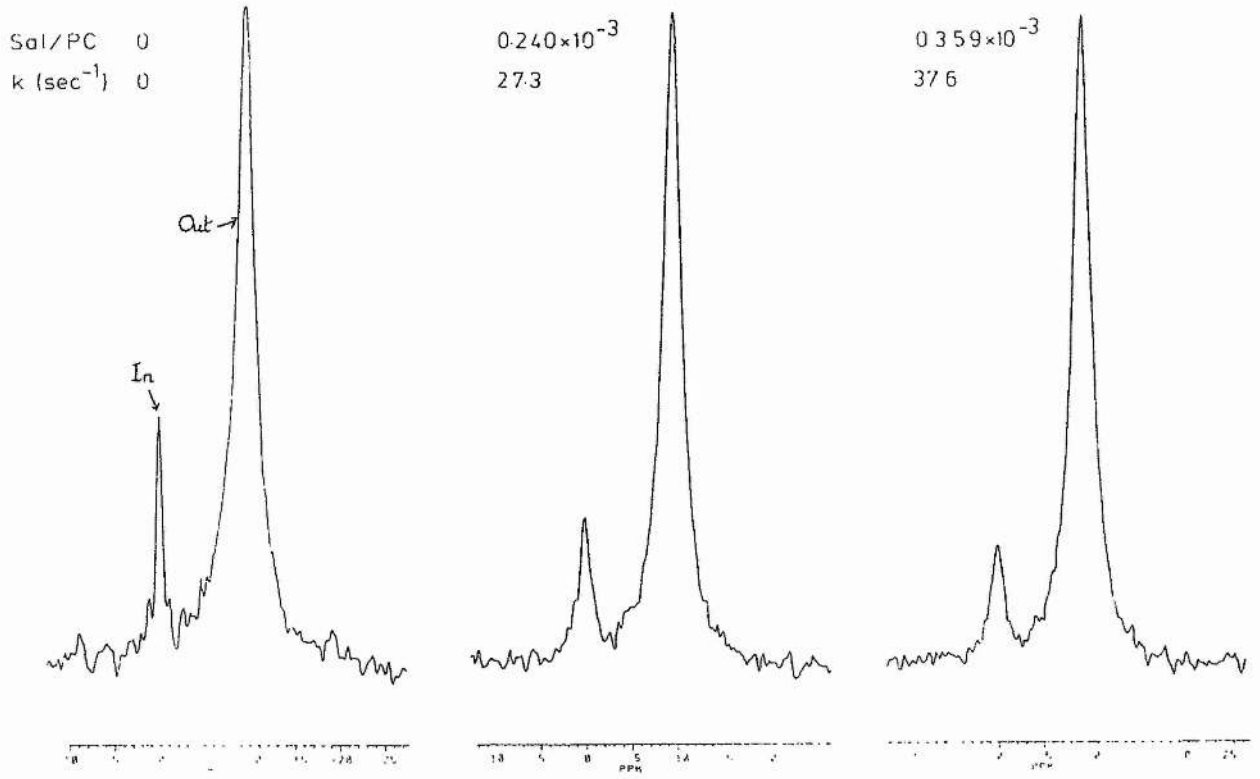

2.4.1.4 Isotope exchange.

The isotope exchange experiments have possibly the simplest procedure. The first step is to prepare vesicles with a different isotope in the extravesicular medium to that inside the vesicles. This was achieved by growing the vesicles in solution of the cation at natural isotopic abundance and changing the extravesicular solution to one enriched in ^{6}Li as a triphosphate/chloride mixture for a short final dialysis, usually for about 2 hours. After the addition of an aliquot of ionophore solution the exchange process is followed in real time by measuring the intensity of the in peak. This decreases as the isotope being observed by the spectrometer is replaced by the nmr invisible isotope originally outside the vesicles. The data are analysed using straightforward kinetic methods applicable to a first order process. A spectrum is obtained before the addition of ionophore to give the initial internal concentration. At time zero the ionophore is added but a spectrum cannot be taken immediately as it takes time to acquire a spectrum to allow the build up of a good signal to noise ratio. The area of the "in" peak is obtained by integration and is usually expressed as a percentage of the area under both peaks. Spectra are acquired at regular intervals after the addition of ionophore. Usually more than a single free induction decay was required to be collected, exactly how many depended on the lithium concentration and the sensitivity of the spectrometer in use. The time of each run is taken to be the midpoint of the acquisition.

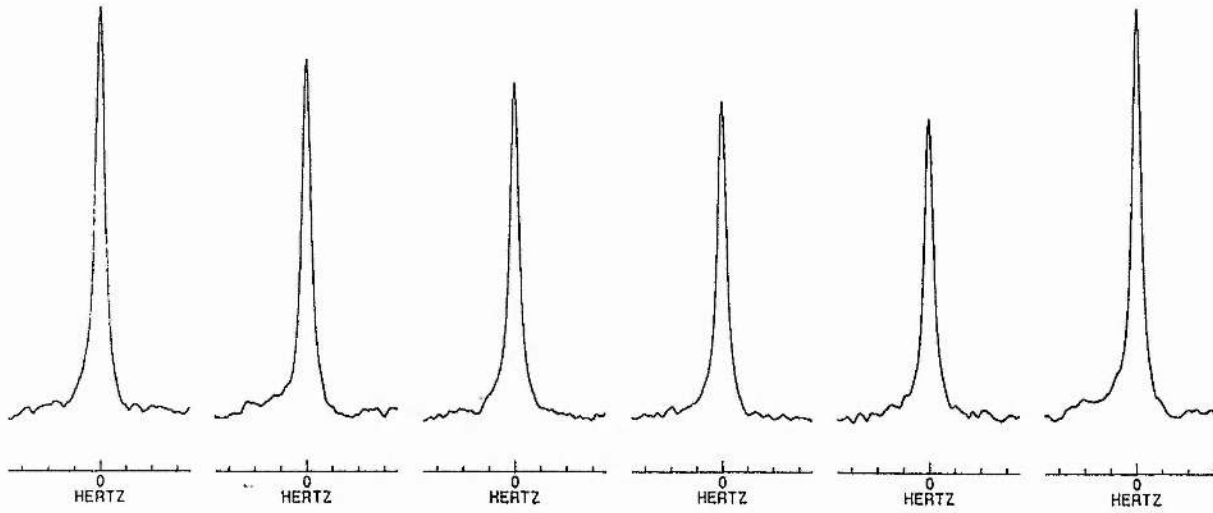

Figure 2-13. ^{7}Li spectra taken during a magnetisation transfer experiment. These spectra were obtained at 75mM [Li^{+}] with an SL/PC ratio of 5.7×10^{-3}.

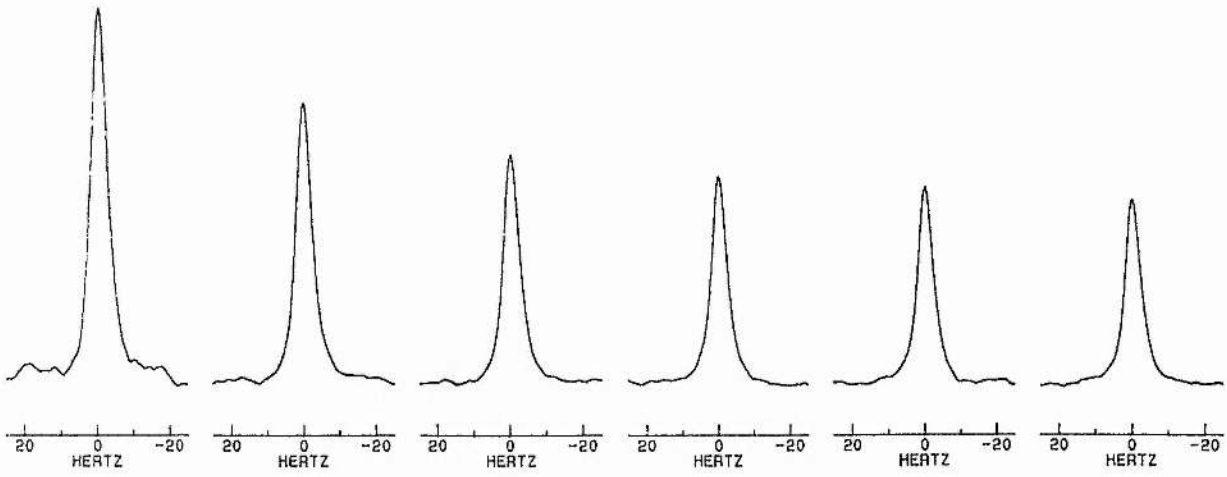

Figure 2-14. ^{7}Li spectra taken during a typical isotope exchange experiment. These spectra were obtained at 100mM [Li^{+}] with an NS/PC ratio of 2.78×10^{-3}.

The limiting factor for rates to be measured by this method was the time taken to accumulate the fid's to give sufficient signal to noise. The problem lies in the large values of T_1(in) for ^7Li (around 13 secs) leading to a relaxation delay of a minute being required. The rate of efflux is obtained by graphical means using a plot of $\ln(I_t - I_\infty)$ vs t. The value of I_∞ was measured after several hours or more commonly after the equilibration was accelerated by the addition of an aliquot of monensin, an ionophore known to mediate lithium exchange on a timescale of less than a minute in these systems. Typical spectra obtained in this experiment are given in Figure 2-14. These are the spectra obtained with a narasin/PC ratio of 2.781×10^{-5} in 100mM lithium chloride and clearly show the loss of intensity of the internal peak with time.

2.4.1.5 Treatment of data.

The procedure for calculating the rate and stability constants (k_f, k_d, and K_s) from the raw kinetic data was the same in each case. This was achieved graphically. Two different graphs were required, the first a plot of $1/\tau_{M^+in}$ vs I/PC ie. the ionophore to phosphatidylcholine ratio. This term, I/PC is used instead of [L]T to normalise between sets of data obtained under different experimental conditions. The gradient of this line is the first order rate constant for efflux, k'. The second graph is a plot of 1/k' vs metal ion concentration. This has a slope of $1/k_d$ and a gradient of $1/k_f$, assuming that the diffusion coefficient is much larger than the dissociation rate constant of the metal/ionophore complex.

2.5 Sodium and Potassium Transport Mediated by Salinomycin and Narasin.

2.5.1 Results.

The results for the ionophore mediated transport of sodium and potassium are given in Tables 2-1 to 2-4. These show a number of interesting features. The values obtained for salinomycin and narasin were somewhat different as might be expected. It was seen that in both cases the potassium transport was faster. This is as expected from the previous experiments carried out on these ionophores (see above). It is of interest to note here that with salinomycin the potassium complex has a higher stability constant than that seen for sodium. It is seen, however, that the more stable complex transports more rapidly which is not the case for any of the other ionophores previously studied using this method.[42-46]

Table 2-1. The rate constants for salinomycin mediated efflux at different sodium concentrations.

$[Na^+](M)$	$k'(mol\ PC.(mol\ SL)^{-1}.s^{-1})$
0.025	2.147±0.250
0.050	2.161±0.038
0.100	1.201±0.018
0.125	1.657±0.044
0.150	1.237±0.035
0.200	1.131±0.019

From these results;

$k'_f = (2.611 \pm 0.277).10^4\ s^{-1}$, $k'_d = (0.425 \pm 0.062).10^4.M.s^{-1}$,

$K_s = 6.1 \pm 1.8\ M^{-1}$.

Table 2-2. The rate constants for efflux for narasin at different sodium concentrations.

$[Na^+](M)$	$k'(mol\ PC.(mol\ NS)^{-1}.s^{-1})$
0.050	0.432±0.093
0.100	0.269±0.010
0.150	0.192±0.005
0.20	0.203±0.007

From these results;

$k'_f = (5.859 \pm 2.229).10^4\ s^{-1}$, $k'_d = (0.535 \pm 0.121).10^4.M.s^{-1}$,

$K_s = 11.0 \pm 8.56\ M^{-1}$.

Table 2-3. The rate constants for efflux for salinomycin at different potassium concentrations.

$[K^+](M)$	$k'(mol\ PC.(mol\ SL)^{-1}.s^{-1})$
0.050	1.179±0.034
0.100	1.068±0.050
0.150	0.860±0.080
0.175	0.524±0.032
0.200	0.561±0.037

From these results;

$k'_f = (28.32 \pm 1.62).10^4\ s^{-1}$, $k'_d = (1.39 \pm 0.30).10^4.M.s^{-1}$,

$K_s = 20.4 \pm 9.5\ M^{-1}$.

Table 2-4. The rate constants for efflux for narasin at different potassium concentrations

$[K^+](M)$	$k'(mol\ PC.(mol\ SL)^{-1}.s^{-1})$
0.050	0.880±0.093
0.100	0.926±0.055
0.150	0.658±0.097
0.200	0.505±0.027

From these results;

$k'_f = (14.7 \pm 3.8).10^4\ s^{-1}$, $k'_d = (1.67 \pm 0.34).10^4.M.s^{-1}$,

$K_s = 8.8 \pm 2.7\ M^{-1}$.

In all cases k'_f and k'_d are calculated assuming that diffusion is not the rate limiting step.

Figure 2-15. Graph showing the linear relationships between k^{-1} and $[M^+]$ from which the values of k'_f and k'_d are obtained, assuming that diffusion is not the rate limiting step.

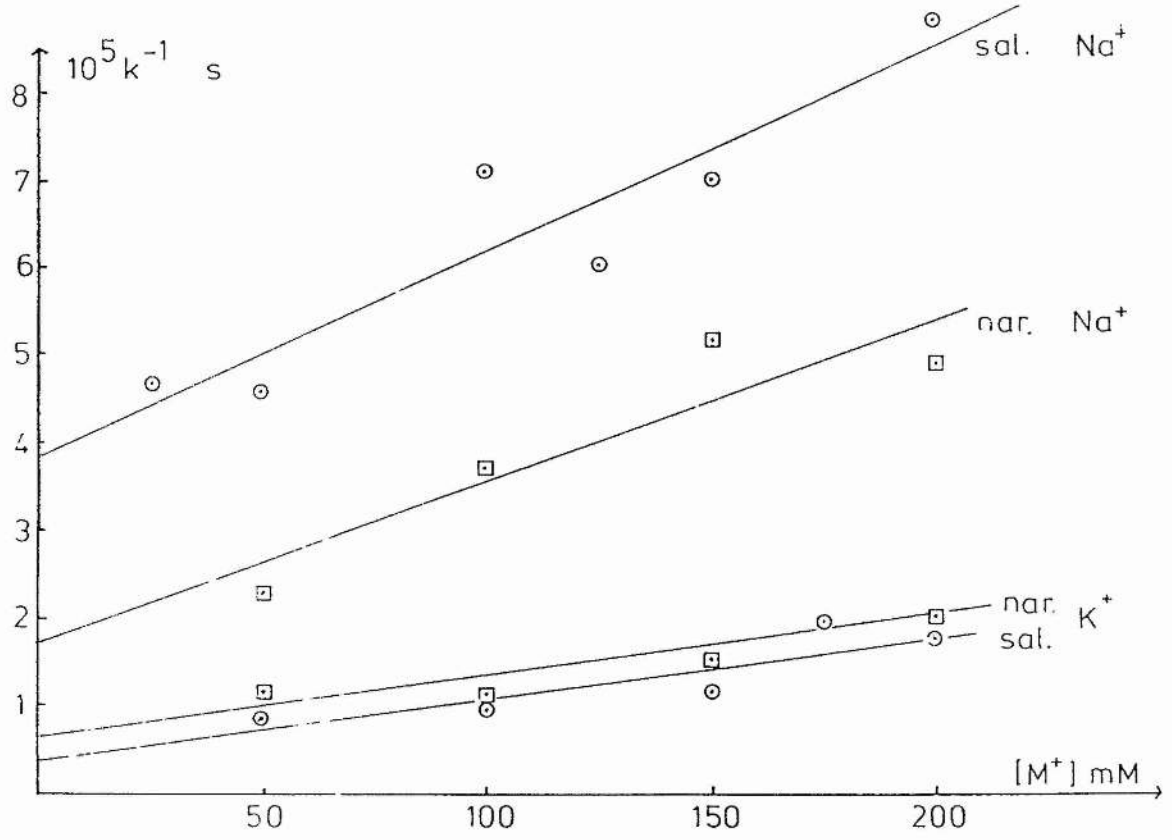

2.5.2 Discussion

The most basic fact which strikes one from these data is that the transport occurs via a 1:1 metal/ionophore complex. This is demonstrated by the linearity of the transport rates vs $[L]_T$ for both salinomycin and narasin, thus showing that transport is first order with respect to ionophore. The linearity of the graph of 1/k' vs $[M^+]$ is in agreement with the process also being first order in metal ion, providing strong evidence for a 1:1 complex (see Figure 2-15).

There are two types of preferences shown by these materials, one is thermodynamic preference, shown by the stability constant of the complex. The other is kinetic preference which is given by the values for the rate constants of the transport process. It is important to distinguish between these two properties. In the data reviewed above the selectivity sequences are thermodynamic preferences and the transport sequences the kinetic preferences. These are not necessarily the same.

Previous studies to determine the ion preference of narasin have produced inconclusive results. The preference exhibited depends upon the system being studied. In erythrocytes potassium is preferred over sodium[36] but the opposite preference is seen in rat liver mitochondria.[35] The results presented here show a kinetic preference for potassium. The kinetic preference is not as great as that seen for potassium with salinomycin, as the lines are closer together. This possibly explains the inconclusiveness of the previous evidence. It is also of interest to

note that in erythrocytes[36] the preference of narasin for sodium over potassium was much greater than that exhibited by salinomycin.

The thermodynamic selectivity is also not as great as for salinomycin as the stability constants of the sodium and potassium complexes are similar. It is seen in fact that the sodium complex is slightly more stable than that formed with potassium.

Not only do these data show the ion preference of the ionophores they also demonstrate where the major difference in the transport occurs. Examination of the graph shows that the lines of one cation with both ionophores are roughly parallel with different intercepts. There are a number of possible explanations for this phenomenon. One is that diffusion has become rate determining. In this case the slope would be proportional to $1/k_{diff}$. The ionophores themselves are of a very similar size and one would expect the complexes with the same cation to be so as well. This would produce roughly parallel lines, as is the case here, but would not explain why the slopes given by the sodium data and those seen for potassium are different. The sodium and potassium complexes of the same ionophore would be expected to be of similar size with the sodium complex if anything the smaller, and certainly the lighter, of the two. This would not explain why the sodium complex for a given ionophore should have a gradient roughly three times that seen for the potassium ionophore. Thus it can be safely said for the sodium complex at least that diffusion is not rate determining. The case for the potassium complexes is less clear cut. These show a transport rate higher than any other

ionophore so far studied by this method so the possibility of rate limiting diffusion cannot be discounted. As was mentioned in the introduction to this chapter whether or not diffusion or dissociation are the dominant expressions in the equation, or even if they are roughly equal, the ratio of slope upon intercept is always the value for the stability constant of the complex.

Table 2-5. The dissociation, formation and stability constants for several naturally occurring ionophores with sodium and potassium.

	Sodium			Potassium		
Ionophore	k'_f ($10^4 s^{-1}$)	k'_d ($10^4 Ms^{-1}$)	K_s (M^{-1})	k'_f ($10^4 s^{-1}$)	k'_d ($10^4 Ms^{-1}$)	K_s (M^{-1})
M139603	20.52	0.855	24.0	5.65	0.804	7.03
Monensin	4.878	0.150	32.6	2.30	0.433	5.3
Nigericin	7.838	0.352	22	9.61	0.0997	96
Salinomycin	2.611	0.425	6.1	28.32	1.39	20.4
Narasin	5.859	0.535	11.0	14.7	1.67	8.8

The difference between the intercepts for salinomycin and narasin with sodium must therefore have a different significance. This is that the formation rates of the complexes must be different and the dissociation rates similar. It can clearly be seen from the figures that k'_f for sodium narasin is roughly twice that for sodium salinomycin (5.86×10^4 s^{-1} vs 2.61×10^4 s^{-1}) but the values for k'_d are comparable (0.545×10^4 Ms^{-1} and 0.425×10^4 Ms^{-1} respectively). Why should the formation rate of these complexes be different but the dissociation rates stay the same? The only structural difference between the two ionophores is an additional methyl group at C(4) in narasin. This therefore must play a part in the observations. If models of salinomycin and narasin are constructed it can be seen that the key difference is a reduction in

the conformational freedom about the C(2) - C(3) bond (see Figure 2-5) caused by the addition of a methyl at C(4). Is this the reason behind the observed difference?

The first approach of a cation must be to the carboxylate moiety of the polyether antibiotic as this is the portion of the structure which protrudes from the membrane into the aqueous solution.[36] It is however believed[49] that the carboxylate oxygen does not play any part in the binding of the metal ion in the stable complex. Instead it is hydrogen bonded to the hydroxyl group at the other terminus. Is it possible that the first approach or subsequent rearrangement of the cation inside the complex leads to this difference in the complexation process? In narasin the carboxyl group has highly restricted rotation due to the steric hinderance of the γ-methyl substituent. It is possible that the sodium ion is held in the correct position for facile further complexation. It must be remembered that the formation of the complex is a multistep process, probably occuring by sequential substitution of water molecules complexed to the metal ion.[37] If however the sodium was sterically fixed in the correct position the formation should be more rapid than for a more mobile ion pair.

In potassium transport the opposite behaviour is seen. Here it is the case that the rate of formation of the salinomycin complex is more rapid than is seen for the narasin complex, assuming of course that diffusion is not the rate limiting step. Both rates are however faster than those seen for sodium. This could be due to the larger size of the potassium ion which would require greater flexibility to accommodate it. In this case the problem would

probably be due to the relative difficulty of the subsequent complexing sites being able to approach the cation sufficiently closely to be able to dislodge the solvent.

Thus small changes in the structure can cause noticeable changes in the complexation rates. This makes the causes of such effects very difficult to identify. Overall the formation rates of the potassium complexes are greater than the formation rates of the sodium complexes for both ionophores.

The thermodynamics of the process can be quantified by calculating the Gibbs free energy (ΔG) of the complexation reactions. For this one uses the equation

$$\Delta G = -RT\ln K_e \qquad \text{Eqn. 2-10}$$

Where K_e is the equilibrium constant

In this case the equilibrium constant is given by the stability constant of the complex (K_s) divided by an arbitrary standard state which cancels the dimensions. This arbitrary state need not be defined as here we are concerned solely with the differences between the free energies of the complexes. This means that the standard state itself is cancelled.

The values obtained from this treatment are given in Table 2-6 and show only small differences in the free energy of formation. In the case of sodium there is a 1.5 kJ mol^{-1} energy difference in the favour of narasin. This is much less than the energy of rotation of a single bond and possibly indicates a greater degree of twist about the C(2)-C(3) bond is required in

salinomycin. In the potassium case the free energy difference is 2kJmol^{-1} in favour of the salinomycin complex. This shows that a smaller conformational change is required for the potassium salinomycin complex to be formed than for the narasin complex. This may imply that the conformation of the carboxylate ion of salinomycin is closer to that found in the potassium complex than is the case for narasin. The carboxylate anion of narasin is in a conformation more like that of the sodium complex than is the case in salinomycin.

Table 2-6. Free energy of formation of the complexes of salinomycin and narasin. These are relative to an arbitrary standard state.

Salt	ΔG kJmol^{-1}
Sodium salinomycin	4.48
Sodium narasin	5.94
Potassium salinomycin	7.47
Potassium narasin	5.39

It is also possible to compare in this way the complexes of narasin and salinomycin with different cations. In this case the free energy difference between sodium salinomycin and potassium salinomycin is 3 kJmol^{-1} in favour of the potassium complex. This implies that the potassium salt requires less conformational adjustment on formation than the sodium complex as it is nearer to the lowest energy conformation. In narasin the sodium complex has a lower energy of formation than the potassium salt but only by 0.5 kJmol^{-1}. This reflects little overall difference in the conformation between these two complexes.

The free energy values obtained are of course overall values ie. they include all the energy changes in the molecule. This means that they reflect changes of energy in the complex as a whole. It is possible that conformational changes at one site are offset by further alterations elsewhere in the molecule. Thus it is possible that an increase in free energy at one place is partially nullified by a concurrent decrease at another site in the molecule. These alterations of free energy due to torsional changes at one bond are not readily elucidated by chemical means.

The ideal way to calculate the diffusion coefficient of these materials through a phospholipid bilayer would be to compare the values obtained for a range of ionophores. If a larger number of ionophores of similar size were studied with different cations and observed to have similar gradients this would be good evidence that diffusion was the controlling step. This would make the measurement of k_{diff} as easy as finding the gradient of a straight line. Unfortunately the diffusion limit has not been approached by sufficient ionophores to make this a feasible method, so an alternative way of checking that diffusion is not rate limiting has to be found.

In this case whether or not diffusion is rate limiting can be found by feeding the data obtained from the graphs back into the overall equation. If the potassium transport is diffusion controlled then there must be an appreciable diffusion contribution to the rate of sodium transport.

The overall transport is given by the equation

$$\frac{1}{k} = \frac{K_m}{V_m} + \frac{[M^+]}{V_m} \qquad \text{Eqn 2-11.}$$

where

$$Vm = \frac{k_d.k_{diff}}{(k_d+2k_{diff})} \qquad \text{Eqn 2-7.}$$

and

$$Km = \frac{k_d}{k_f} \qquad \text{Eqn 2-6.}$$

So if $k_d \gg k_{diff}$ then $V_m = k_{diff}$

In this case the gradient of a plot of 1/k vs $[M^+]$ will have a gradient of $1/k_{diff}$. Assuming that this is the case for potassium transport and that the diffusion constants are the same for the sodium and potassium complexes gives a value of $1.5 \times 10^4 s^{-1}$ for k_{diff} which can be substituted into equation 2-9 such that:

$$\text{Slope} = \frac{(k_d + 2k_{diff})}{k_d.kdiff} \qquad \text{Eqn 2-12.}$$

and

$$\text{Intercept} = \frac{k_d.(k_d + 2k_{diff})}{k_f.k_d.k_{diff}} \qquad \text{Eqn 2-13.}$$

The first of these enables a value to be obtained for k_d.

$$k_d = \frac{2}{(\text{slope}-(1/k_{diff}))} \qquad \text{Eqn 2-14}$$

which can then be substituted into the second equation to calculate a value for k_f.

$$k_f = \frac{(k_d+2k_{diff})}{\text{intercept}.k_{diff}} \qquad \text{Eqn 2-15}$$

If this is a valid procedure then the ratio of k_f/k_d should

match the value of K_s obtained graphically. In this case the calculated values are given below in Table 2-8.

Table 2-8. The calculated and actual values of K_s for Na^+.

	k_f^c ($10^4 s^{-1}$)	k_d^c ($10^4 Ms^{-1}$)	K_s^c (M^{-1})	K_s^a (M^{-1})
Salinomycin	5.74	1.19	4.8	6.1
Narasin	13.32	1.66	8.02	11.0

The values of K_s are roughly two thirds of those expected. Thus implying that one of the assumptions was invalid. It is probably incorrect to assume that the potassium tranport is completely governed by diffusion, but the values are close enough to make a diffusion contribution to the gradient a possibility.

The thermodynamic stability of the metal/ionophore complex does not have a great effect on transport in a system like ours. The transport rates here are determined by the kinetic parameters k_f, k_d and k_{diff}. The stability constant of the complex is derived from the ratio of k_f and k_d but it is only of significance in transport if the complex is so stable that the cation is never released or so unstable that the complex is never formed. In a competition experiment, however, the stability of the complex can be of key importance. If a lot of the ionophore is sequestered in the membrane as a stable complex of one of the competing ions it cannot also be transporting an ion of the other type. This means that the concentration of ionophore involved in transporting the more stable complex will be high and the more rapidly transported ion will only have a low concentration of ionophore with which to complex.

2.5.3 The effect of structural changes on the transport abilities of salinomycin.

Miyazaki et al had published a study of the effect of structural modification on the transport and antimicrobial properties of salinomycin.[29] This was an attempt to see how changes affected the transport as seen in our system. Some transport studies were made on dihydrosalinomycin and it was also attempted to make C(20) keto salinomycin.

These compounds were prepared from the sodium salt of salinomycin using the methods of Asukabe et al.[50] Dihydrosalinomycin (DSL) was prepared by hydrogenation of salinomycin over a palladium-carbon catalyst. The preparation of 20-ketosalinomycin was attempted unsuccessfully by oxidation with pyridinium chlorochromate. The samples were identified using HPTLC and ^{1}H nmr. There was also only one spot in the TLC of the sample of dihydrosalinomycin. This and the loss of the distinctive vinylic protons in salinomycin showed that reduction of the double bond had been successful.

A number of studies in phosphatidylcholine vesicles were attempted, using both ^{23}Na and ^{39}K nmr. These used the dynamic line broadening experiment above. Only one of these studies, at 200 mM sodium concentration, was successful. The others all showed initial broad lines. This meant that there was either no further line broadening seen, or the lines merged before a sufficient number of experiments could be carried out. The data obtained was a value for the rate of efflux at 200mM sodium. This

is given in Table 2-9 where it is compared with that seen for salinomycin under the same conditions.

Table 2-9. Comparison betwen the transport rates of salinomycin and dihydrosalinomycin at 200 mM sodium concentration.

	Dihydrosalinomycin	Salinomycin
Rate of efflux (s^{-1})	6.145 ± 0.200	11.310 ± 0.198

From these data it can be seen that dihydrosalinomycin transports sodium ions at about half the rate of salinomycin. This agrees with the previously published work[29] that reducing the vinylic function decreases the activity of salinomycin.

2.6 Lithium transport with salinomycin and narasin.

Using magnetisation transfer and $^{6}Li/^{7}Li$ exchange it is possible to study the rate of ionophore mediated lithium transport through phospholipid bilayers. This is a preliminary study of the rates of transport of Li^{+} mediated by salinomycin and narasin in phosphatidylcholine vesicles.

2.6.1 A comparison between magnetisation transfer and isotope exchange.

The aim of this work was to measure the transport rates and calculate stability, formation and dissociation complexes of the lithium complexes with salinomycin and narasin as had been done for the sodium and potassium complexes.[38] We were also interested in the comparison of the rates obtained using magnetisation and isotope exchange experiments. Would these

procedures, the former an exchange of nuclei with different magnetisations and the latter an exchange of nuclei with different masses produce the same results?

The comparison of magnetisation transfer with isotope exchange was carried out at 100mM [Li^+] with narasin as the ionophore. The vesicles were grown using the same method as given above and the experiments were carried out at 25°C as usual. The results are given in Table 2-10.

Table 2-10. Comparing the values obtained for narasin mediated lithium transport by different methods.

Experiment	Magnetisation transfer	Isotope exchange
Rate constant/s^{-1}	77.1 ± 0.99	19.96 ± 0.69

There is a qualitative agreement between the rate constants obtained but the values are seen to differ by a factor of four, the isotope exchange producing the more rapid rate. There are important differences in the experimental procedure which may account for this deviation. One is that a different set of vesicles are used for each measurement when using isotope exchange as the method of study. In measurements by magnetisation transfer only one set of vesicles are used. This means that there is an extra possibility of error in the former method. If the vesicles are not all the same size, which was the case here, or have different size distributions then the rates will be different. This reduces the correlation between experiments run on different sets of vesicles and explains the much larger percentage error seen for the isotope exchange experiments. The other problem lies in the difference in ionophore concentration used. There was a 200 fold

difference in the ionophore/PC ratio used in the two experiments, with the isotope exchange the more dilute. This would magnify any errors in the preparation of the ionophore solution and its addition to the experimental medium. The data for the isotope exchange takes into account the passive transport of lithium across the vesicle membranes. This was measured by running an experiment with no ionophore added and was seen to have a rate of $2.25 \times 10^{-5} s^{-1}$.

2.6.2 A comparison of salinomycin and narasin to other naturally occuring polyether antibiotics.

Magnetisation transfer experiments were carried out at a range of cation concentrations to try to determine the stability, dissociation and formation constants of the ionophore / lithium complexes. This was attempted for both salinomycin and narasin but unfortunately the data were insufficiently reproducible to allow values for these constants to be obtained. The data was sufficiently good, however, to give some idea of the rate and compare it to the known values for M139603 (see Figure 2-16),[46] monensin,[45] nigericin[51] and some synthetic ionophores which had been studied by other members of the group.[52,53] The transport rates are given in Table 2-11. From these data it is possible to see that salinomycin and narasin both give rates in the same region (20-80 s^{-1}) with salinomycin possibly the faster. This would be borne out by the difficulty we, and Caughey et al,[54] found in preparing a stable sample of lithium narasin for study by 2D nmr, see chapter 3. The transport data is insufficiently good to be sure.

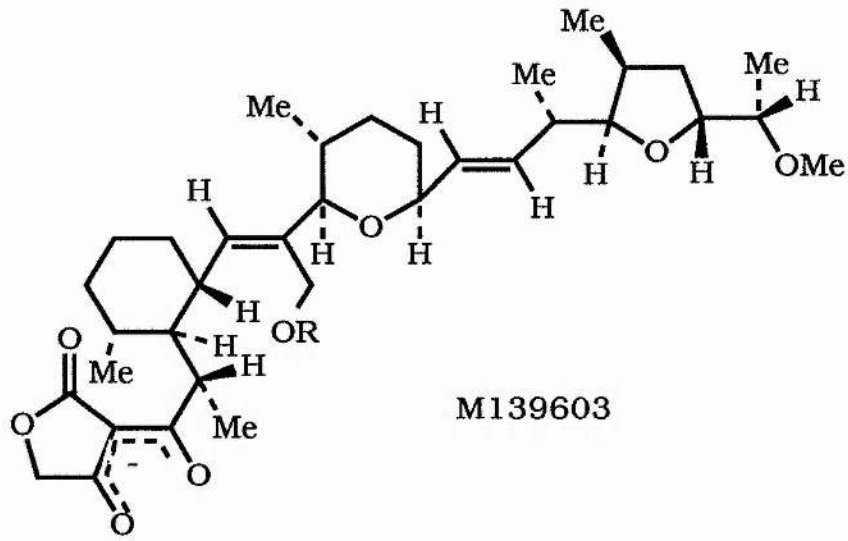

M139603

Figure 2-16. The structure of M139603.

It is obvious however that the transport rates for lithium are a lot slower than those seen for sodium and potassium. There is a difference of roughly three orders of magnitude in the observed rates. This is as would be expected from the previous studies on salinomycin and narasin which have all observed a much lower lithium preference for these materials. This is the first study in phospholipid membranes to demonstrate lithium transport with either of these two ionophores.

Table 2-11. The rate constant for efflux at 100mM cation concentration.

	LiSL	LiNS	NaSL	NaNS	KSL	KNS
$k'(s^{-1})$	31.7	19.96	12010	29100	106800	92630

It is interesting to compare these results with those obtained with a number of different ionophores with the same system. The first type of ionophore to consider is the naturally occurring polyether antibiotics, three of which have been studied using our system namely M139603, monensin and nigericin. Of

these M139603 and monensin are sodium selective ionophores and the other is potassium selective. The observed transport rates for lithium show, as might be expected that the former pair are more efficient lithium ionophores than any of the latter group. The rates of exchange, at 100mM lithium are given in Table 2-12.

Table 2-12. Typical values of rate constants for lithium transport mediated by naturally occuring polyether antibiotics at 100mM [Li^+].

Ionophore	M139603	Monensin	Nigericin	Salinomycin	Narasin
k (s^{-1})	2402	339	25.3*	31.7	19.96 77.1*

The values denoted * are from isotope exchange experiments, all others are derived from magnetisation transfer experiments.

The transport rates of all these ionophores are much lower for lithium than for sodium and potassium. The size of the cavity in the lowest energy form of the ionophore is obviously of key importance, the less adjustment required for complexation to occur, the more efficient the transport process will be. So the ionophores with a larger cavity, eg nigericin or salinomycin, will select large cations like potassium or rubidium, whereas those with a smaller cavity, eg. monensin or M139603, will be better able to complex with a smaller cation like sodium or lithium.

2.6.3 A comparison of salinomycin and narasin to synthetic lithium ionophores.

The synthetic ionophores studied were three very similar materials, Figure 2-17.

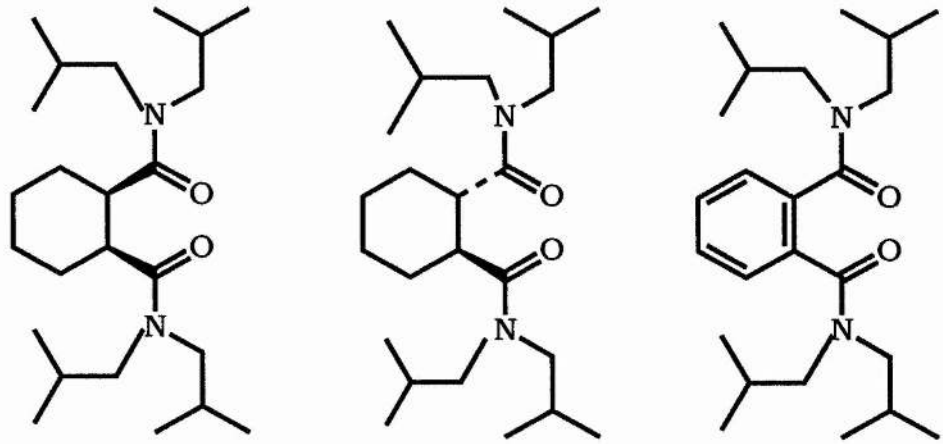

Ionophore 1 Ionophore 2 Ionophore 3

Figure 2-17. The structures of three synthetic lithium ionophores.

The results of this work show that these are much less efficient ionophores than the naturally occuring ones. Exact quantification of the differences is difficult as these materials do not transport with first order dependence on the ionophore concentration. The results measured at 100mM lithium are given in Table 2-13.

Table 2-13. Comparison of the rate of efflux obtained for narasin and three lithium ionophores at 100mM [Li^+].

Ionophore	Narasin	Ionophore 1	Ionophore 2	Ionophore 3
I/PC (10^4)	0.278	6.47	66.4	55.1
Rate ($10^4 s^{-1}$)	21.1	14.9	5.17	1.31

Here narasin is first order, ionophores 1[54] and 2 second order and ionophore 3, 0.54 order with respect to the ionophore concentration.[53] Narasin can be seen to give a higher rate than its nearest rival, ionophore 1, even though present at only 4% of the concentration of the latter ionophore. Even without taking the second order dependance of the exchange mediated by the latter into account this is nearly a 200 fold increase in the rate. There is another order of magnitude between this and the other two ionophores.

So in conclusion narasin and salinomycin are, for naturally occuring polyether antibiotics, relatively inefficient lithium ionophores. Even so they still give transport rates several orders of magnitude greater than those for the synthetic ionophores which were examined.

2.7 Experimental.

The phospholipid vesicles were grown using the general method below for all experiments with different concentrations of salt solutions. The spectra were measured on Bruker WP80 spectrometers at Stirling and St Andrews (Na) and on the Bruker AM 300 spectrometer at St Andrews (Na, K, and Li). The WP80 required only 1.5 cm^3 of vesicle suspension with 2 cm^3 used for the AM 300, the phospholipid was always at about 15mM concentration. The egg yolk phosphatidylcholine (EPC) was purchased from Lipid Products as a solution in chloroform/methanol. The salinomycin was kindly donated by Hoechst AG as the sodium salt and the narasin by Eli Lilly Inc. as the free acid. Both were used without further purification. The n-octylglucopyranoside was purchased from Sigma and Aldrich Analar grade materials were used for all other. All dialyses were carried out under nitrogen. Distilled water was used throughout. Ionophore 1 was prepared by Miss F. McMillan, ionophores 2&3 were prepared by Miss H. Forbes.

The preparation of phosphatidylcholine vesicles.

EPC solution 344 µl (258 µl) was measured into a weighed clean round bottomed flask and the solvent evaporated under vacuum (< 0.1 mbar) for at least 3 hours. n-Octylglucopyranoside 160 mg (130 mg) was dissolved in 2 cm^3 (1.5 cm^3) of a standard solution of MCl at the required concentration. This solution was then added quantitatively to the weighed EPC and stirred carefully

to avoid foaming in a stoppered flask for about one hour at room temperature until the lipid had completely dissolved. 2.0-2.5 dm^3 of the standard MCl solution were preheated to 40°C and flushed with nitrogen for ~12h. before being transferred to a thermostatically controlled dialysis vessel at 40°C under nitrogen. The lipid solution was transferred quantitatively into a piece of presoaked dialysis tubing which was sealed and placed in the dialysis vessel. The dialysis solution was changed every 12 hours. Each time the new solution was preheated and flushed with nitrogen for 12 hours. After 36 hours of dialysis the external solution was changed to one containing triphosphate. The exact method varied depending on the cation under study but the solution was always of the same cation concentration as the chloride solution. The ionic strength was maintained by the addition of choline chloride. The following numbers are all for 100mM solutions in the cation for other concentrations simply multiply by the correct factor.

For sodium the mixture would consist of 50 mM NaCl, 10 mM $Na_5P_3O_{10}$ and 20 mM choline chloride. The vesicles would be dialysed against 2.0-2.5 dm^3 of this twice for 12 hours at 40°C under nitrogen.

For potassium the mixture would be 20 mM $K_5P_3O_{10}$ and 40 mM choline chloride. The vesicles were dialysed against 300 cm^3 of this solution twice for 12 hours at room temperature under nitrogen.

For ^{7}Li the mixture would be 50mM LiCl 10 mM $Li_5P_3O_{10}$ and 20 mM choline chloride. Dialysis was carried out against 20 cm^3 of this solution twice for 12 hours at room temperature under nitrogen.

For ^{6}Li the mixture was the same but the final dialyses were carried out twice for 1.5 hours at room temperature under nitrogen against 20 cm^3 of solution.

The $Li_5P_3O_{10}$ was prepared by titrating LiOH against tripolyphosphoric acid obtained by running sodium tripolyphosphate solution down a cation exchange column charged in the H^+ form. The end point pH 7 was found using a pH electrode. $^{6}LiCl$ was prepared by titrating $^{6}LiOH$ with HCl again to pH 7.

The vesicles were transferred quantitatively to a 10mm nmr tube. The lock signal was obtained from a 4mm coaxial insert of D_2O. The shift difference was obtained by the addition of sufficient aqueous 1M $DyCl_3$ (for Na) 100mM $DyCl_3$ (for Li) or 1M $Tb(NO_3)_3$ (for K) to give a clear baseline between the peaks. The quantity needed depended on the cation concentration and was typically a few microlitres of a 1M solution (sodium and potassium) or of a 100 mM solution for lithium.

The ionophore was used as a standard solution in HPLC grade methanol. Typical concentrations were $5x10^{3}M$ and aliquots were of 0-10 microlitre amounts i.e. picomoles.

Preparation of dihydrosalinomycin.[50]

Sodium salinomycin (110mg) was dissolved in methanol ($5cm^3$). To this solution palladium-carbon catalyst (20 mg) was added. The mixture was stirred under hydrogen for 36 hours at room temperature and the catalyst removed by filtration. The ethanol was removed by distillation at reduced pressure. The HPTLC plate of the final product showed a single spot at a position slightly different to that of salinomycin. The ^1H nmr spectrum of this material was seen to be lacking the vinylic peaks, although the rest of the spectrum looked the same.

References to Chapter 2.

[1]Pressman, B.C., *Ann. Rev. Biochem.* (1976), **45**, 501-530.

[2]e.g. Mollenhauer, H.H., Morre, D.J. and Rowe, (1990), L.D., *Biochim. Biophys. Acta.*, **1031**, 225-246.

[3]Taylor, R.W., Kauffman, R.F. and Pfeiffer, D.R. (1982) in *Polyether Antibiotics* , Westley, J.W. (Ed), Marcel Dekker, New York. pp 103-184. This is a good review of all the transport work done uptil 1981.

[4]Harrison, R. and Lunt, G.G., (1975), *Biological Membranes, Their Structure and Function*, Blackie & Son, Glasgow.

[5] For three determinations of pK_a for monensin see: a) Gertenbach, P.G. and Popov A.I., (1975), *J. Am. Chem. Soc.*, **97**, 4738-4744. b)Agtarap, A., Chamberlin, J.W., Pinkerton, M. and Stainrauf, L.K.(1967), *J. Am. Chem. Soc.*, **89**, 5737-5739. c)Pressman, B.C.(1973), *Fed. Proc.*, **32**, 1698-1703.

[6]de Ligny, C.L., Luykx, P.F.M., Rehbach, M. and Wieneke, A.A. (1960), *Recl. Trav. Chim. Pays-Bas.*, **79**, 699-730.

[7]Hoogerheide, J.G. and Popov, A.I., (1978), *J. Solution Chem.*, **7**, 357-372.

[8]Chock, P.B., Eggers, F., Eigen, M. and Winkler, R. (1977), *Biophys. Chem.*, **6**, 239-251.

[9]Krishnan, C.V., Friedman, H.L. and Springer, C.S., Jr. (1978), *Biophys. Chem.* **9**, 23-25.

[10]Lutz, W.K., Wipf, H.K. and Simon, W. (1970), *Helv. Chim. Acta.*, **53**, 1741-1746.

[11]Pfeiffer, D.R., Hutson, S.M., Kaufman, R.F. and Lardy, H.A. (1976), *Biochemistry*, **15**, 2690-2697.

[12]Cornelius, G., Gaertner, W. and Haynes, D.H. (1974). *Biochemistry*, **13**, 3052-3057.

[13]Degani, H., Friedman, H.L., Navon, G. and Kosower, E.M. (1973), *J. Chem. Soc. Chem. Commun.*, **1973**, 431-432.

[14]Pressman, B.C. (1973), *Fed. Proc.* **32**, 1698-1703.

[15]Pressman, B.C., Harris, E.J., Jagger, W.S. and Johnson, J.H. (1967), *Proc. Nat. Acad. Sci. USA..*, **59**, 1949-1956.

[16]Cox, B.G, Firman, P. and Schneider, H., (1985), *J. Amer. Chem. Soc.* ,**107**, 4297-4300.

[17]Knoche, W. (1974), In. *Techniques of Chemistry*, vol. **6**, pt. 2, Hammes, G.G.(Ed), Wiley-Interscience, New York. pp 187-210.

[18]Jost, A. (1966), *Ber. Bunsenges. Phys. Chem.*, **70**, 1057-1060.

[19]Eigen, M. and DeMaeyer, L. (1963), In *Techniques of Organic Chemistry*, vol. **8**, pt. 2, Friess, S.L., Lewis, E.S. and Weissberger, A. (Eds). J. Wiley and Sons. New York.pp. 895-1054.

[20]Pressman, B.C. and deGuzman, N.T. (1974)m *Ann. N.Y. Acad Sci.*, **227**, 380-391.

[21]Amman, D., Bissig, R., Guggi, M., Pretsch, E., Simon, W., Borowitz, J. and Weiss, L., *Helv Chim Acta.*, **58**, 1535-1548.

[22]Johnson, D. and Lardy, H.A. (1967), In *Methods in Enzymology.* Estabrook, R.W. and Pullman, M.E. (Eds), vol. **10**, Acad. Press. pp. 94-96.

[23]e.g. Painter, G.R. and Pressman, B.C. (1983) in *The Biochemistry of Metabolic Processes* , Lennan, D.L.F., Stratman, F.W. and Zahlten, R.N. (Eds), Elsevier, Amsterdam. pp 41-54.

[24]e.g. Sharvit, N. and Pietro, A.S. (1967), *Biochem. Biophys. Res. Commun.*, **28**, 277-283.

[25]e.g. Katoh, K. and Tsuda, T. (1986), *Res. Vet. Sci.*, **41**, 207-210.

[26]Pfeiffer, D.R., Taylor, R.W. and Lardy, H.A. (1978), *Ann. NY. Acad. Sci.*, **307**, 402-423.

[27]Miyazaki, Y., Shibuya, M., Sugawara, H., Kawaguguchi, O., Hirose, C., Nagatsu, J. and Esumi, S. (1974) ,*J. Antibiot.* ,**27**, 814-821

[28]Mitani, M., Ymanishi, T. and Miyazaki, J., (1975), *Biochem. Biophys. Res. Commun.*, **66**, 1231-1236.

[29]Miyazaki, J., Kinashi, H., Otake, N., Mitani, M. and Yamanishi, T. (1976), *Agric. Biol. Chem.* ,**40**, 1633-1640.

[30]Berg, D.H. and Hamill, R.L. (1970), *J. Antibiot.*, **31**, 1-6.

[31]Caffarel-Mendez, S., Demuynck, C. and Jeminet, G. (1987), *Reprod. Nutr Develop.*, **27**, 921-928.

[32]Henderson, P.J.F. (1971), *Ann. Rev. Microbiol.*, **25**, 393-428.

[33]Graven, S.N., Estrada-O, S. and Lardy, H.A. (1966), *Proc. Nat. Acad. Sci. USA.*, **56**, 654-658.

[34]e.g. Gomez-Puyou, A., Sandoval, F., Chavez, E. and Tuena, M. (1970), *J. Biol. Chem.*, **245**, 5239-5247.

[35]Wong, D.T., Berg, D.H., Hamill, R.H. and Wilkinson, J.R. (1977), *Biochem. Pharmacol.*, **26**, 1373-1376.

[36]Painter, G.R. and Pressman, B.C. (1982), *Top. Curr. Chem.*, **101**, 83-110.

[37]Katoh, K. and Tsuda, T. (1986), *Tohoku J. Agric. Res..*, **37**, 1-4.

[38]F.G. Riddell and S.J. Tompsett, (1990), *Biochim. Biophys. Acta,*, **1024**, 193-197.

[39]For an introduction to CD see eg. Velluz, L., Legrand, M. and Grosjean, M. (1965) *Optical Circular Dichroism.* Academic, New York.

[40]Painter G.R. and Pressman, B.C. (1979) *Biochem. Biophys. Res. Commun.*, **91**, 1117-1122.

[41]Caughey, B., Painter, G.R. and Gibbons, W.A. (1986) *Biochem. Pharm.*, **35**, (22), 4103-4105.

[42] Riddell, F.G., Arumugam, S., Brophy, P.J., Cox, B.G., Payne, M.C.H. and Southon, T.E. (1988), *J. Am. Chem. Soc.*, **110**, 734-738.

[43]Riddell, F.G., Arumugam, S. and Cox, B.G. (1988), *Biochim. Biophys. Acta.*, **944**, 279-284.

[44]Riddell, F.G. and Arumugam, S. (1988), *Biochim. Biophys. Acta.*, **945**, 65-72.

[45]Riddell, F.G., Arumugam, S. and Cox, B.G. (1987) *J. Chem. Soc. Chem. Commun.*. **1987**, 1890-1891.

[46]Riddell, F.G. and Arumugam, S. (1989) *Biochim Biophys Acta.*, **984**, 6-10.

[47]Mimms, L.T. Zampighi, G. Nozaki, Y. Tanford, C. and Reynolds, J.A. (1981), *Biochemistry*, **20**, 833-840.

[48]Riddell, F.G. and Hayer, M.K. (1985), *Biochim. Biophys. Acta.*, **817**, 313-315.

[49]Anteunis, M.J.O. and Rodios, N.A. (1981) *Bull. Soc. Chim. Belg.*, **90**, 715-735.

[50]Asukabe, H., Yonegama, H., Mori, Y., Harada, K., Suzuki, M., and Oka, I. (1987) *J. of Chromatogr.*, **396**, 261-271.

[51]Chippa, M.A. (1990) MSc thesis. University of St Andrews.

[52]Forbes, H. (1990) 4th year project, University of St Andrews.

[53]Riddell, F.G. and Patel, A., Unpublished results.

[54]Caughey, B.W., Gibbons, W.A. and Painter, G.R. (1989), *Magn. Res. in Chem.*, **27**, 403-406.

CHAPTER 3.

Chapter 3 The study of the molecular conformations of salinomycin and narasin using ^{1}H and ^{13}C nmr.

3.1 Introduction.

Nuclear magnetic resonance is a very powerful and widely used analytical tool providing direct information about the chemical environment of a particular atom, as long as the nucleus is magnetic. As such it can be used to study the structure and conformation of many materials. Most chemists use nmr regularly to identify whether or not their reaction product is that which they require.

There are however some limitations of this technique. One is the relative insensitivity. Milligram quantities of material are normally required to obtain a ^{13}C spectrum in a practical timescale. A second problem is the embarasssment of riches obtained in a spectrum. If a spectrum is taken of a complex material the lines will tend to overlap one another making their identification and assignment difficult. This is a particular problem in proton spectra, as there is only a small spectral width and the lines tend to be relatively broad with multiplet character. It is possible to resolve this difficulty by the use of a second dimension in the acquisition. If the resonances are separated in two dimensions then there is less likelihood of peak overlap occurring.

3.1.1 Two dimensional nmr.

Two dimensional (2D) nmr was first proposed in 1971 by Jeener[1]. The technique which he pioneered used two $\pi/2$ pulses

and has since become widely used. It is more commonly known as COSY one of the acronyms beloved by nmr spectroscopists in this case it is taken from COrrelation SpectroscopY.[2] The initial method has spawned a large number of variants most of which are some kind of correlation spectroscopy. These techniques all rely on what is known as frequency labelling for their utility. The general procedure can be represented schematically as follows:

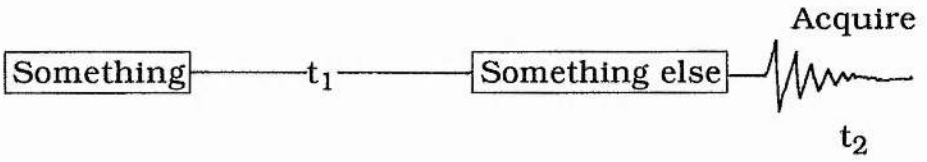

where t_1 and t_2 are both time delays and the nature of the operations vary. Exactly what these operations are will depend on the aim of the experiment and examples will be given later. In general the sample is modulated as a function of t_1 and detected as a function of t_2. The sample will initially evolve at some frequency ν_1 during t_1 ie. it is labelled with this frequency. During t_2 the evolution will occur at a different frequency, ν_2. This will lead to peaks in the spectrum at (ν_1,ν_2) where $\nu_1 \neq \nu_2$. These are known as off diagonals or cross peaks and are the object of all 2D nmr techniques.[3]

This process is best explained using the simplest system ie a single spin 1/2 nucleus. If the longitudinal relaxation T_1 is ignored for simplicity's sake the behaviour of the magnetisation in the rotating frame with two $\pi/2$ pulses will be as shown in Figure 3-1.

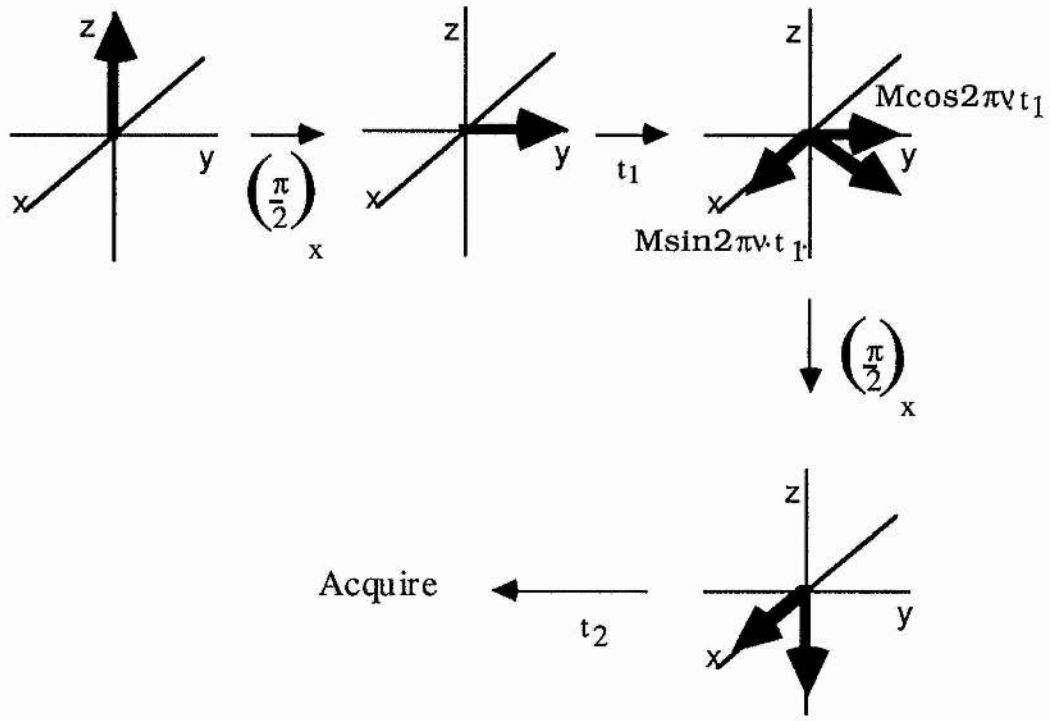

Figure 3-1. A two dimensional nmr pulse sequence.

The acquisition samples the magnetisation only in the x-y plane where the signal intensity is $M.\sin 2\pi.\nu.t_1$. So the signal will fluctuate sinusoidally with t_1 and decay exponentially with time as

$$M = M_0 e^{-t_1/T_2} \qquad \text{Eqn. 3-1.}$$

If a series of experiments are performed at intervals of t_1 starting from zero to several seconds the amplitude of the peak would be seen to fluctuate sinusoidally with frequency ν, see Figure 3-2. Observing the top of this peak will produce a pattern like that in Figure 3-3 known as an interferogram. This can be seen to bear a remarkable resemblence to a free induction decay and it can be Fourier transformed in the same way. If this is performed for every column of points obtained from an FID then a two dimensional spectrum can be obtained with a peak at (ν_1,ν_2). In this case ν_2 is the chemical shift ν of the peak. In this case the

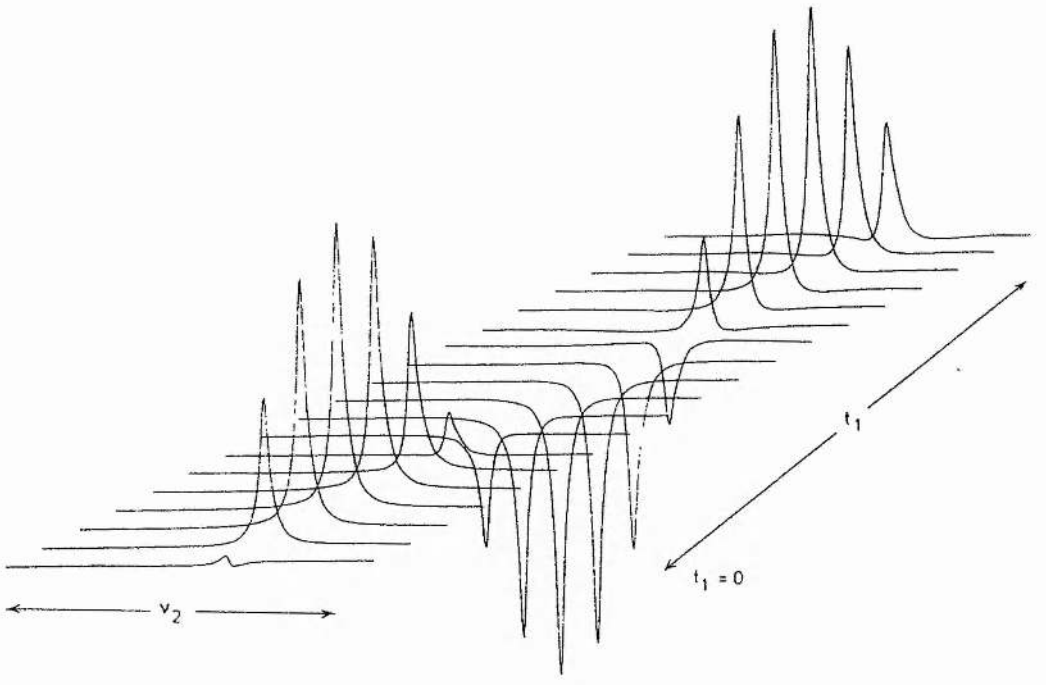

Figure 3-2. The result of applying the pulse sequence in Figure 3-1 with variable t_1.[4]

Figure 3-3. A slice from the data of Figure 3-2 taken parallel to t_1 through the tops of the peaks.[4]

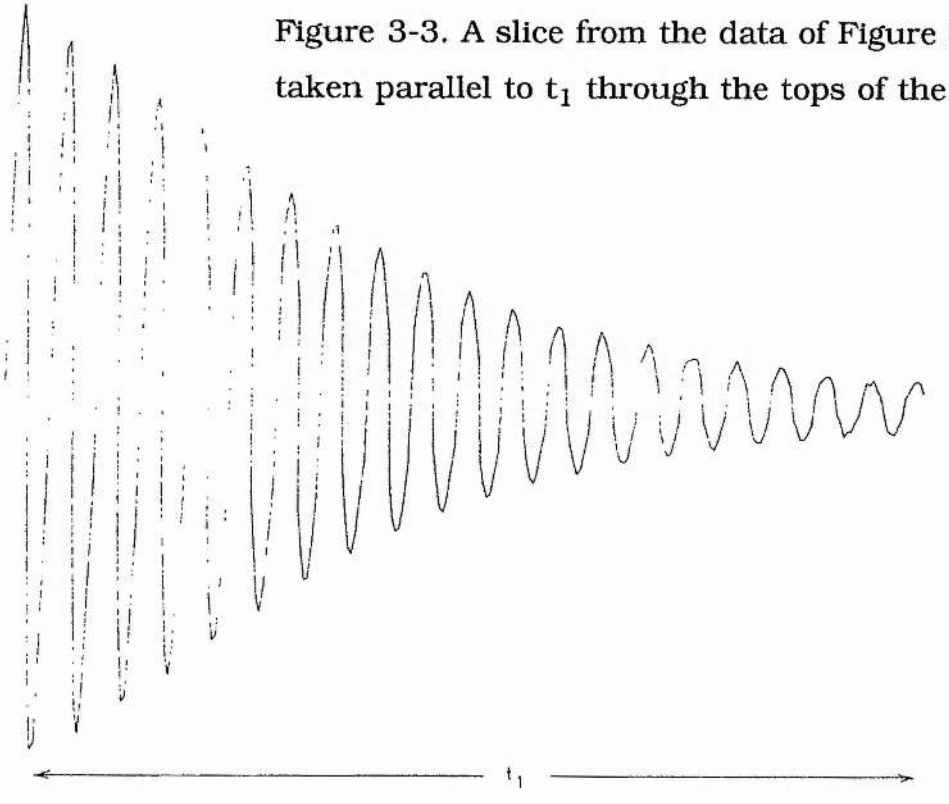

interferogram produced was oscillating with frequency ν so the frequency ν_1 is also the chemical shift. This leads to a square spectrum with a peak at (ν,ν) ie on the diagonal. This spectrum in itself is not particularly useful but if the same pulse technique is applied to a system with J coupling then this is an entirely different matter.

3.1.2 Coherence transfer.

It is possible to identify adjacent groups in a spectrum using homonuclear decoupling.[3] For a complex spectrum this will be made more difficult as the peaks will tend to overlap. This makes it hard to decouple only one specific resonance and also difficult to identify the changes in the spectrum. If it were possible to spread the data out over two dimensions then peaks are less likely to overlap and cross peaks off the main diagonal will become obvious. This should enable the chemist to identify easily couplings between adjacent centres and so assign the spectrum. The problem is how to produce these off diagonal peaks.

This can in fact be achieved using the above pulse sequence.[2] The reasons for this become clear if one considers a system with homonuclear coupling. In a coupled system the second pulse causes the magnetisation in one transition which arose during t_1 to be shared amongst all its associated transitions. The reason for this lies in the concept of coherence. Considering a saturated transition and one which has just undergone a $\pi/2$ pulse it can be seen that neither have a z component of the magnetisation. The populations of the α and β states must therefore be the same. However in the former case there is no net magnetisation, whilst

in the latter there is a magnetisation component precessing in the x-y plane. This arises from the x-y components of the nuclei precessing with the same phase, which they derived from the pulse. In the saturated sample the nuclei are precessing with random phase or incoherently. Thus experiencing a pulse creates a phase coherence between the α and β states.[4]

A coherence like this across a transition is called a single quantum coherence. This is in fact the root cause of the nmr signal. This phase coherence is useful as once created it can be transferred to other states. In an AX system (Figure 3-4) if a single quantum coherence is created across say the A_1 transition, what are its possible fates? A π pulse will excite all the population excess and transfer all the phase data to the receiving level. So if such a pulse were to be applied to the X_1 transition a phase coherence between $\alpha\alpha$ and $\beta\beta$ would be created. This would be a double quantum coherence as there is a difference of two in the quantum levels of the two states. As the selection rule for a transition to be seen is $\Delta M = \pm 1$ these cannot be observed. However they are used in certain nmr experiments as an extra pulse can convert them back to a single quantum coherence which is observable. The evolution of the invisible multiple quantum coherence will proceed along different pathways to those of the observable spectrum and so may be of practical use.

If we return to our single quantum coherence between the $\alpha\alpha$ and $\alpha\beta$ states we can consider what happens if a pulse of other than π is administered. This will lead to only partial transfer of coherence so there will now be three phase coherences $\alpha\alpha - \alpha\beta$, $\alpha\beta - \beta\beta$, both single quantum coherences and the double quantum

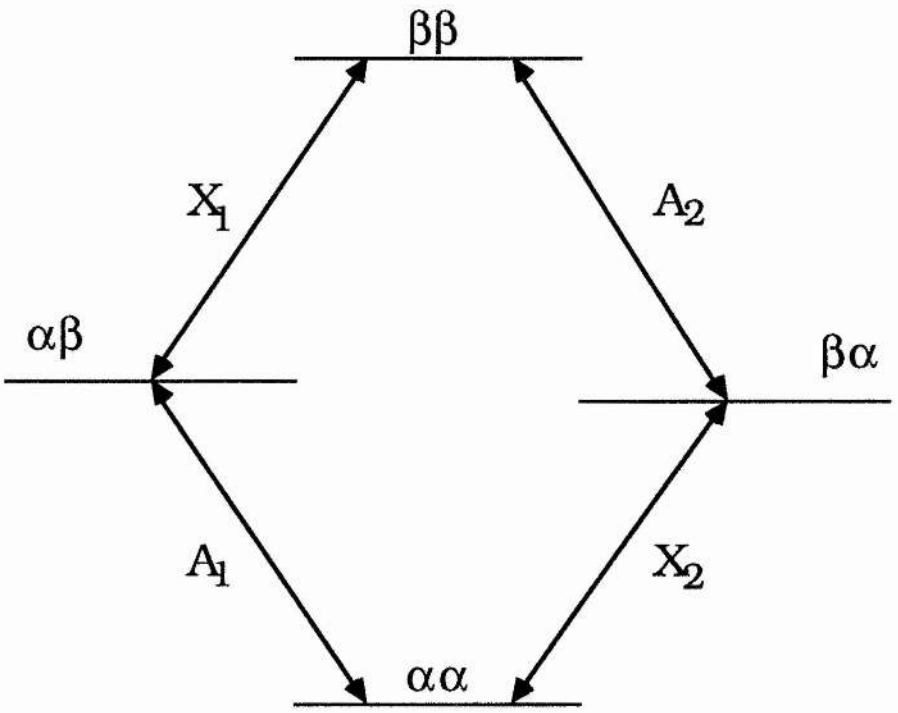

Figure 3-4. The energy levels in an AX system

coherence, αα – ββ. It is the second of these, the single quantum coherence across the X_1 transition which gives rise to the COSY cross peak. This component should be called coherence transfer. In a real COSY experiment the pulses are not applied selectively to a single transition, instead a non-selective pulse is applied across the whole spectrum.[4] This pulse can be seen as a sequence, or cascade, of selective pulses in quick succession. This means that while the phase information in αβ is being partially transfered to ββ the same is happening for all the other pairs of states. Thus during this second pulse phase coherence is spread out amongst all the possible coherences (in the AX case there are 6, 4 single, 1 zero and 1 double quantum coherence). Exactly how much coherence is transferred to each state depends on t_1, J and the duration of the second pulse.

3.1.3 Data handling and presentation.

One problem in 2D nmr is the amount of data which is accumulated. Consider a 10ppm ^1H spectrum with 0.2 Hz/pt resolution at 500MHz. In the one dimensional spectrum this gives an acquisition time of 5s and uses 50,000 words of memory space. This is well within the capacity of any modern spectrometer. The equivalent 2D experiment with the same resolution in each dimension requires 50,000 words for each t_2 spectrum and 2 x 25,000 for each t_1. Thus leading to a total of 2,500,000,000 words of computer memory which is roughly equivalent to the memory of 60 personal computers. The other problem is the acquisition time. This is 7.5s for each spectrum (mean $t_1 + t_2$) so for 25,000 spectra with eight scans each to allow for phase cycling the total acquisition time is aroud 17 days. So some decrease in the digital resolution and/or sweep width is required to make this a viable operation.[4]

The spectrum which results from this pulse sequence contains cross peaks showing which resonances are coupled to each other. There are also peaks on the main diagonal which are those due to untransferred coherence. The diagonal is in fact the 1D spectrum. The other fact to note is that a coupling from A to X must also mean a coupling from X to A of the same magnitude. This means that the spectrum is symmetrical about the main diagonal. This factor can be used in the processing to eliminate spurious signals by the process of symmetrisation.[4] This is a process which rejects any data which is not symmetrical about the main diagonal. In this manner it removes a lot of noise and unwanted features thereby improving the appearance of the

spectrum. It is however only of use if the magnitude spectrum is being considered and the peaks are all of the same phase and both the spectral widths and the sizes of the two blocks are the same.

There are two ways of presenting 2D spectra, as stacked plots or contour plots. Stacked plots are where rows of spectra are plotted slightly offset. This seems to give a three dimensional representation of the spectrum as the peaks can be seen to build up in both dimensions. This makes the peaks easy to see but as the spectra become more complicated they rapidly become cluttered. Contour plots look rather like an Ordanance Survey map of a mountain range. Points of equal intensity are linked by contours. This makes the spectrum clearer and enables the couplings to be readily measured off. All that is required is a straight edge, good eyesight and some patience and the lines are relatively easy to follow.

3.1.4 Phase cycling.

There are a number of problems in setting up a COSY spectrum to obtain a good result. One factor common to all 2D or 3D spectra is the need for phase cycling. This removes unwanted peaks in a number of ways given below. The first problem arises due to the longitudinal relaxation, T_1. This was ignored when the COSY spectrum was first discussed but it is an important factor. The effect of T_1 is to return the magnetisation to the z axis during the t_1 evolution delay. Therefore on the application of the second $(\pi/2)_x$ pulse it will give rise to a peak in the 2D transformed spectrum at $\nu_1 = 0$. So this will be a copy of the spectrum along this line which is probably in the middle of the spectrum. If a

$(\pi/2)_{-x}$ pulse is applied then the magnetisation will be along the -y axis as opposed to the +y axis as seen earlier. So alternating a +x and -x pulse should average this signal out to zero.[4] The component of the magnetisation of interest in the spectrum lies along the x axis so is unaffected by the sign of the second pulse. This gives us the phase cycle:

Scan	Phase 1	Phase 2	Rec
1	x	x	x
2	x	-x	x

The experiment will also suffer from the problems in quad detection seen for one dimensional spectra so the same pulse sequence can be applied.

3.1.5 Quadrature detection.

Quad detection is a way of improving the signal to noise and decreasing the required computer power by measuring from the centre of a spectrum.[5] The problem with this is that the one component of the magnetisation is insufficient to distinguish betwen positive and negative frequencies. This is like watching a rotating stick from the side. It is impossible to disinguish the direction of rotation it just looks like it is oscillating up and down see Figure 3-5. If it is observed from a second orthogonal direction at the same time the sense of rotation can be elucidated. In terms of an nmr spectrometer this requires two separate phase sensitive detectors with identical reference frequencies but a 90° phase difference between them.

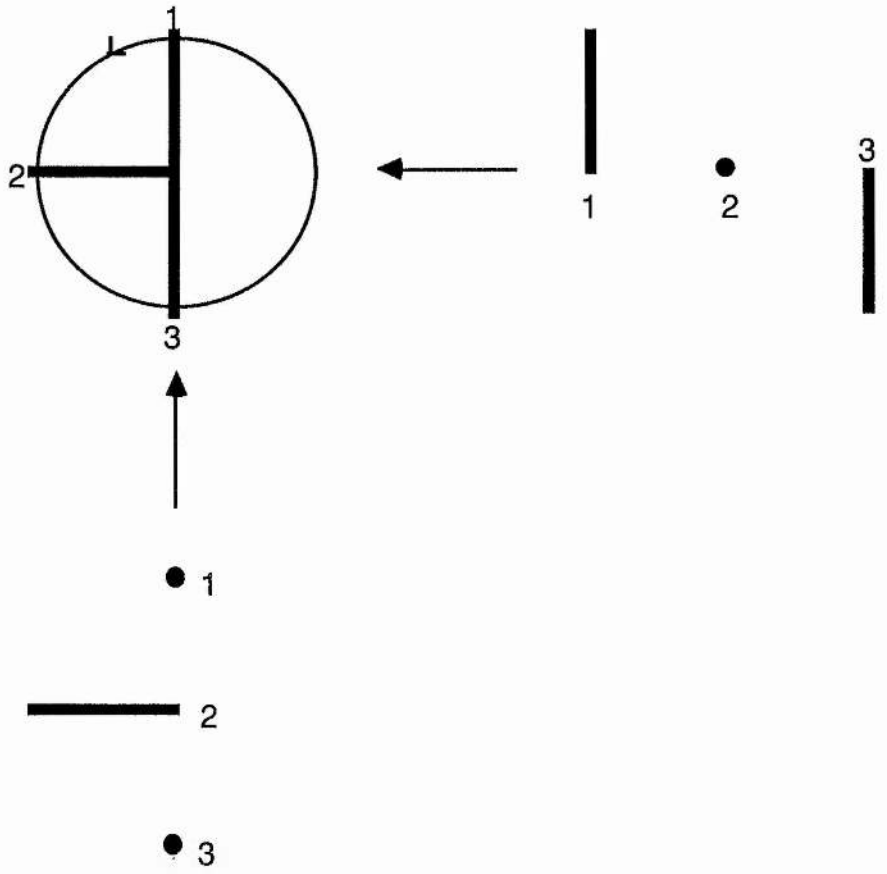

Figure 3-5. Schematic diagram to show the effect of observing a rotating stick in the plane of rotation.

This procedure enbles the direction of motion to be observed but unfortunately also leads to problems in the hardware. For quad detection to be successful both channels have to be identical, otherwise the even and odd components will not cancel exactly. To minimise this problem a phase cycle can be implemented, in conjunction with alternating the receiver channel. The data is obtained by alternating the phase of the signal and the receiver channel used. Thus the data with one phase is stored together and that with the other phase also stored together in a separate memory block. This produces two fid's one real and one imaginary which are both part of a complex spectrum.

There may also be faults which will lead to spurious signals whose phase is independent of the applied pulse. A 180° phase difference followed by subtraction of the stored spectrum will eliminate these. Put together this gives a four pulse cycle.

Scan	Pulse	Rec	A	B
1	x	x	+1	+2
2	y	y	-2	+1
3	-x	-x	-1	-2
4	-y	-y	+2	-1

A and B are the memory blocks, 1 and 2 are the receiver channels.

The problem with this method of quad detection is that it requires two digitisers (ADC's) which are expensive. To get round this it is possible to collect both phases through a single ADC by treating the signal as if it were being detected as a single phase.[5] The receiver phase is advanced by 90° after each point has been detected. Each sample point will then have a phase 90° higher than expected so it looks like a sample of higher frequency. This works because if the sweep width is F we are digitising at 2F. The phase shift is 90° ie 1/4 cycle so the frequency seems to have been increased by F/2. The signal is measured from the centre of the spectrum so the observed frequencies are at -F/2 to F/2 relative to the reference frequency. So if this is increased by F/2 this will seem to range from 0 - F removing the negative portion of the spectrum. This process is known as Time Proportional Phase Increments (TPPI) and will crop up later as a method for phase sensitive COSY experiments.

3.1.6 COSY spectra in magnitude mode.

The simplest form of COSY is referred to as the magnitude spectrum. Less data is produced than with the phase sensitive COSY discussed later but is simpler to carry out. This method works by combining the two signals with 90° phase difference either by addition or subtraction.[6] In the latter case which is most often used the pulse sequence is:

Scan	Pulse 1	Pulse 2	Rec
1	x	x	x
2	x	y	-x
3	x	-x	x
4	x	-y	-x

This method leads to lines with a mixture of the absorption and dispersion parts of the spectrum ie there are both positive and negative areas. This is rectified by calculating the magnitude spectrum ($\mathcal{M}$) using

$$\mathcal{M} = \sqrt{\mathcal{R}^2 + I^2}$$

Where $\mathcal{R}$ is the real spectrum and I is the imaginary spectrum. This gives a star shaped line with a very wide base. To eliminate this a sine-bell window function can be applied to the fid.[6] This is half the cycle of a sine wave possibly squared and/or phase shifted. The problem with this method is although it does sharpen the line it also loses sensitivity. This is particularly serious if there are lines with markedy different widths in the spectrum. The sine bell works by reducing the intensity at the beginning and end of the fid but emphasising the middle. Thus a

sharp line will show up well but a broad line will have lost much intensity in the resolution enhancement procedure. Therefore this method is not ideal to use, although it is the approach used in all of the spectra used in this work.

3.1.7 Phase sensitive COSY.

A better technique is the phase sensitive COSY.[7] This produces a spectrum which gives the relative phases of the cross peaks enabling the signs of coupling constants to be determined. This procedure also gives extra data about the type of coupling observed and has none of the drawbacks associated with the magnitude spectrum listed above.[5] One method of obtaining such spectra is to use TPPI (time proportional phase increments) as mentioned under quad detection.[5] In a 2D experiment this works by increasing the phase of the initial pulse by 90° with each increase in t_1. As in the one dimensional equivalent t_1 is sampled at twice the rate but only half of the values are stored.

3.1.8 The nuclear Overhauser effect and NOESY spectra.

A second type of homonuclear two dimensional nmr technique is the so called Nuclear Overhauser Effect correlation SpectroscopY (NOESY).[8] This shows which protons are near in space but not necesarily in the structure. From such interactions it is possible to extract a lot of structural information. This technique is widely used in the study of protein folding patterns.

The nuclear Overhauser effect (nOe) is observed as a change in intensity of one resonance when another is perturbed.[9] It is caused by direct interaction of the magnetic dipoles of nuclei with

each other and is proportional to $1/r^6$ where r is the internuclear distance. In some cases the nOe data can be quantified to give direct comparison with similar compounds.[10] In more complex materials where a greater number of factors can contribute to the magnitude of the nOe a qualitative comparison is all that is realistically possible. In a NOESY spectrum it is the presence of a cross peak which is important. In protein nmr this is taken to mean that the two groups thus correlated are close to each other.[11] Each of the protein folding structures eg β-sheet or α-helix show distinctive patterns of NOESY cross peaks and so can be identified.

The origin of the nOe, as stated above, is in magnetic dipolar interactions. The reason for this lies in the system trying to maintain itself at thermal equilibrium.[9] So, as the population difference across one transition is changed, those across other transitions alter to try and balance out the difference. The transitions affected must be in some way connected to those being stimulated. In this case the interaction is through space so is not limited to groups which are close together in the molecular structure. It is possible to see interactions between nuclei at opposite ends of the molecule if they are close to each other in space. Therefore the information is complementary to that from the COSY spectrum.

In a COSY experiment the component of magnetisation along the y-axis before the second pulse is ignored. It is this component, however, which is monitored in the NOESY spectrum. This component is frequency labelled, as is the component used in the COSY spectrum and as such can be used to aquire a 2D

spectrum. This component is along the z-axis while the COSY spectrum is acquired and so can be involved with chemical transfer, nOe or possibly both. If this component is returned to the x-y plane after an evolution delay then a spectrum can be acquired. The pulse sequence used is:

$$\frac{\pi}{2} \text{---} t_1 \text{---} \frac{\pi}{2} \text{---} \tau_m \text{---} \frac{\pi}{2} \text{---} t_2 \text{---} \text{Acquire}$$

This is very similar to the magnetisation transfer sequence seen in the previous chapter. Indeed it is a two dimensional version of this experiment. If during the evolution delay, τ_m, a nucleus labelled with a particular frequency migrates to another site there will be a cross peak between the two sites. If there are two nuclei in the molecule which would show an nOe then as the z components of their magnetisations can also interact there may be a cross peak between these two sites.

3.1.9 Heteronuclear correlation spectroscopy.

A further type of two dimensional nmr experiment used in this work were heteronuclear correlation experiments. These are a method of determining which protons are attached to which carbons and as such make the assignment of the ^{13}C spectrum a simple matter, once the ^{1}H spectrum has been assigned. These methods work by a similar method to the COSY experiment discussed above relying on polarisation transfer between protons and ^{13}C nuclei.[11] The polarisation is transferred via the J-couplings which allows for selection of the cross peaks seen. The ^{1}J coupling constants will be of the order of 160Hz for ^{1}H to ^{13}C so can easily be selected. Longer range, ^{2}J, coupling constants are of

the order of 10-15 Hz so it is also possible to select them. The selection is achieved by means of a fixed delay of $1/(2J_{CH})$ which allows the two proton vectors arising from the J-coupling to precess into an anti parallel alignment. This allows magnetisation transfer to occur. Changing this delay allows different coupling constants to be selected. Two experiments, called XHCORD and COLOC, were used for the work in this thesis. The former selects for single bond couplings while the latter identifies longer range interactions.

The general pulse sequence for this type of experiment is as given in Figure 3-6.

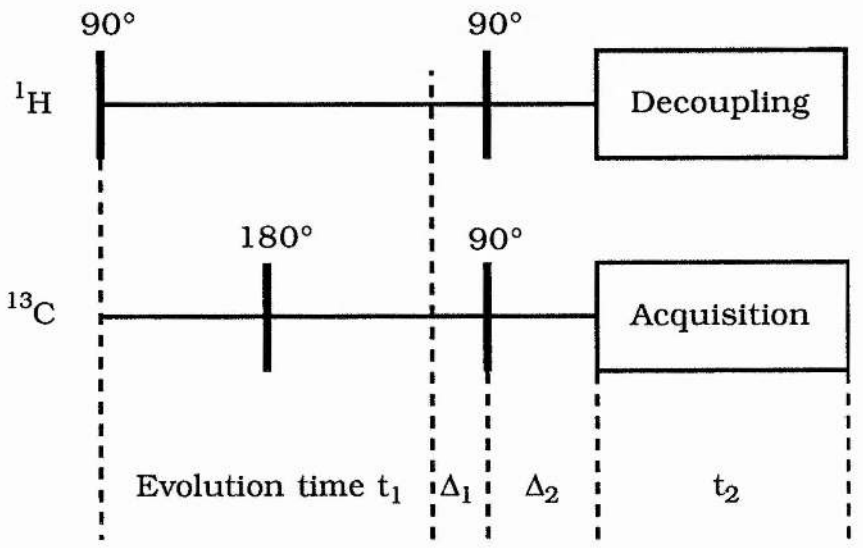

Figure 3-6. The pulse sequence used for Heteronuclear shift correlation spectroscopy.

The 180° pulse applied to the carbon channel serves to decouple the proton signal. The delays t_1 and t_2 and the two 90° pulses in the 1H channel are analogous to those in the COSY experiment. The delay Δ_1 selects for the coupling constant and the delay Δ_2 is to allow the carbon vectors to align in a parallel

orientation. The 90° pulse in the ^{13}C channel is a read pulse to place the ^{13}C magnetisation in the x-y plane where it can be measured.

3.1.10 One dimensional ^{13}C nmr experiments.

Two one dimensional nmr experiments were also used in the assignment of the 13C spectra these were WALTZ and DEPT. WALTZ 16 is a pulse sequence developed to achieve broadband 1H-13C decoupling.[12] The WALTZ experiment consists of a sequence of composite pulses which refocus the components arising from the ^1J couplings. This means that there is no residual splitting due to the ^1J interactions. DEPT is a spectrum editing method which is used to identify the number of protons attached to a particular carbon.[13] The DEPT experiment consists of three pulses, two in the 1H channel and one in the 13C channel. The pulse sequence is given in Figure 3-7.

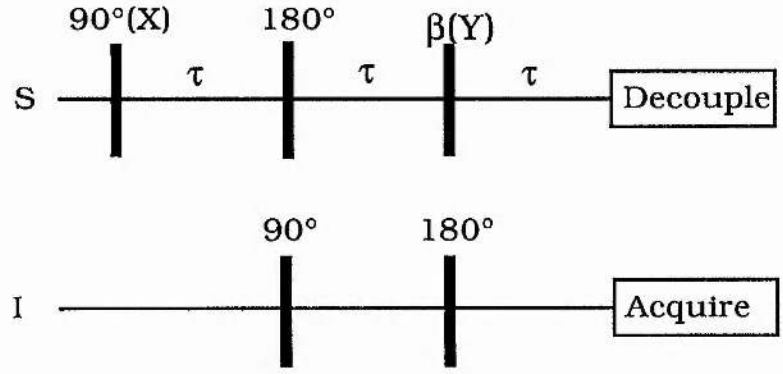

Figure 3-7. The pulse sequence used in DEPT experiments.

The second pulse in the ^1H channel (β(Y)) is the composite pulse $(\pi/2)_x$, $(\beta)_z$, $(\pi/2)_{-x}$. This sequence creates I-spin coherences dependent on the number of nuclei attached to a particular S nucleus, IS, single quantum coherence, I_2S double

quantum coherence and I_3S both single and triple quantum coherences. The second pulse has variable flip angle and is where the selectivity arises. If this is a 90° pulse then only CH signals occur, a 45° pulse selects all but quaternary carbons and a 135° pulse inverts the signals from CH_2 groups. The final part of the composite pulse converts the multiple coherences into observable ^{13}C magnetisation.

3.2 NMR on salinomycin and narasin.

There have been a number of nmr studies on salinomycin and narasin published over the years since their discovery. These have been using both ^{13}C and ^{1}H nmr and have been concerned with the structure, conformation and biosynthetic origins of these materials. The work on all the polyether antibiotics published up until 1982 was reviewed in Westley's book with chapters on both ^{1}H and ^{13}C nmr.[14,15]

3.2.1 ^{13}C nmr of salinomycin and narasin.

The first papers on the nmr properties of these materials were carried out using ^{13}C nmr. Three papers were published in 1976-77 on the ^{13}C nmr of both narasin and salinomycin the latter being studied as the sodium salt as well as the free acid.

In 1976 Dorman et al from Eli Lilly published a paper on the ^{13}C nmr of narasin.[16] They used a 25MHz ^{13}C spectrometer in continuous wave mode collecting and adding multiple spectra. To obtain reasonable signal to noise and to aid in the study of the biogenesis, ^{13}C enriched samples were used. The narasin was prepared by fermentation of Streptomyces aureofaciens with ^{13}C

enriched substrates. The aim of the study was to work out the biosynthetic pathway by identifying the source of the observed enrichments. Six different substrates were used, acetate, propionate and butyrate, each labelled at only one site. This means that the list is Ac(2), Pr(2), Pr(3), Bu(2), Bu(3) and Bu(4), the number in brackets noting the site of enrichment. The results showed that the molecule was derived from 5 acetate, 7 propionate and 3 butyrate units, as expected from the structure. This also enabled an assignment of the structure to be made. There were a large number of uncertainties in this assignment with nearly half of the published values uncertain. It was also seen that enrichment occurred at different sites from those expected. This is due to the alteration of the substrates by the process of α-oxidation. This will produce for example a propionate from a butyrate.

This showed that ^{13}C enrichment can be used to study such materials and that the biosynthesis follows the polyketide pathway. There are however certain complications in the fermentation process. This paper also showed that the structure of narasin as proposed from the mass spectrum[17] was in fact correct.

In 1977 Seto et al published a second study of the ^{13}C nmr of narasin.[18] This was only a partial assignment of spectrum relating to the salinomycin assignment published later that year.[19] The aim of this work was to identify the position of the extra methyl in narasin. It was known that this group was in fact substituted on ring A, ie that nearest to the carboxyl grouping, but the actual site and orientation of substitution were uncertain. A comparison of the ^{13}C nmr spectra of salinomycin and narasin

showed where the extra methyl occurred in the spectrum and the effect this substituent had on the other resonances. It was observed that the signal from C(4) and C(5) underwent shift changes of ca 9ppm with a 3ppm shift change at C(3) and no change at C(6). Comparisons of these values with those observed in methyl substituted cyclohexanes showed that the methyl must be bonded to C(4) in an equatorial position. It was also observed that Me(41) showed a much smaller T_1 than the other methyls, but that it was similar to those of the methylenes. This was explained by the restriction of rotation of this group by the protons attached to C(42). see Figure 3-8.

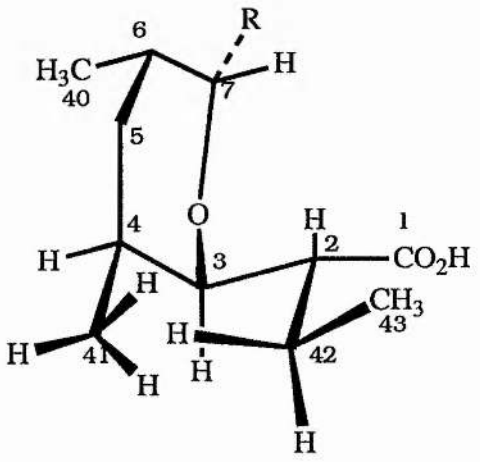

Figure 3-8. Showing the steric hinderance of the carboxyl chain in narasin.

The other paper mentioned was a complete assignment of the ^{13}C spectra of salinomycin as the free acid, sodium salt and also assignments of 20-deoxysalinomycin and methyl salinomycin.[19] This was achieved by comparisons with similar compounds and by using ^{13}C enriched materials. In this case 1,2 doubly labelled acetate and propionate were used, demonstrating which pairs of carbons were adjacent. The assignments were

better than those of Dorman et al.[16] for narasin with far fewer inconsistencies. There were, however, still some uncertainties about the assignments.

3.2.2 ^{1}H nmr on salinomycin and narasin.

The later work on these materials has all been concerned with the ^{1}H spectra. These are more complicated than the ^{13}C spectra as the spectral width is much smaller and the spectral complexity greater, due to the presence of J coupling. This meant that these have only been studied since the advent of superconducting magnets and Fourier Transform (FT) nmr techniques. The first papers on salinomycin and narasin were by Anteunis and Rodios in 1981. There were two studies one of 17-epi, deoxy(O-8)salinomycin[20] and the other on salinomycin and narasin themselves.[21]

It had been shown that the conformation of the crystalline C(17)-epimer[22] was similar to that observed in the crystal structure of salinomycin,[23] differences being seen in only four of the bond rotations. NMR was used to see whether this was just an effect of the crystal packing or if it persisted in the solution state. It was seen that in fact the nmr signals, except near the epimeric centre, were for the most part within 0.1ppm of those seen in salinomycin. The sites where the largest differences are observed are C(10)-H, C(12)-H, C(36)-H, Me(37), C(22)-H, C(25)-H, C(16)-H, C(18)-H, C(19)-H and C(20)-H. The differences at C(20)-H are due to the loss of the hydroxyl at this site and those at C(16)-H, C(18)-H, C(19)-H and C(22)-H to conformational changes expected on epimerisation. An interesting feature is the

difference along the C(10) to C(12) stretch of the molecule. This shows that there is a large conformational change here which is possible due to the lack of steric constraints. The change at C(25) may echo the ability to flex in this area of the molecule as well. This seems to say that the conformation of these ionophores is largely preset by the chemical structure. This means that there are only certain sites at which conformational changes are possible to allow complexation to occur.

The second paper was published later the same year studying narasin and salinomycin as both free acids and sodium salts[21]. The conformation was determined by measurement of the apparent coupling constants. This showed that the conformation was almost as seen in the crystal structure, the only major difference being a rotation about the C(24) to C(25) bond. The other factor determined from these data was the position of the two "hinge" regions in the molecule. These are the areas in which conformational change occurs by facile bond rotations. The bonds are not prevented from rotation by substituents on neighbouring carbon atoms. The two "hinge" regions identified are the C(24) - C(25) bond mentioned above and the C(10) to C(12) stretch of the molecule. It is in these areas that conformational change must occur to allow complexation of a cation. It is interesting to note the observed loss of activity when this ketone is reduced to the alcohol.[24] This may be due to an increase in the steric crowding in this area increasing the barrier to rotation, thereby decreasing the efficiency of the complexation procedure. Another explanation for this loss of activity is that this is one of the cation binding sites in the molecule, it is possible that the hydroxyl cannot complex

where the ketone can, due to the difference in orientation. From the Circular Dichroism studies mentioned earlier,[25,26] it was seen that the conformation of the anion at this site was different from that of both the complexed and free acid forms of these ionophores. During the course of this work aromatic solvent induced shift (ASIS) measurements were made. This compares the chemical shift values from an aromatic solvent, in this case benzene-d_6, with those of an aliphatic solvent; here $CDCl_3$ was used. The chemical shifts of some resonances are seen to move on this change of solvent. If they move upfield they are from a lipophilic area and downfield shifts arise from a hydrophilic area. The magnitude of the shift represents the degree of lipophilicity or hydrophilicity of the site. In this case the results showed that in sodium salinomycin there were 33 protons in hydrophilic areas and 29 in lipophilic zones. The downfield and upfield shifts almost balanced out showing that the sodium salts are virtually neutral membrane-carriers. The free acid showed slightly less overall lipophilicity than the sodium salt. The overall pattern was different from that observed in smaller ionophores in that there were two hydrophilic areas. One of these was around the (closed) head-tail portion of the molecule and the other in the central portion of the structure around O(4), O(8), C=O and C(18)=C(19). In the free acid this zone is somewhat less pronounced.

The hinge areas of narasin were further studied by Caughey et al.[27] They applied two dimensional nmr techniques to the assignment of the ^1H spectra in a range of solvents. The transport of cations across membranes involves passage through two

completely different environments. The membrane is a non-polar highly anisotropic lipophilic phase whereas the ion solutions are polar, isotropic and lipophobic. The study of cation complexation should incorporate an investigation of the conformation in both of these types of environments. This is what was attempted by Caughey et al with the effect of solvent polarity on the conformational equilibrium being assessed. The solvents used were cyclohexane, chloroform, acetone and methanol all in totally deuterated forms. It was observed that the chemical shifts of most sites were unaffected by solvent polarity. However some of the sites, specifically C(10)-H, C(12)-H, C(13)-H, C(14)-H and C(25)-H showed large (> 0.15 ppm) changes on going from cyclohexane to methanol. These changes occured with a large step between chloroform and acetone and all occur in the areas previously described as "hinges".[21] The conformation was believed to be more extended in a more polar environment, similar to the differences seen on epimerisation of salinomycin. These data showed that the conformation of narasin acid is dependent on solvent polarity. Taken in conjunction with the CD data[26] this shows that narasin is an efficient protonophore. The mechanism for cation transport is pH dependent and, for example, in the control of Eimeria (chapter 1) and transport in erythrocytes (chapter 2) it involves the transport of alkali metal ions in one direction and protons in the reverse direction, so this is as would be expected.

The most recent published paper on the ^{1}H nmr of these compounds was by Caughey et al in 1989.[28] This was again a study on narasin this time as the apo, free acid, sodium and potassium

bound forms. The spectra were taken using deuterated methanol as solvent using two dimensional and nOe nmr techniques. The data published were a list of assignments and coupling constants, as a first step in the conformational analysis of narasin. It is of interest to note that the observed values at specific sites vary with the cation present.

The ^{1}H and ^{13}C nmr spectra of these two materials have thus been assigned in a range of solvents and with a range of cations present. Changes in the chemical shift can be seen at certain sites in the spectra. NMR is therefore a good tool for this type of study and soon, as the fund of knowledge increases, an unambiguous conformation of these materials in solution should be obtained. The problem will then to be to repeat the measurements in an actual lipid bilayer.

3.3 Results and Discussion.

3.3.1 Preparation and confirmation of samples.

NMR is a very powerful tool for elucidating the chemical structure of molecules. It can also be used to study conformations of complex molecules including proteins with molecular weights of up to 15,000 Daltons. If the conformations of polyether antibiotics can be determined in solution, as both free acids and cation/ ionophore complexes this should help provide an understanding of the fundamental processes governing the complexation reaction. If the conformational differences between the complexed and free acid forms of the ionophore can be elucidated then information on the intermediate processes can be extrapolated from these data. Once the solution state behaviour of ionophores has been studied it should be possible to investigate the more complex behaviour at the solution/membrane interface. The following work is a study of the cation complexes of narasin and salinomycin in chloroform solution.

The first step in such a study is an assignment of the nmr spectra. Although on the scale of proteins these are small molecules, with a molecular weight of about 800D, there are still over 40 ^{13}C and over 45 ^{1}H signals in the spectra, with many of the latter overlapping. This makes the assignment of the spectra a far from trivial matter.

Initially the proton spectra for all the alkali metal salts of both ionophores and narasin acid, were studied and assigned. The spectra were all fundamentally similar but there were specific

differences with some peaks shifting by up to 0.5 ppm and many changing their relative positions. The general method of assignment was the same in all cases using COSY and NOESY spectra obtained at 500MHz.

The first thing to do was prepare samples of the alkali metal salts of narasin and salinomycin. In the first attempt at this narasin acid was dissolved in deutero-chloroform and stirred with sodium chloride crystals for an hour. This proved to be unsuccessful, but addition of a few drops of water to the mixture and vigorous stirring produced the desired product. This procedure of stirring a chloroform solution of ionophore with a saturated solution of the desired metal chloride was used for all samples. The chloroform solution was then dried through a plug of the corresponding anhydrous metal carbonate, which also ensured complete neutralisation of the acid. This method was successful for all the salts except lithium narasin. In the preparation of the salinomycin salts the only difference was that the starting material was the sodium salt rather tha the free acid. This is greatly favoured over cæsium and lithium but the equilibrium was forced by the much higher concentration of the latter in the mixture, ca 5g of chloride to 50mg of sodium salinomycin.

Although distinctly different nmr spectra were obtained for each salt it was important to show that the materials prepared were what they were thought to be. This was tried in a number of ways. The first attempt was using atomic absorption. If the material was a 1:1 complex then atomic absorption experiments on a standard solution should show this. The concentration of the

alkali metal in a solution, measured by atomic absorption, should match the known concentration. The problem with this approach lay in the almost complete lack of water solubility of these materials. This meant that the solutions had to be made up in aqueous methanol, from 50% methanol for the lithium salt to 10% methanol for cæsium. This disrupted the calibration of the spectrometer leading to non-reproducible results. The data showed that the desired cation was present in each case but did not prove the presence of a 1:1 complex.

The second method tried was C,H microanalysis. This was tried on three salts of salinomycin (lithium, potassium and cæsium, after evaporation of the $CDCl_3$) with the results shown in Table 3-1. This shows that the values were close to those expected but not within the accepted limits for such analyses. This again is not proof of a 1:1 complex with the correct cation. The low carbon value is consistent with small amounts of $CDCl_3$ and or H_2O remaining in the material.

Table 3-1. The actual and theoretical values obtained from the microananlysis of the salts of salinomycin.

	LiSL	KSL	CsSL
Theoretical Carbon (%)	66.6	63.9	57.1
Actual Carbon (%)	65.93	57.7	54.52
Theoretical Hydrogen (%)	9.19	8.81	7.88
Actual Hydrogen (%)	9.37	8.84	8.06

A completely different approach was then used: try to make what would be expected to be the most difficult salt to form, in this case cæsium narasin was chosen, by a completely different route. If the nmr spectra are the same then this is strong evidence that the method of preparation of the samples was valid. The first attempt at this was by running narasin acid in methanol down a cæsium charged cationic exchange column, also made up in methanol. The solution which emerged from the bottom of the column was evaporated and the product, a purple solid, was dissolved in $CDCl_3$. A ^1H spectrum showed that this was not the desired product, and was not in fact a narasin derivative at all. The ketal functions in the molecule are acid sensitive, so if the column had not been fully neutralised from the proton form, hydrolysis of these functions would be expected.

The final, successful, approach was using a titrimetric method with the nmr spectrometer acting as a rather expensive indicator. This was achieved by dissolving a known amount of narasin acid in $CDCl_3$ and placing the solution in an nmr tube. A standard solution (0.2M) cæsium hydroxide solution was prepared by diluting ca 6M cæsium hydroxide solution with D_2O to reduce the interference of the water peak. A spectrum was taken initially and then aliqouts of the cæsium hydroxide solution were added. The aliquots of solution added were 50µl, 20µl, 20µl, 10µl, 20µl and 20µl, the narasin present was equivalent to 100µl of the added solution, so the neutralisation was taken well past equivalence. The final solution was dried over cæsium carbonate and a final spectrum taken.

The resulting ^1H spectra are shown in Figures 3-9 to 3-12 including the entire spectra of the starting (Figure 3-9), half neutralised, (Figure 3-10), finishing products (Figure 3-11) and cæsium narasin prepared by the usual method, Figure 3-12. There are also expansions of the olefinic regions of the spectra for each point during the titration, these are two signals which move by a large amount and are easy to identify, Figure 3-13. During the neutralisation process certain lines are seen to broaden and move e.g. C(19)-H, C(33)-H and C(7)-H. These are all peaks with very different positions in the spectra of the free acid and the cæsium salt. This broadening is probably due to a dynamic exchange process with the cæsium ions exchanging between molecules of the free acid and cæsium narasin or between different binding sites in the same molecule. This process can be used to study the kinetics of the complexation process, similar studies have been carried out for for a number of ionophore/cation pairs.[29] Once complete neutralisation had occurred, at 1:1 CsOH : narasin the lines sharpened and moved no further. This is sufficient evidence that the samples prepared using our method are the expected salts.

Figure 3-9. The ^{1}H nmr spectrum of narasin acid before the addition of CsOH.

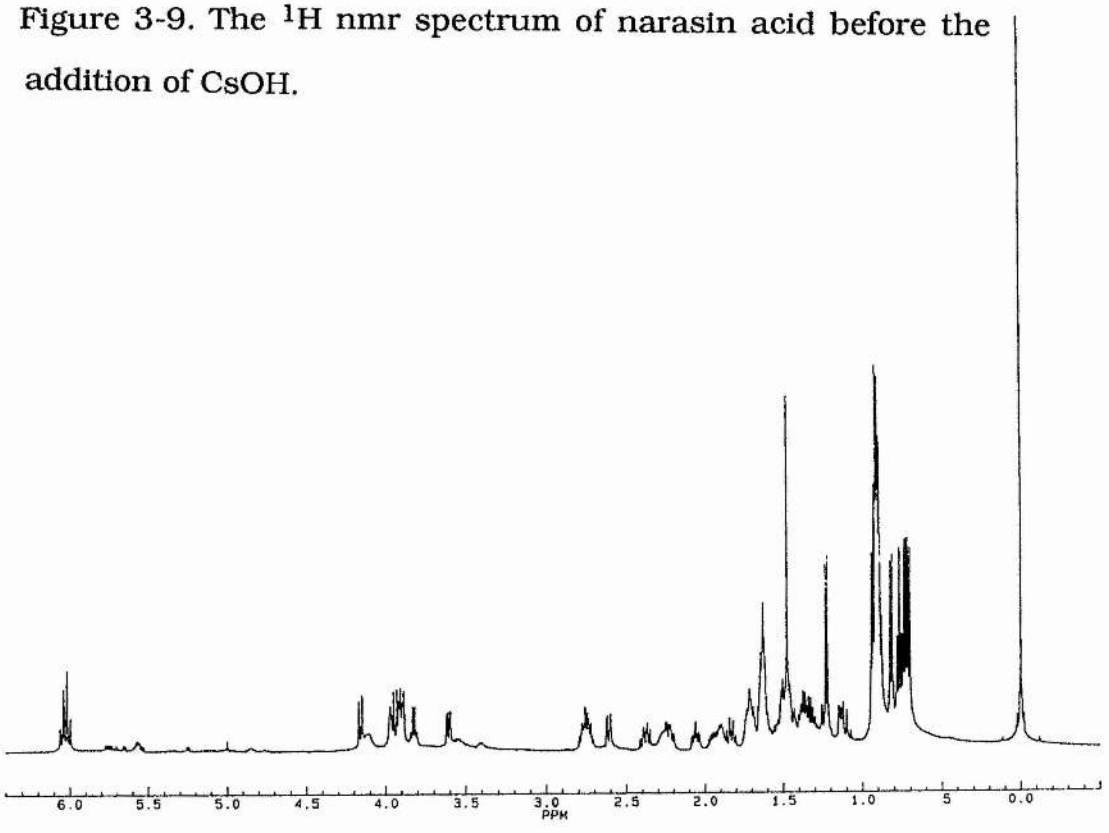

Figure 3-10. The ^{1}H nmr spectrum of narasin acid after the addition of 50% CsOH.

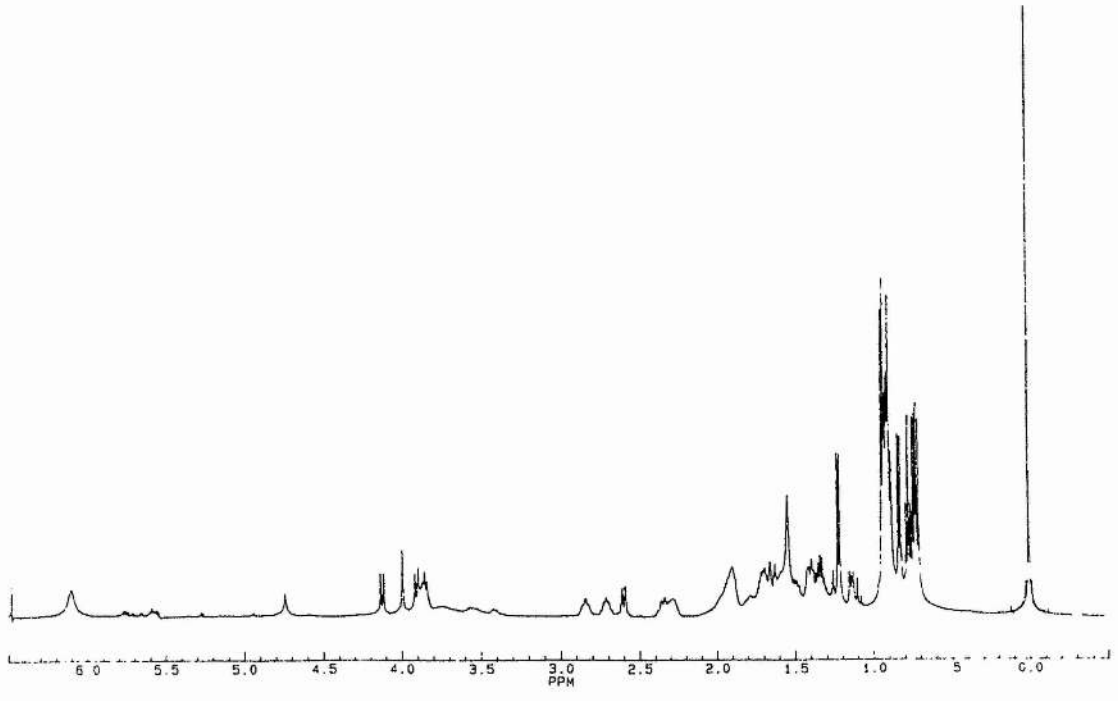

Figure 3-11. The ^{1}H spectrum of narasin acid completely neutralised with CsOH.

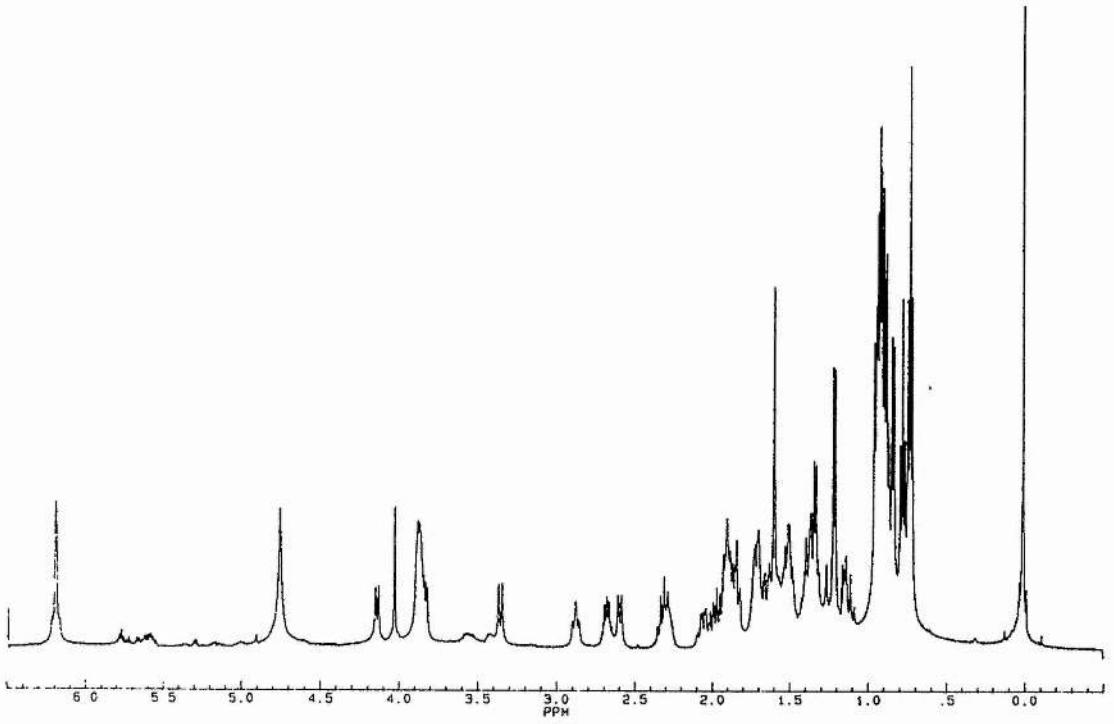

Figure 3-12. The ^{1}H spectrum of Cæsium narasin obtained by the usual method.

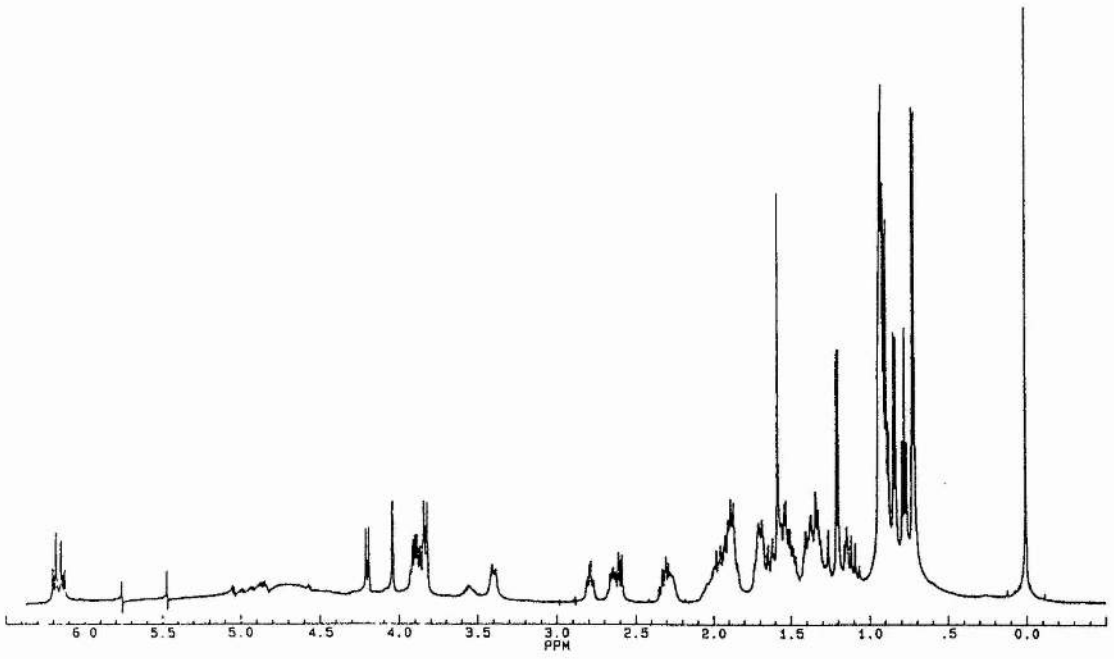

Figure 3-13. An expansion of the vinylic region of the ^{1}H spectrum of narasin during the titration.

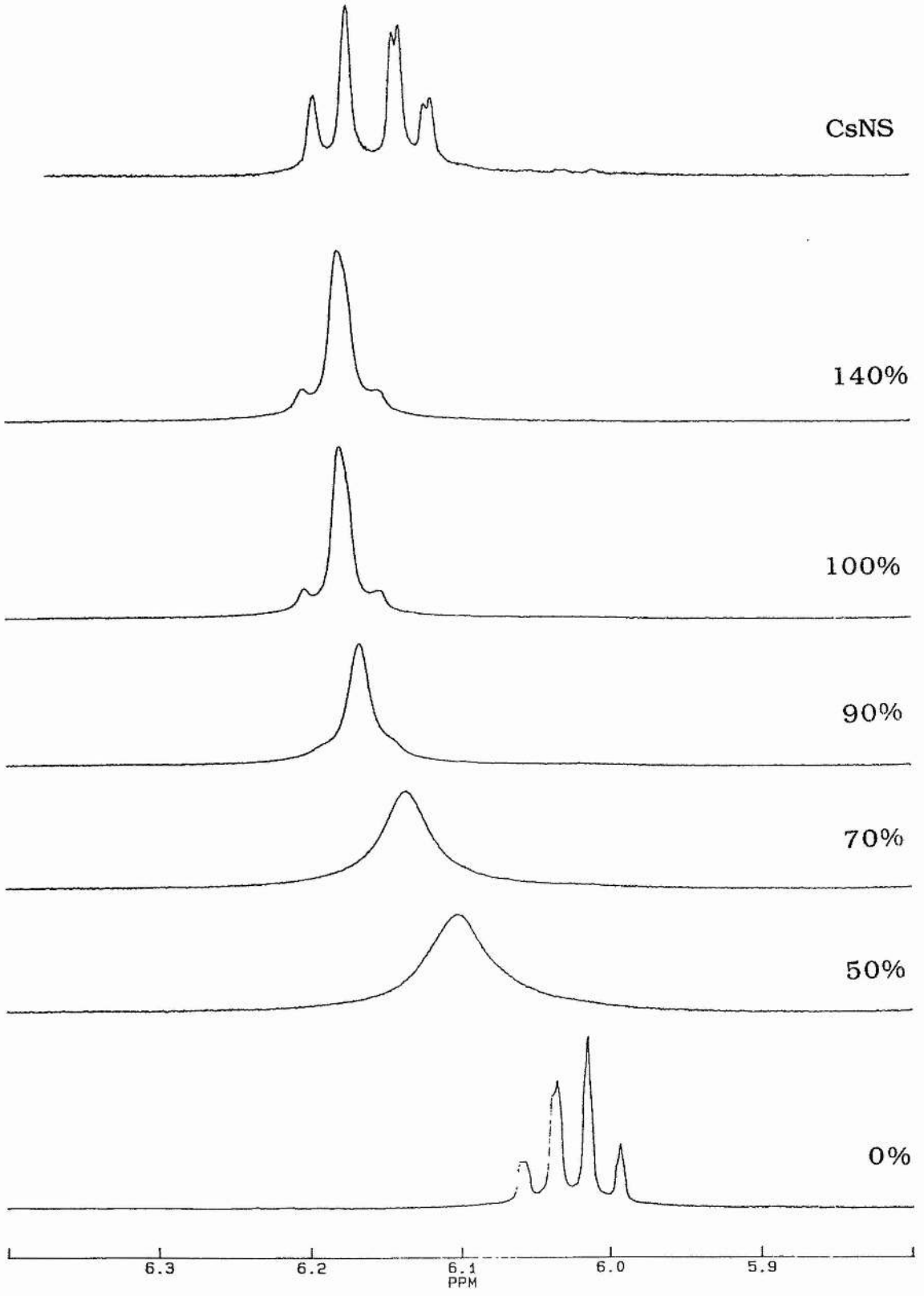

3.3.2 Assignment of the ^{1}H and ^{13}C spectra.

On looking at the structure of narasin and salinomycin (Figure 3-14) it can be seen that there are seven distinct chains of adjacent carbon atoms with attached protons and one singlet methyl. The assignment consisted of identifying one of the protons by chemical shift and utilising the homonuclear couplings in the COSY spectrum to step along the chains of connectivity. Some of them fall out readily such as C(18)-H, C(19)-H and C(20)-H, the only olefinic site in the molecule. C(29)-H and C(30)-H also drop out as this is the only etheric proton adjacent to a methyl. The other obvious signal is the singlet due to Me33.

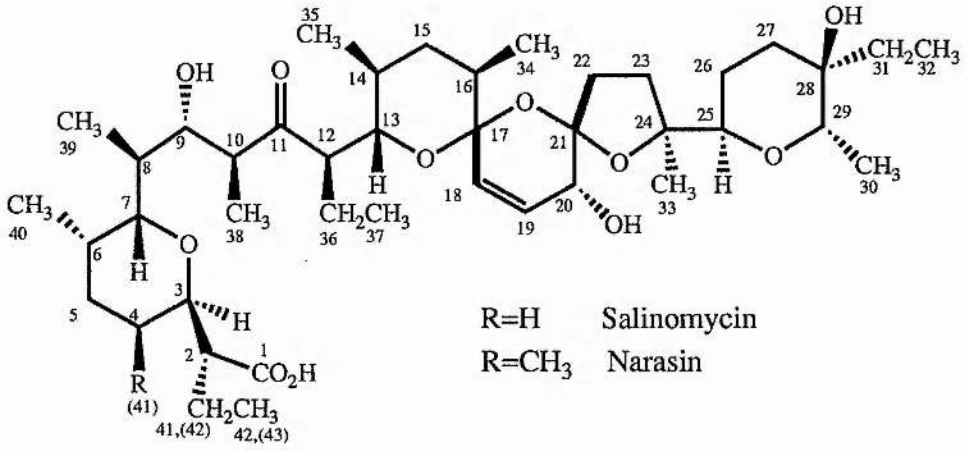

Figure 3-14. The structures of salinomycin and narasin showing the numbering system used in the assignments.

The most extended regions of connectivity in the molcules are at the "left-hand" end of the molecule nearest to the carboxylic acid group. The key signals to assigning this area are the 3 protons at 2.6 to 2.95 ppm attributable to sites adjacent to carbonyls. One of these, C(10)-H, shows a vicinal coupling to a methyl enabling its identification. This gives one end of the chain

which can be followed to C(7)-H and on to C(2)-H. By elimination, the unassigned signal must be due to C(12)-H allowing the assignment of the C(12) to C(16) fragment. C(25)-H is now the only unassigned peak above 3ppm which leads to assignment for C(26)-H and C(27)-H. Et(31, 32) is assigned by elimination as are C(22)-H and C(23)-H to finish the gross assignment.

The NOESY spectra were useful to study the areas which could not be unambiguously assigned solely referring to the COSY spectra. The ^{13}C-^{1}H correlated (XHCORD) spectra obtained later also helped to assign some proton resonances by providing separation in a second dimension. Often there were two or more resonances from nearby protons at very similar chemical shift for example C(14)-H and C(16)-H exhibit very similar shifts. One area for which the NOESY and XHCORD were useful was C(18)-H and C(19)-H. These two resonances formed an AB quartet and both showed similar coupling to C(20)-H. However the NOESY cross peaks enabled them to be unambiguously assigned, which could be confirmed by the C-H correlation experiments. A similar procedure was required to separate the resonances from C(22)-H and C(23)-H.

The assignment became easier with practice as the cross peaks between the resonances tended to look similar in all the salts enabling the easy identification of readily confusable peaks.

The ^{13}C assignment was achieved using XHCORD, WALTZ and DEPT data. This was a relatively simple process for the carbons with bonded protons, just reading off the ^{13}C resonance using the proton signals for identification. There are, however, six

quaternary carbons which are more difficult to assign. The two carbonyls can be assigned by chemical shift alone but a different strategy must be used for the others. A COLOC experiment on potassium salinomycin gave C(24), by a correlation with C(33)-H and hence by elimination C(28), with the assignments for the other salts by extrapolation. This was no help however for the two acetal carbons. A further COLOC on lithium salinomycin showed a different cross peak. This time there was a correlation between C(19)-H and a resonance at ~ 107ppm. This is inconclusive so the assignment of Seto et al.[19] for these two resonances is taken as correct. They. assigned these resonances on the basis of the differences between salinomycin and 20-deoxysalinomycin. The signal at 106.4ppm was seen to move by a large amount whilst that at 99.2ppm was almost invariant. This was taken to show that the former was C(21) and the latter C(17). Examples of the above spectra are shown in Figures 3-15 (1H), 3-16 (COSY), 3-17 (NOESY), 3-18(13C), 3-19 (XHCORD).

The chemical shifts of certain atoms were observed to vary with cation whilst for other atoms they are almost constant. These variations show where the largest changes in conformation occur on complexation with different cations. Once the areas which alter have been indentified, a greater understanding of the molecular recognition and ion selectivity properties of these materials should be possible. If the actual conformations of the complexes with different ions can be determined, then the reasons for the observed selectivities should be identifiable. In this situation calculation of the energy differences betwen complexes should be relatively facile, enabling the ion preferences

Figure 3-15. The ^{1}H spectrum of potassium narasin.

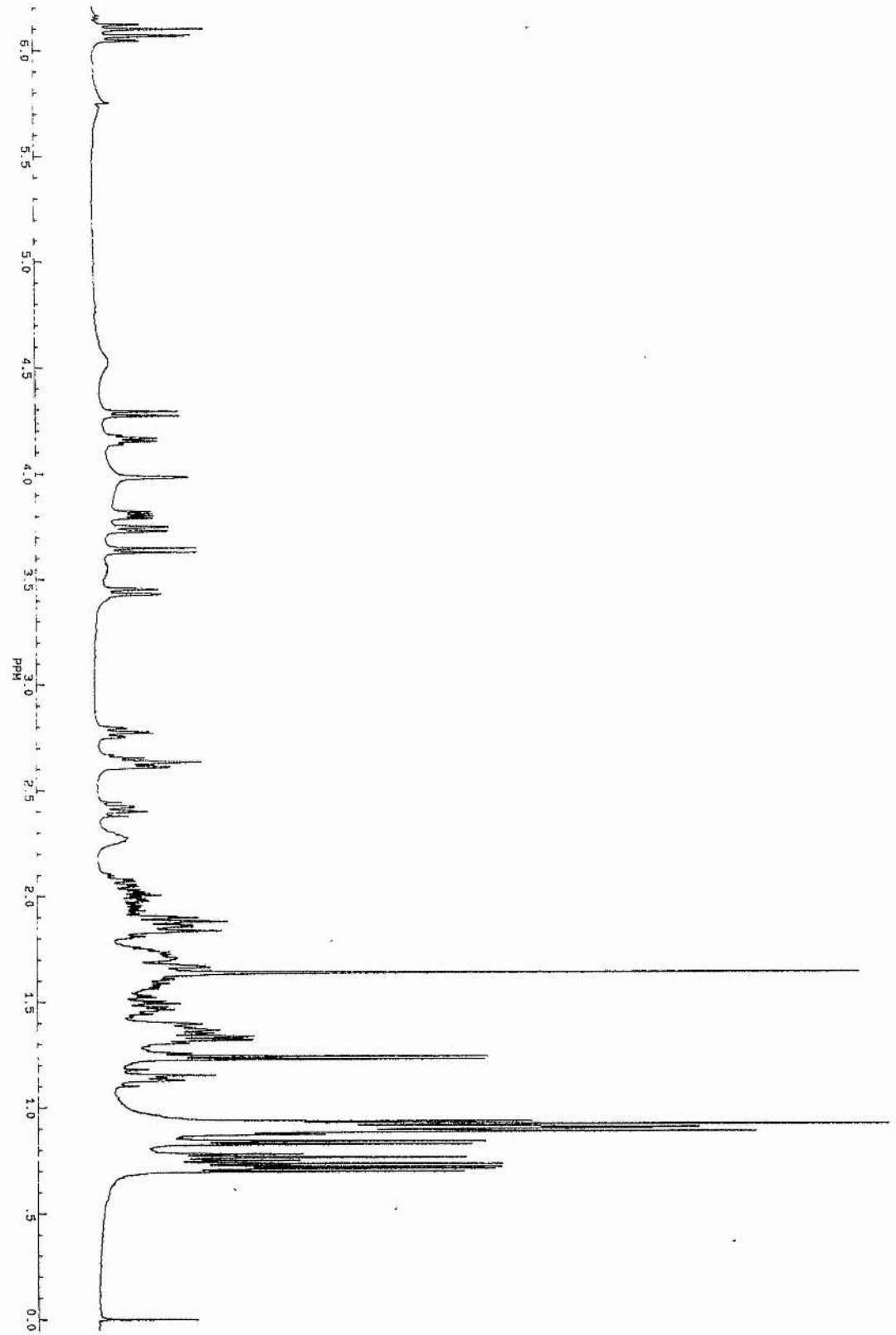

Figure 3-16. An expanded region of the COSY spectrum of rubidium salinomycin.

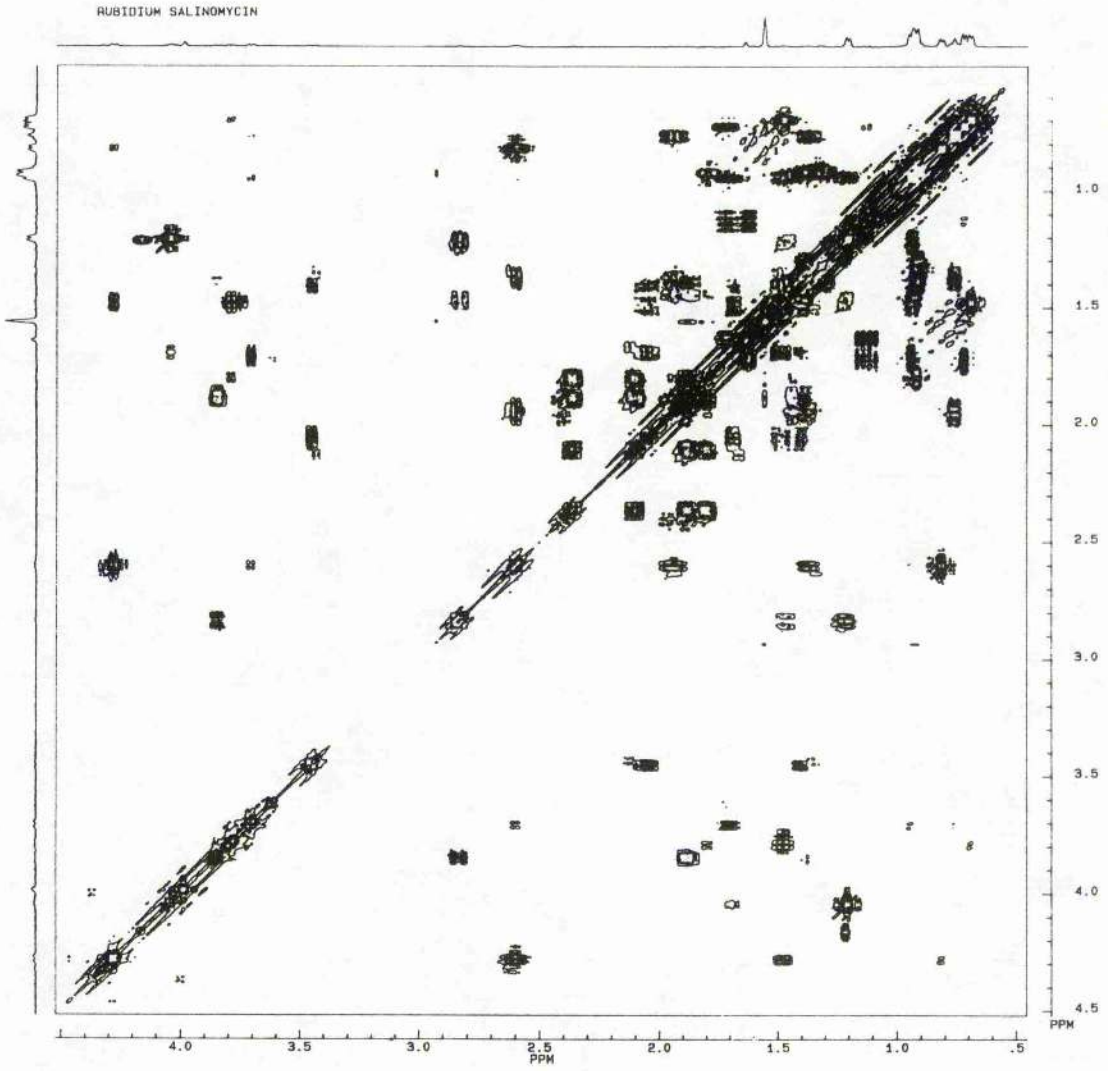

Figure 3-17. An expanded region of the NOESY spectrum of sodium narasin.

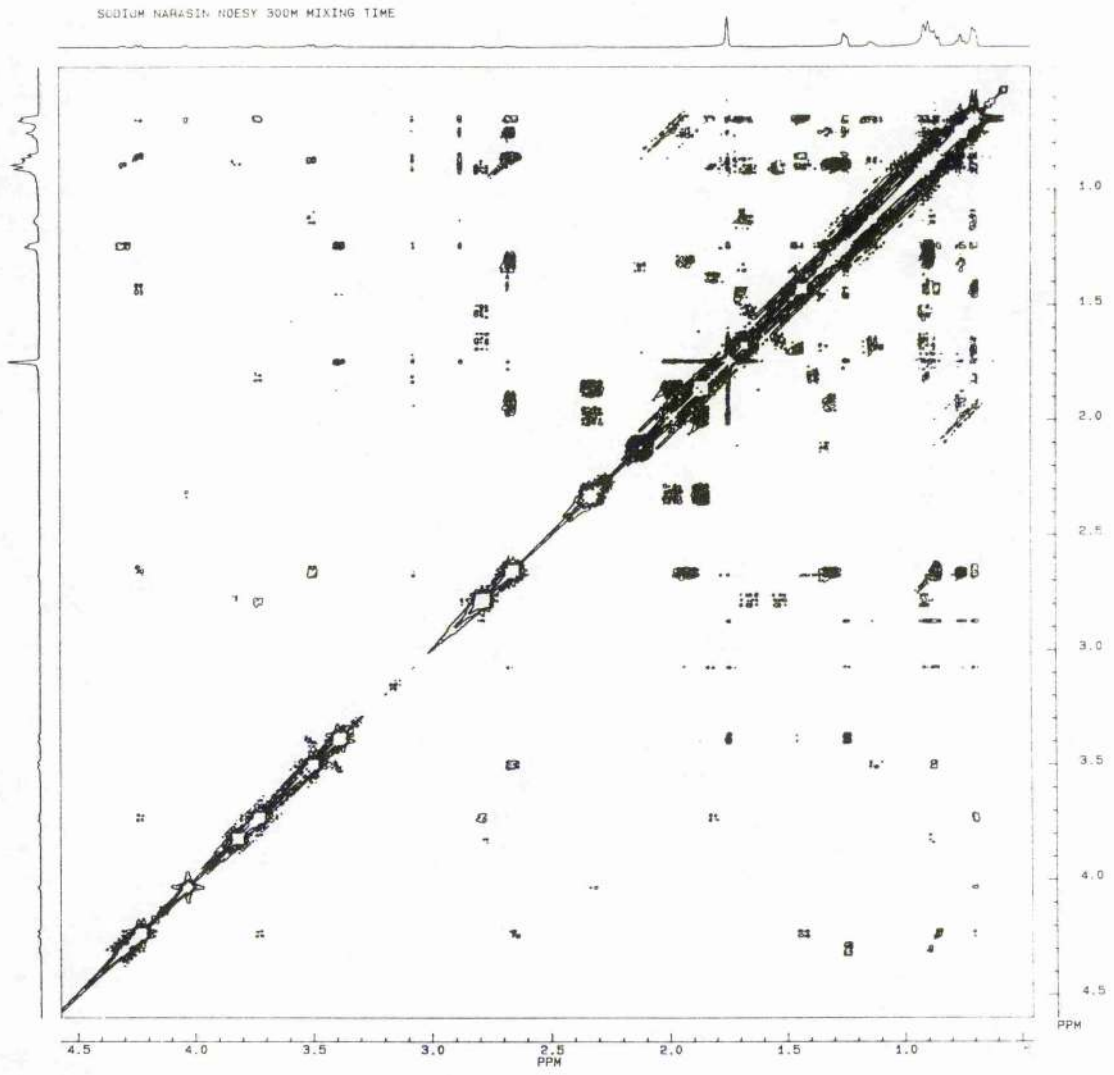

Figure 3-18. The ^{13}C spectrum of lithium salinomycin obtained with WALTZ-16 decoupling.

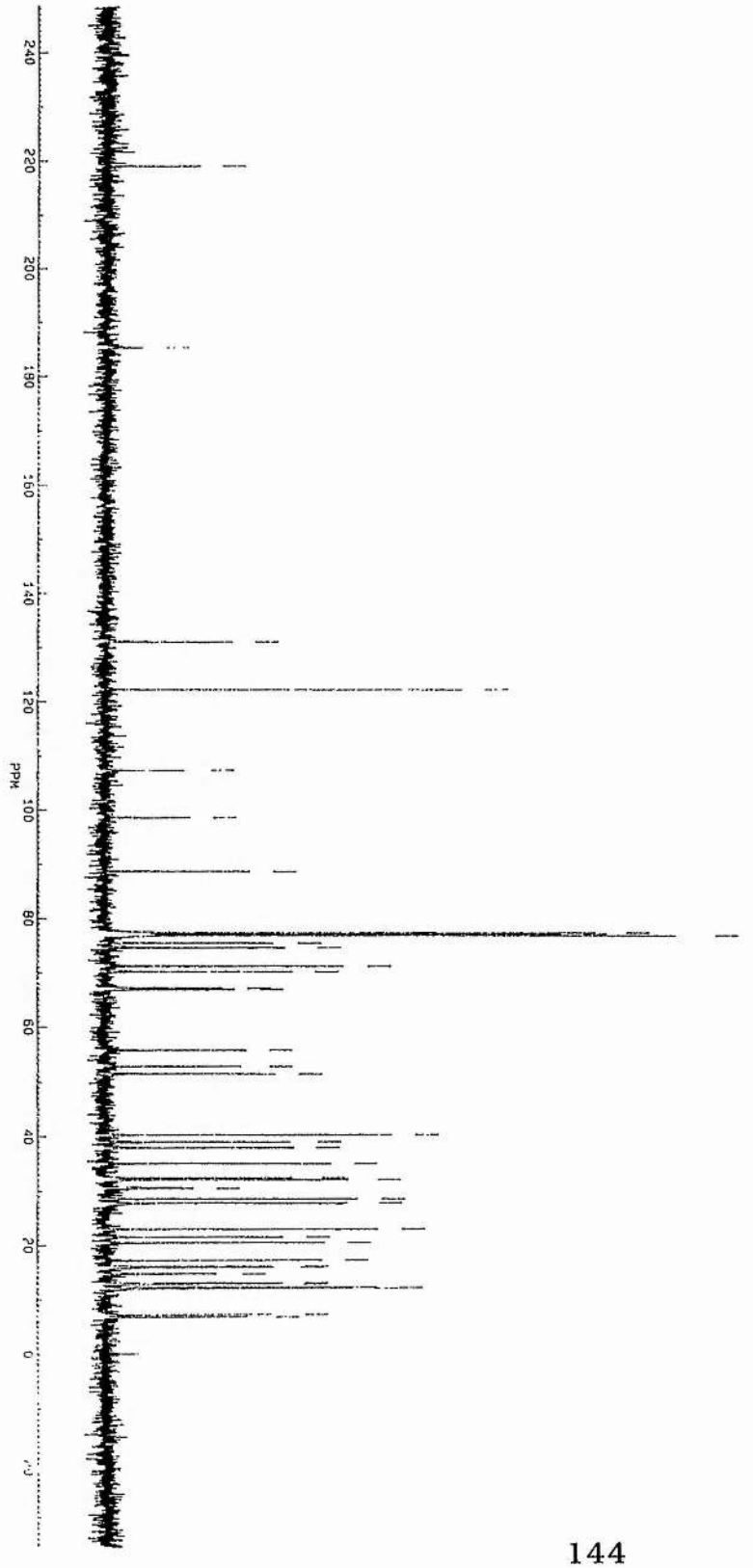

Figure 3-19. An expanded region of the XHCORD spectrum of sodium salinomycin.

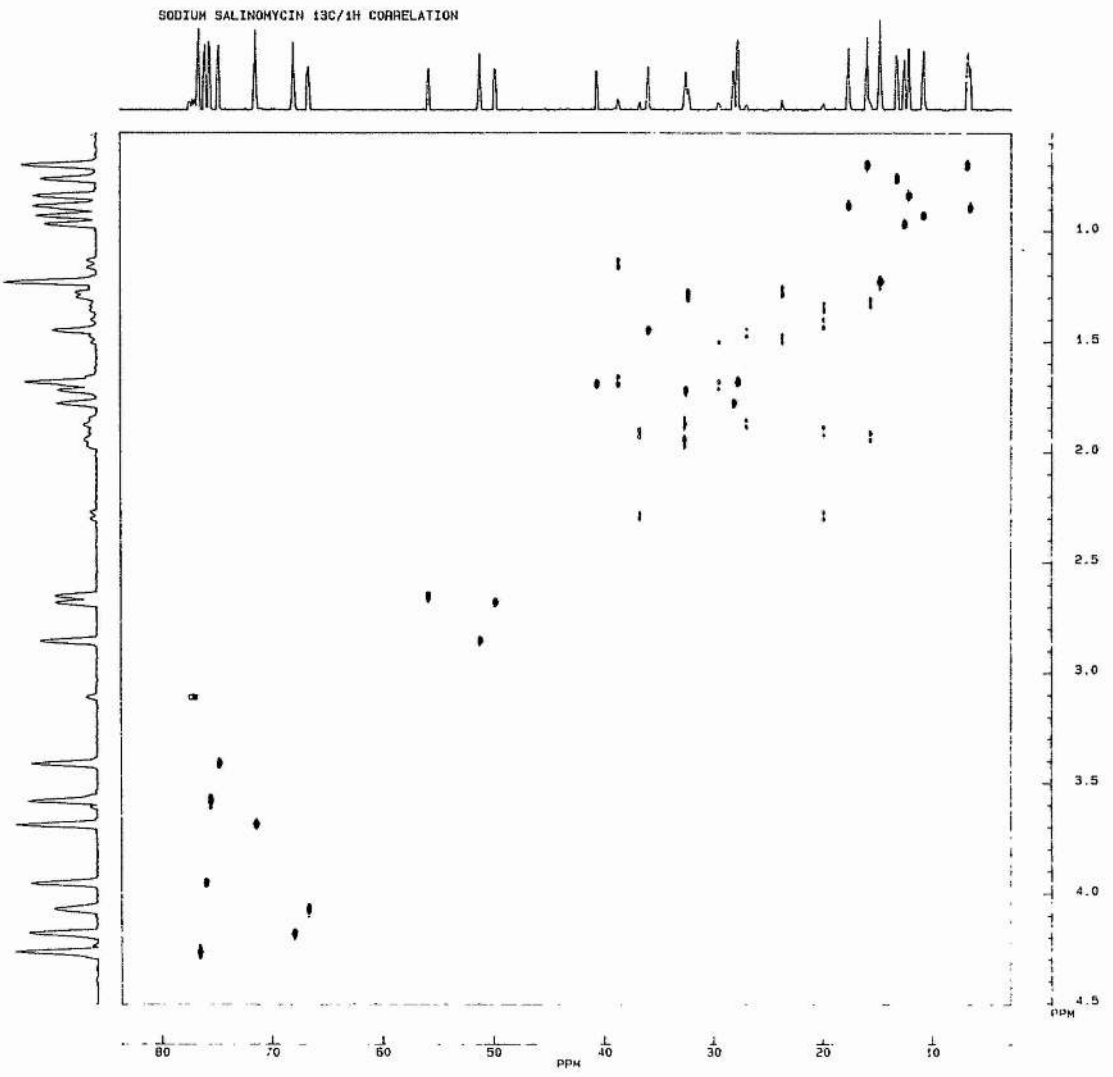

to be quantified at a molecular level. In this way the design of more ion selective ionophores should be possible on a more reasoned basis than trial and error. Areas where a greater, or lesser, degree of flexibility in the molecule would be advantageous can be identified and the required adjustments made.

This and the preceding work is a start on this road. The "hinge" areas, where the molecular flexibility lies, have been identified and the effect of different ions on the chemical shifts of these sites studied. There are computer programmes available to calculate structures from observed nmr data such as coupling constants and nuclear Overhauser effects.[30] The application of such a programme to this problem should be highly informative but unfortunately beyond the scope of this work. The data in this thesis is sufficiently good to show that changes occur in the conformation of these molecules and partially to explain them. To obtain more information the use of sophisticated software and powerful computers will be required.

In the following explanations of the trends seen in the chemical shifts, results for salinomycin acid from previously published papers have been used. The ^{1}H values used were those obtained by Anteunis and Rodios[21] in their study of this species. The ^{13}C values were those of Seto et al.[19] corrected to allow for possible misassignment. In this case what I believe to be the correct value for the resonance, from their published data, has been used. The assignments are given in Tables 3-2 to 3-5.

Table 3-2. The ^{1}H chemical shifts of the alkali metal complexes of salinomycin

Atom	H*	Li	Na	K	Rb	Cs
2	2.90	2.71	2.85	2.86	2.83	2.94
3	3.98	4.05	3.93	3.85	3.85	3.89
4d	1.93	1.85	1.89	1.89	1.88	1.92
4u		1.41	1.42	1.37	1.40	1.42
5d	1.60	1.84	1.88	1.95	1.93	1.89
5u		1.34	1.45	1.47	1.45	1.38
6	1.83	1.77	1.78	1.82	1.80	1.86
7	3.64	3.69	3.68	3.73	3.79	3.92
8	1.47	1.47	1.45	1.48	1.48	1.54
9	4.16	4.32	4.20	4.29	4.28	3.96
10	2.75	2.72	2.68	2.65	2.60	2.64
12	2.63	2.74	2.65	2.64	2.60	2.59
13	3.88	3.48	3.55	3.62	3.70	3.98
14	1.72	1.71	1.71	1.72	1.70	1.67
15d	1.61	1.70	1.68	1.65	1.62	1.62
15u	1.09	1.15	1.14	1.14	1.13	1.09
16	1.71	1.69	1.70	1.74	1.72	1.68
18	5.98	6.05	5.99	6.15	6.13	6.33
19	6.03	5.95	6.05	6.07	6.05	6.20
20	3.98	4.10	4.05	4.00	3.99	4.06
22d	2.40	2.27	2.31	2.41	2.36	2.28
22u	2.09	2.00	1.92	1.97	2.10	1.82
23d	2.23	2.00	1.95	1.89	1.88	1.97
23u	1.84	1.90	1.88	1.89	1.80	1.88
25	3.93	3.47	3.40	3.42	3.45	3.30
26d	1.54	2.25	2.25	2.09	2.05	2.10
26u	1.62	1.44	1.35	1.35	1.40	1.33
27d		1.77	1.70	1.67	1.68	1.70
27u		1.52	1.49	1.50	1.48	1.51
29	3.83	4.35	4.28	4.15	4.05	3.93
30	1.24	1.23	1.23	1.21	1.21	1.19
31d	1.39	1.31	1.28	1.33	1.39	1.40
31u	1.32	1.31	1.28	1.33	1.33	1.33
32	0.89	0.92	0.90	0.89	0.92	0.94
33	1.48	1.71	1.69	1.64	1.56	1.62
34	0.70	0.70	0.70	0.72	0.72	0.69
35	0.90	0.87	0.85	0.93	0.95	0.90
36d	1.93	1.98	1.90	1.94	1.94	1.93
36u	1.39	1.33	1.32	1.35	1.37	1.37
37	0.76	0.78	0.70	0.77	0.76	0.77
38	0.81	0.87	0.85	0.83	0.82	0.79
39	0.72	0.72	0.70	0.70	0.70	0.73
40	0.94	0.92	0.92	0.93	0.93	0.98
41d	1.54	1.48	1.49	1.48	1.46	1.49
41u	1.40	1.31	1.26	1.25	1.21	1.21
42	0.95	1.00	0.96	0.93	0.95	0.97

* These values are from the paper of Anteunis and Rodios.[21]
d, is the downfield proton, u, is the upfield proton.

Table 3-3. The ^{13}C chemical shifts of the alkali metal complexes of salinomycin.

Atom	H*	Li	Na	K	Rb	Cs
1	177.2	185.20	184.85	184.06	183.21	182.36
2	48.9	52.81	51.10	51.76	51.20	49.56
3	74.9	76.79	75.98	75.72	76.00	76.56
4	20.1	20.38	19.86	20.02	19.97	20.42
5	26.4	27.71	26.89	26.53	26.36	26.27
6	28.0	28.48	28.04	27.98	28.03	28.24
7	75.2[a]	71.18	71.37	71.25	71.06	71.43
8	32.6[b]	34.98	35.86	36.28	36.30	36.36
9	68.7	67.10	68.00	67.92	67.78	68.21
10	49.2	51.53	49.71	48.82	48.88	49.78
11	214.5	218.96	218.06	215.21	215.28	215.14
12	56.5	55.73	55.89	55.26	55.48	56.24
13	71.7[a]	74.53	75.54	76.40	76.13	74.88
14	36.5[b]	32.37	32.43	32.79	33.02	33.17
15	38.6	38.92	38.67	38.35	38.16	38.75
16	40.7	40.22	40.55	41.40	41.54	41.56
17	99.2	98.56	98.89	99.96	99.97	99.86
18	121.6	122.10	122.11	121.92	122.04	123.42
19	132.4	130.94	133.61	133.06	133.35	132.64
20	67.2	66.79	66.62	67.46	67.78	66.96
21	106.4	107.31	106.98	107.82	107.68	107.49
22	36.2	37.86	36.85	34.70	35.36	35.14
23	30.2	32.11	32.52	32.67	32.77	33.46
24	88.5	88.54	88.47	88.57	88.29	87.63
25	73.7	75.47	74.71	74.01	73.84	74.96
26	21.9	20.38	19.86	19.25	19.31	19.95
27	29.3	30.44	29.36	28.04	27.90	28.88
28	70.9	70.13	70.25	71.25	71.20	71.43
29	77.2	77.39	76.56	76.50	76.81	76.56
30	14.5	14.61	14.63	14.68	14.67	14.90
31	30.6	32.06	32.21	32.06	31.74	31.96
32	6.3	6.74	6.50	6.19	6.16	6.77
33	25.8	27.69	27.59	27.71	26.84	27.90
34	17.9[c]	15.80	15.85	15.59	15.60	15.75
35	15.6[c]	17.09	17.57	18.11	18.31	18.28
36	22.7[d]	16.00	15.55	15.85	15.94	16.41
37	11.9[e]	12.93	13.15	13.22	13.22	13.61
38	12.8	11.92	12.05	12.43	12.60	12.75
39	7.0	7.12	6.75	6.64	6.71	7.14
40	11.2	12.10	10.74	10.98	11.24	12.21
41	16.6[d]	22.88	23.56	24.17	23.79	23.08
42	13.2[e]	12.77	12.44	12.26	12.30	12.94

* These values are from the paper of Seto et al[19] and are given here as published. [a-e], we believe these pairs of values should be exchanged.

Table 3-4. The ^{1}H chemical shifts of the alkali metal complexes of narasin.

Atom	H	Na	K	Rb	Cs
2	2.77	2.80	2.78	2.75	2.78
3	3.91	3.82	3.80	3.79	3.82
4	2.27	2.28	2.27	2.27	2.27
5d	1.72	1.79	1.82		1.84
5u	1.45	1.40	1.39	1.37	1.36
6	1.89	1.83	1.84	1.83	1.86
7	3.61	3.74	3.73	3.80	3.87
8	1.49	1.45	1.45	1.45	1.48
9	4.16	4.26	4.28	4.28	4.20
10	2.78	2.67	2.63	2.60	2.64
12	2.62	2.69	2.61	2.59	2.60
13	3.86	3.50	3.64	3.70	3.82
14	1.74	1.72	1.72	1.71	1.68
15d	1.64		1.64	1.63	1.63
15u	1.11	1.14	1.14	1.14	1.09
16	1.72	1.72	1.75	1.75	1.70
18	6.05	6.05	6.05	6.04	6.11
19	6.01	6.00	6.11	6.09	6.18
20	3.97	4.04	3.98	4.00	4.03
22d	2.39	2.34	2.41	2.36	2.31
22u	2.06	1.87	2.00	2.15	1.96
23d	2.24	1.98	1.87	1.89	1.88
23u	1.83	1.87	1.87	1.76	1.88
25	3.89	3.40	3.43	3.46	3.40
26d	1.65	2.11	2.06	2.01	2.03
26u	1.52	1.36	1.37	1.43	1.39
27d	1.63	1.70	1.68	1.70	1.69
27u	1.63	1.47	1.50	1.49	1.53
29	3.84	4.32	4.15	4.09	3.90
30	1.23	1.26	1.22	1.21	1.20
31	1.35	1.30	1.32	1.35	1.32
32	0.89	0.90	0.90	0.93	0.91
33	1.47	1.78	1.63	1.55	1.57
34	0.70	0.72	0.73	0.72	0.72
35	0.91	0.89	0.93	0.95	0.93
36d	1.95	1.94	1.95	1.95	1.92
36u	1.38	1.33	1.34	1.36	1.39
37	0.77	0.76	0.77	0.77	0.77
38	0.83	0.87	0.83	0.82	0.84
39	0.75	0.70	0.71	0.70	0.71
40	0.94	0.91	0.92	0.92	0.92
41	0.90	0.89	0.89	0.90	0.92
42d	1.63	1.67	1.62	1.60	1.54
42u	1.63	1.53	1.56	1.54	1.54
43	0.92	0.92	0.88	0.88	0.89

d, is the downfield proton, u, is the upfield proton.

Table 3-5. The ^{13}C chemical shifts of the alkali metal complexes of narasin

Atom	H	Na	K	Rb	Cs
1	177.70	184.65	184.08	183.01	182.03
2	49.83	51.21	51.42	51.24	50.78
3	77.97	79.08	79.18	79.49	79.92
4	28.15	28.56	28.46	28.61	29.05
5	35.65	36.33	36.05	35.91	35.77
6	28.94	29.15	29.26	29.26	29.43
7	72.74	71.62	71.41	71.28	71.13
8	36.02	36.02	36.40	36.43	36.57
9	68.75	68.57	68.29	68.15	68.29
10	49.50	49.38	48.81	48.95	49.16
11	216.20	217.70	215.79	215.15	214.94
12	56.27	55.83	55.40	55.57	55.82
13	73.73	75.99	76.40	76.13	77.02
14	32.83	32.48	32.77	33.03	33.35
15	38.76	38.72	38.30	38.09	38.55
16	40.95	40.70	41.33	41.40	41.53
17	99.61	99.24	99.91	99.94	99.88
18	122.35	122.24	122.03	122.17	122.86
19	132.35	130.94	132.96	133.34	132.78
20	67.74	66.49	67.57	67.94	67.15
21	106.62	107.31	107.71	107.47	107.44
22	36.48	35.60	34.94	35.50	35.41
23	30.33	32.66	32.55	32.69	33.15
24	88.62	88.37	88.57	88.30	87.91
25	75.57	75.16	73.90	73.69	74.46
26	22.11	19.97	19.23	19.31	19.67
27	29.28	29.36	27.67	27.66	28.83
28	71.07	70.48	71.52	71.49	71.25
29	77.14	77.06	76.75	76.93	75.53
30	14.30	14.88	14.63	14.69	14.74
31	30.67	32.20	31.93	31.67	31.62
32	6.33	6.49	6.18	6.18	6.38
33	25.71	28.20	27.43	26.61	27.35
34	15.69	15.74	15.57	15.54	15.71
35	17.89	17.54	18.13	18.29	18.37
36	16.58	15.60	15.77	15.98	16.29
37	13.19	13.10	13.18	13.21	13.38
38	13.07	12.43	12.47	12.65	13.00
39	7.37	6.86	6.78	6.90	7.19
40	12.74	11.64	11.79	12.07	12.50
41	18.33	19.41	19.76	19.73	19.83
42	23.63	24.82	25.07	24.55	23.95
43	12.09	12.65	12.47	12.55	12.76

3.3.3 Conformational variations identified by changes in chemical shift.

As has been stressed before, salinomycin and narasin have very similar structures, differing only in the presence of a methyl group at C(4). It is this group therefore which must cause any differences in the selectivity or transport properties exhibited by these materials. It is in the vicinity of this group that one would expect the greatest differences to be seen between the behaviours of salinomycin and narasin. If a molecular model is constructed then one sees that a *cis*-methyl substituent on C(4) hinders the rotation about the C(2)-C(3) bond. This is borne out by the evidence in both the ^{1}H and ^{13}C spectra. In the proton spectrum for salinomycin the chemical shift due to C(2)-H is observed to decrease by 0.2 ppm on complexation with lithium. The value is then seen to increase along the series of alkali metals until it has returned to roughly its original position in the cæsium salt. With narasin the observed change is only very small, 0.05ppm, across the entire sequence. In the ^{13}C chemical shifts a similar difference of behaviour is observed. In both cases there is a change in the chemical shift on complexation but it is much larger for salinomycin than narasin, 3.9ppm as opposed to 1.4ppm. After this a 3.3ppm increase is observed along the series for salinomycin with the narasin chemical shift remaining virtually constant. As in the ^{1}H spectra the largest changes observed are for the free acid and cæsium salt. These values show that these two species require the greatest conformational reorganisation at this site. It is of interest to note the similarity between the chemical shifts for the acid and cæsium complexes at this site in both ^{1}H and ^{13}C spectra.

This may mean that the conformations of these species around this site are similar.

The early ^{13}C work included measurements of T_1 relaxation times of the signals in the spectra. Of interest was C(41) in narasin which was seen to relax with abnormally rapidity, the T_1 being more like those of the methylene groups than the other methyls. This was attributed to the methyl being prevented from rotating by a proton on C(42), Figure 3-8. This would bring these protons into very close proximity and would be expected to produce a large NOESY cross peak. No such peak was observed in any of our spectra so possibly this reasoning is incorrect.

In this portion of the molecule the other atom for which the chemical shift varies is C(1). This is the carbon of the carboxylic acid group and as such would be expected to be considerably affected by the cation present. A large increase in chemical shift of over 7.0 ppm is seen for both salinomycin and narasin on complexation. The examination of tables of chemical shift data[31] shows that this is a typical value for the difference between the acidic and anionic forms of a carboxyl group. There is a further marked decrease, over 2.5ppm, across the rest of the series of alkali metal ions. This change may be due to the diffuseness of the charge on the metal ion. If this were the case the difference between the lithium and sodium complexes would be expected to be the greatest, not the least as is seen here. This is evidence that this site is not directly bound to the complexed ion. The anomalous differences observed may be due to orientation effects with the cation complexed at sites remote from the anionic centre, with other groups masking the charge.

Two "hinge" regions have been identified in the molecule.[21] These are areas where the skeleton is flexible and can alter to accommodate different sized ions, as well as enabling the molecules to "wrap" themselves around the cation during the complexation process. In salinomycin and narasin these "hinge" regions are located at either end of the rigid dispiroketal moiety in the molecule. That there are conformational changes in the molecules at these sites can be seen from the chemical shift data. It is in these areas that the largest changes occur when the bound cation is changed.

The simpler of these regions to study is at C(24) to C(25) as only one carbon - carbon bond is involved. In the ^{1}H spectra very similar behaviour is seen in this area for both narasin and salinomycin. On complexation there is an increase of ca. 0.5ppm for C(25)-H, an increase of ca. 0.5ppm for one of the protons on C(26) and an increase at Me(33) of ca 0.2ppm in salinomycin and 0.3ppm in narasin. These changes must reflect large changes in the conformation on complexation but interestingly there is little change along the rest of the series, except for Me(33) in narasin. This possibly reflects the formation of the hydrogen bond between the carboxylate anion and C(28)-OH. In the free acid this bond may be absent and the conformation different in this portion of the molecule. In the paper by Anteunis and Rodios[21] some predicted values of the chemical shifts were published. These came from some empirical rules derived by comparing the chemical shifts of many polyether antibiotics.[32] They noticed that if the equivalent atoms to C(25) were in contact with the solvent then the predicted value of the chemical shift was ca 0.3ppm higher than

expected. This would explain in part the difference seen in these values. Similar behaviour was observed at C(29)-H which probably has its origins in the same effect.

The changes in conformation about the C(24) - C(25) bond are also shown in the ^{13}C spectra. The largest changes for C(33) are observed on complexation, where there is a change of 2.5ppm in narasin and 1.8ppm in salinomycin. After this the salinomycin resonance remains roughly constant but the narasin spectrum shows a 1.6ppm decrease to the rubidium salt with the cæsium salt at a slightly higher chemical shift. This mirrors the behaviour of the proton resonances. There are also large changes (>2.0ppm) in the chemical shifts at C(23) and C(26) between the free acid and the sodium salt. Again there is little change along the rest of the series of alkali metals. This implies that this area undergoes a large conformational change on complexation with little change as the ions increase in size. It is interesting to note that there is more conformational rearrangement in this region with narasin, than is the case for salinomycin. This is possibly due to the loss of flexibility about the C(2)-C(3) bond. This holds the carboxylate group in a fixed position. If the hydrogen bond is to be maintained the flexibility must arise somewhere.

The other hinge region is in the C(7) to C(13) portion of the molecule specifically between C(10) and C(12). This area also exhibits changes in the chemical shift with different cations. Again the changes only occur at certain atoms and there are differences between the behaviour of salinomycin and that of narasin in this region. The resonances of greatest interest in the ^{1}H spectra are those due to C(7)-H, C(9)-H and C(13)-H. In the

carbon spectra the resonances of interest are C(11) and C(13). It is C(13)-H that shows the greatest variation implying that this is of key importance in the complexation. The basic trends are the same for salinomycin and narasin but there are interesting differences. On complexation a large decrease in the chemical shift is seen from 3.88 to 3.48ppm in salinomycin and from 3.86 to 3.50ppm in narasin. In both cases there is an upward trend of ca. 0.2ppm to the rubidium salt. It is at this point that the major difference occurs. In narasin there is a further increase of 0.12ppm between the rubidium and the cæsium salts, in the case of salinomycin the equivalent difference is 0.28ppm. This possibly reflects a large change in the conformation at this site between rubidium salinomycin and cæsium salinomycin.

Is there any other evidence for this hypothesis? It is seen that in salinomycin the COSY cross peak from the C(12)-H to C(13)-H coupling varies in intensity with the cation present. There are no large changes across the series with narasin. In lithium salinomycin this cross peak is of relatively low intensity but it is much stronger in the sodium, potassium and rubidium salts it is however completely absent in the cæsium spectrum. This coupling is always small, usually between 0.5 and 1Hz, and is rather difficult to measure from the normal spectrum. Even under resolution enhancement the coupling for cæsium salinomycin could not be resolved. This means that, from the Karplus equation,[33] the angle about this bond is almost 90°. For the other salts the angle here is in the region of either 75° or 105°. It is difficult to know for certain due to the symmetry of the dependence of coupling constant on the angle between the planes

containing the two groups. It is also of interest to note that there is a COSY cross peak between C(13)-H and Me(37)-H, a five bond coupling, in all the spectra except lithium salinomycin and cæsium salinomycin.

In the ^{13}C spectra the behaviour at C(13) is different for salinomycin and narasin. In narasin there is a 2.3ppm increase in the chemical shift on complexation with sodium. Along the rest of the series there is a further increase of 1.0ppm. This pattern of a large initial change followed by a more gradual alteration is also seen in the ^{1}H spectrum. In this case the shift is probably due to γ-gauche interactions so a rotation about the C(11) - C(12) bond or possibly the C(12) - C(36) bond could be a causal factor. The presence of a five bond coupling from C(13)-H to Me(37)-H is evidence that in narasin it is not rotation of the ethyl group that is the cause of this change. This means that the rotation is almost certainly about the C(11) - C(12) bond. This is more likely to allow the complexation of a larger cation than the mere rotation of a side arm. In salinomycin the trends are more difficult to identify as this is one of the sites where it appears that there was a misassignment of the ^{13}C resonance by Seto et al.[19]. If this is in fact the case then there is no large shift at C(13) on complexation but there is a rise of 1.9ppm between the lithium and potassium complexes followed by a drop of 1.5ppm to cæsium. So the behavour around this site is different in narasin from that exhibited by salinomycin.

The carbonyl at C(11) is the sterically least hindered group in this portion of the molecule. The observed shifts seen on changing the solvent polarity are attributed to changes in the

orientation of this group[27]. This would have an effect on the shielding of the adjacent protons. This is one of the conformationally best characterised areas of the molecule due to the circular dichrosim studies mentioned earlier.[25,26] These showed that the conformation is similar at this site in the free acid and the cation bound forms as the differential absorptions are similar. Those of the anionic form are greatly different.

The data in this thesis disagrees on several counts with the early assignments of the ^{13}C work. There appear to be fifteen misassignments in the work of Dorman et al[16] for narasin acid. The assignments of sodium salinomycin from Seto et al[19] seem to be more accurate with only five pairs of values which should be exchanged. It is impossible to state unequivocally from the data presented here, that the resonances for the free acid are similarly misassigned, but they have been treated as such in the above discussion.

The ^{1}H assignments agree on almost all points with those previously published. The assignments given here are more complete than those published by Anteunis and Rodios[21] and only disagree on the assignment of C(18)-H and C(19)-H in narasin acid. It is easy to identify these from the carbon-hydrogen correlation spectra and the assignments here agree with those of Caughey et al.[28]

3.3.4 The effect of solvent on complex conformation.

It is interesting to note the effect of solvent on the chemical shifts of the cation bound ionophores. It has been seen[27] that in narasin free acid there is a large change in the chemical shifts at

certain sites on changing solvent from chloroform to methanol. Comparing the values given here for sodium and potassium narasin with those published by Caughey et al.[28] shows similar, but less marked, changes at certain sites. The sites where the largest changes are observed are in the C(10) to C(12) region of the spectrum which is as may be expected. Interestingly there is little change observed at C(25)-H in the sodium and potassium salts. The observed stability of the chemical shift here implies that there is no large conformational rearrangement. The effect seen here in this data is probably due to the loss of a solvent interaction on complexation. Once the complex was formed there was little difference in chemical shift with different cations. Thus, the complex is conformationally fixed at this site independent of solvent polarity or cation size.

The observed changes at C(10) are much smaller for the cation bound forms than for the free acid ca. 0.10ppm and 0.46ppm respectively. The observed changes for C(12)-H are roughly comparable, increases of 0.17ppm in narasin free acid, 0.18ppm in potassium narasin and 0.11ppm in sodium narasin on changing solvent from chloroform to methanol. The observed changes at C(13)-H are also very different. This is one of the sites at which a large change is seen on altering the bound cation. A 0.3ppm decrease is seen in narasin acid on changing solvent from chloroform to methanol. In the sodium salt there is a decrease of 0.11ppm on the same change being made, but the chemical shift of the potassium salt stays the same. From the published data it seems that in methanol-d_4 the chemical shifts of all three forms is the same. This is far from true in chloroform where there is a

0.36ppm decrease on complexation with sodium and a 0.14ppm increase on replacing the sodium with a potassium ion. This implies that there is a much larger conformational rearrangement required in chloroform than methanol to allow complexation. So in a less polar solvent the conformation of the free acid is markedly different from that of the final complex whereas in a polar complex the conformations are similar. The chemical shift of the apo (anionic) form in methanol is also similar to those of the cation bound and free acid forms.

A site at which there is an unexpected variation in the chemical shifts is in the vinylic region of ring C. This is the middle ring of the dispiroketal moiety and as such would be expected to be rigid. There is a variation observed in both the ^{1}H and ^{13}C spectra with changing cation and in the ^{1}H spectra with changing solvent. In the ^{13}C spectra the largest change is seen at C(19) with a ca 2.4ppm increase in both salinomycin and narasin. The highest value for C(19) is for the rubidium salt in both cases with the lowest for the sodium salt in narasin and the lithium salt in salinomycin. In salinomycin there is also an increase of 1.8ppm at C(18) from the free acid to the cæsium salt. In the 1H spectra the trends are similar with there being more change at C(18)-H in salinomycin than narasin. In salinomycin there is an increase of 0.35ppm from the free acid to the cæsium salt atC(18)-H. The comparable increase at C(19)-H is only 0.17ppm but the lithium salt is 0.08ppm lower than the free acid. It can be seen that in salinomycin acid and sodium salinomycin it is the C(18)-H which gives the upfield peak with the reverse being true for all the other salts.

The reverse of this is seen in the narasin series. In narasin the larger change, 0.18ppm, is seen at C(19)-H on changing cation. On changing solvent it is at C(18)-H that the larger change is observed for all three derivatives. In this connection it may be worth noting the effect of altering the structure in this area has on the transport properties.[24] Hydrogenation of the double bond decreases the activity as also does oxidation of the vinylic hydroxyl. Acylation of this hydroxyl however was seen to have a beneficial effect on the transport rates and antimicrobial activity.[24] This site must be important in the complexation for some reason, even if only geometric. The flexibility in this area is somewhat limited but there could still be a ring flip or at least a slight flex. The coupling constants between C(18)-H and C(20)-H and C(19)-H and C(20)-H are always small but do vary with changing cation see Table 3-6. This means that there is some change in the relative conformations of the two sites. There is also a change on changing solvent. The first thing to notice is that in salinomycin it is the coupling constant between C(19)-H and C(20)-H that is the larger whereas in narasin the greater coupling is between C(18)-H and C(20)-H. The C(18)-H to C(19)-H coupling is constant as would be expected.

In salinomycin there is a large change in the C(18)-H to C(20)-H coupling constant. This decreases from 2.0Hz in lithium salinomycin to ca. 0.5Hz in both the free acid (as given by Anteunis and Rodios[21]) and the cæsium salt. From the examination of a

Table 3-6. The apparent coupling constants for the vinylic region of salinomycin.

	H*	Li	Na	K	Rb	Cs
18-19	10.9	10.8	11.0	11.0	10.8	11.0
18-20	0.6	2.0	1.5	1.3	1.0	0.5
19-20	1.7	2.5	2.7	2.8	2.5	3.0

The values denoted * are taken from the data of Anteunis and Rodios.[21]

Table 3-7. The apparent coupling constants for the vinylic region of narasin.

	H	Na	K	Rb	Cs
18-19	11.0	10.8	11.2	10.5	11.0
18-20	2.0	2.2	2.7	2.5	2.0
19-20	0.5	1.0	0.8	0.7	0.5

model there is at most ca 55° of twist possible about the C(19)-C(20) bond , roughly 30° to 85°. From the Karplus equation[33]

$$^3J = 8.5\cos^2\phi - 0.28$$

the coupling constants would be ~ 6Hz at 30° and ~ 0Hz at 85°. Applying these equations to this system shows that there is about a 20° twist about this site. In narasin there is little change in the coupling constants with either solvent or cation. The maximum difference being about 0.5 Hz a less than 10° rotation.

The Karplus equation was postulated for ethane, an sp^3-sp^3 system, so it is uncertain how accurate these values actually are in an sp^2-sp^3 system such as there is here. The coupling constant will vary with the angle between the planes containing the protons, so there is a much more flexibility around this site in

salinomycin than is the case in narasin. So there are changes of conformation in even the most rigid portions of the molecule. The hydroxyl on C(20) is one of those which takes part in the complexation of a cation. It is possible that the observed change is due to this group changing orientation to allow a stronger interaction to occur. It is unusual that the ^{4}J C(18)-H-C(20)-H coupling in narasin should be larger than the three bond coupling C(19)-H to C(20)-H. This must be due to the vinylic nature of this interaction, although this does not explain why this is not the case in salinomycin.

Summing up the effect of solvent polarity on the conformation of the cation bound ionophore it seems to be safe to say that there are differences in the conformations. The changes are smaller however than for the corresponding free acid. Thus the ionophore/cation complex is well defined conformationally and not greatly affected by the polarity of the solvent.

3.4 Experimental.

All spectra were taken on a Bruker MSL500 nmr spectrometer using the decoupler coils of the high resolution probe. For the 2D spectra 2048 fid's of 4k each were collected zero filled to 4k in the second dimension. Fourier transform was carried out in magnitude mode with sine bell apodisation in each dimension. The spectral quality was further improved by symmetrisation about the main diagonal. NOESY spectra were acquired with mixing times of between 100 and 300 ms . A recycle time of around 1.6-2.5s was used for all the ^1H spectra. For the XHCORD spectra 512 fid's of 4k datapoints were collected these were zero filled in the ^1H dimension to 1 or 2k. Spectra were selected for both 160Hz and 12Hz coupling constants.

The salinomycin, as the sodium salt, was donated by Hoechst A.G. The narasin, as the free acid, was donated by Eli Lilly Inc. Both of these were use without further purification.

The samples were all prepared using a similar method. Ionophore 50mg was disolved in $CDCl_3$ (~ 0.5 cm^3) in a sample bottle. To this metal chloride (~3g) and distilled water (~0.5cm^3) was added and the mixture stirred for at least 1h at room temperature. The organic layer was removed in a Pasteur pipette and dried by filtration through a plug of anhydrous metal carbonate into a 5mm nmr tube. Samples of rubidium carbonate and cæsium carbonate were made by reaction of the metal hydroxide in solution with solid carbon dioxide. Most of the water was removed by distillation at reduced pressure. The salt was further dried on an oil pump and stored over silica gel in a vacuum desicator.

References to Chapter 3.

[1]Jeener, J., 1971 Ampere International Summer School, Basko Polje, Yugoslavia.

[2]Freeman, R., (1980), *Proc. R. Soc. Lond.*, **A373**, 149-178.

[3]For a general introduction to modern nmr techniques see, Derome, A.E., *Modern NMR Techniques for Chemical Research.* (1987), Pergamon. Oxford.

[4]Derome, A.E., (1987), *Modern NMR Techniques for Chemical Research.*, Pergamon. Oxford. Ch 8.

[5]Redfield, A.G. and Kunz, S.D., (1975), *J. Magn. Reson.*, **19**, 250-254.

[6]Bax, A. (1982), *Two dimensional NMR in Liquids.*, Delft University Press, Dordtrecht.

[7]Marion, D. and Würtrich, K., (1983), *Biochem. Biophys. Res. Commun.*, **113**, 967-974

[8]Meier, B.H. and Ernst, R.R. (1979), *J. Am. Chem. Soc.*, **101**, 6441-6442.

[9]Overhauser, A.W. (1955), *Phys. Rev.*, **92**, 411-415.

[10]Bell, R.A. and Saunders, J.K., (1970), *Can. J. Chem.*, **48**, 1114-1122.

[11]Freeman, R. (1988), *A Handbook of Nuclear Magnetic Resonance*, Longman, Harlow.

[12]Shaka, A.J., Keeler, J. and Freeman, R. (1983), *J. Magn. Reson.*, **53**, 313-340.

[13]Doddrell, D.M., Pegg, D.T. and Bendall, M.R. (1982), *J. Magn. Reson.*, **48**, 323-327.

[14]Anteunis, M.J.O. (1982), In *Polyether Antibiotics*, Westley, J.W. (Ed), Marcel Dekker, New York. pp 245-334.

[15]Seto, H. and Otake, N. (1982), In *Polyether Antibiotics*, Westley, J.W. (Ed), Marcel Dekker, New York. pp 335-398.

[16]Dorman, D.E., Paschal, J.W., Nakatsukasa, W.M., Huckstep, L.L. and Neuss, N. (1976), *Helv. Chim. Acta*, **59**, 2635-2634.

[17]Occolowitz, J.L., Berg, D.H., Debono, M. and Hamill, R.L. *Biomed. Mass. Spect.*, **3**, 272-277.

[18]Seto, H., Yahagi, T., Miyazaki, Y. and Otake, N. (1977), *J. Antibiot.*, **30**, 530-537.

[19]Seto, H., Miyazaki, Y., Fujita, K-i. and Otake, N. (1977), *Tetrahedron Lett.*, **28**, 2417-2420.

[20]Anteunis, M.J.O. and Rodios, N.A. (1981), *Bull. Soc. Chim. Belg.*, **90**, 471-480.

[21]Anteunis, M.J.O. and Rodios, N.A. (1981), *Bull. Soc. Chim. Belg.*, **90**, 715-735.

[22]Westley, J.W., Blount, J.F., Evans, R.H. Jr. and Choa-Min, L. (1977), *J. Antibiot.*, **30**, 610-612.

[23]Kinashi, H., Otake, N., Yonehara, H., Saito, S. and Saito, Y., (1975), *Acta. Cryst.*, **B31**, 2411-2415.

[24]Miyazaki, Y., Kinashi, H., Otake, N., Mitani, M. and Yamanishi, T., (1976), *Agric. Biol. Chem.*, **40**, 1633-1640.

[25]Painter, G. and Pressman, B.C., (1979), *Biochem. Biophys. Res. Commun.*, **91**, 1117-1122.

[26]Caughey, B.W., Painter, G.R. and Gibbons, W.A. (1986), *Biochem. Pharmacol.* **35**, 4103-4105.

[27]Gibbon, W.A., Painter, G.R. and Pressman, B.C., (1983), *Biochem. Biophys. Res. Commun.* **113**, 832-838.

[28]Caughey, B.W., Gibbons, W.A. and Painter, G.R., (1989), *Magn. Res. Chem.*, **27**, 403-406.

[29]e.g. Shen. C. and Patel, D.J., (1976), *Proc. Nat. Acad. Sci. USA.* **73**, 4277-4281.

[30]e.g. Kessler, H. Will, M., Antel, J., Beck, H. and Sheldrick, G.M., (1989), *Helv. Chim. Acta.*, **72**, 530-555.

[31]Breitmaier, E., Haas, G. and Voelter, W., (1979), *Atlas of ^{13}C data.*, Heyden, London.

[32]Borremans, F. and Anteunis, M.J.O., (1981), *Bull. Soc. Chim. Belg.*, **90**, 1045-1053.

[33]Karplus, M. (1959), *J. Chem. Phys..*, **30**, 11-15.

Chapter 4

Chapter 4. A study of some synthetic ionophores for both anions and cations.

4.1 Introduction.

4.1.1 Anion Transport.

The transport of anions, in particular chloride, across the limiting membranes of cells is very important. For example, chloride is the counter-ion transported by the Band 3 protein to replace bicarbonate ions inside the cells. This is the process by which the carbon dioxide produced during respiration is removed from the cells to the blood stream.[1] It is also believed that cystic fibrosis is caused by abnormalities in the chloride transport.[2] For these reasons an understanding of the chloride transport process, and the development of nmr methods for monitoring it, are important.

NMR has been widely and successfully used to study cation transport across membranes, see chapter 2, and the halides should be equally amenable to study using this technique. ^{35}Cl, ^{37}Cl, ^{79}Br and ^{81}Br are all nmr active and relatively easy to observe although they are all quadrupolar nuclei.[3] Their sensitivities are all greater than that of ^{13}C but as they are quadrupolar they give greater linewidths. In compensation, the shorter relaxation times allow data to be acquired much more rapidly. The problem with studying the transport of halide ions in phospholipid vesicles is to generate a contrast between the signals due to the ions inside the vesicles and those outside. Such contrast reagents were encountered earlier, in the work on cation

transport (Chapter 2) so no further discussion of their desired properties will be entered into here.

There have only been very few studies of chloride transport through biological membranes using nmr. These have tended to concentrate on erythrocytes[4] where the internal chloride signal is invisible due to rapid quadrupolar relaxation. This is caused by interactions between the ^{35}Cl and proteins inside the cell. Quadrupolar relaxation is governed by the equation:

$$T_{1q}^{-1} = T_{2q}^{-1} = \frac{3\pi^2}{10} \cdot \frac{(2I + 3)}{I^2 (2I - 1)} \cdot \chi^2 \cdot (1 + \eta^2/3) \cdot \tau_c$$

$$\chi = \frac{e^2 . q_{zz} . Q}{h}$$

where:

I	=	spin quantum number.
χ	=	nuclear quadrupole coupling constant.
τ_c	=	correlation time.
e	=	charge on an electron.
Q	=	quadrupole moment.
q_{zz}	=	the largest component of the electric field gradient.

I	1	3/2	5/2	3	7/2	9/2
$\frac{(2I+3)}{I^2 (2I-1)}$	5	$\frac{4}{3}$	$\frac{8}{25}$	$\frac{1}{5}$	$\frac{20}{147}$	$\frac{2}{27}$

Thus, the relaxation is slowest and the line sharpest when I is large, Q is small and the electric field gradient is small.

Inside the cell there will be many species, e.g. proteins, containing cationic groups if the chloride ion is attracted to such a species it will be at a site with a high electronic field gradient and

its mobility will be reduced. The less mobile a nucleus is the broader its line will be so a chloride ion attached to a large protein will be very restricted in its mobility and so will show a broadened line possibly to the point of making the line invisible.

The only published work on a contrast reagent for halide ions inside vesicles is by Riddell et al.[5] This study used manganous ions as a relaxation agent for the chloride signal. This broadens but does not shift the "out" peak leaving the "in" peak unchanged enabling the two to be distinguished. It was observed that although manganous ions produced good line broadening they also rapidly destroyed the vesicles. This was believed to be due to interactions between the coordination sites on the manganese and the bilayer surface. Stable manganese (II) complexes were prepared to try, unsuccessfully, to retard this process to enable measurements to be taken. If a phosphate was added to the solution in the ratio of 8:1 PO_4:Mn then the vesicles were found to be stabilised sufficiently for rates to be measured. This was found to be due to the lowering of the pH of the solution, required to dissolve the manganese (II) phosphate, rather than any property of the phosphate ions themselves.

Once a contrast system had been found this enabled rate measurements to be made with ionophoric materials. The first such material tried was tetrabutylammonium chloride, known to be a phase transfer reagent.[6] This was observed to mediate transport in phospholipid bilayers at a rate ca 3.5 times that of vesicle destruction. The other material studied was valinomycin, a naturally occurring neutral ionophore, (see Figure 1-4). It has been postulated that valinomycin, which is potassium selective,

carries a chloride ion as an ion pair when complexed with a cation,[7] much as is seen to occur in crown ethers (see below). If this is the case then chloride transport must occur at the same rate as potassium transport. The data reported however did not show any evidence of such chloride transport. The rate of loss of chloride(in) intensity with valinomycin present, was the same as the rate seen in the absence of valinomycin. By contrast the rate of potassium/rubidium exchange in a similar system was much more rapid, with complete exchange occurring within 7 minutes. Thus the ion-pair theory of valinomycin mediated transport does not hold true, at least in this system.

4.1.2 Synthetic anion ionophores.

The simplest type of anion carrier are alkyl ammonium ions, with medium length chains e.g. tetrabutylammonium. These have been used as phase transfer materials (see above) making anions soluble in an organic solvent. These materials transport anions as an ion pair and are relatively nonselective of the anion carried. A similar type of nonselective transport is that mediated by crown ethers.[8] These form positively charged complexes with a cation and also take an anion with them as an ion pair. Anion transport has also been seen to be mediated by certain organometallic complexes such as the vitamin B_{12} derivative seen in Figure 4-1.[9] This last method has been seen to favour transport of lipophilic cations over hydrophilic ones.[10] This is because the transition energy of formation of the complex is lower if the anion is lipid soluble.

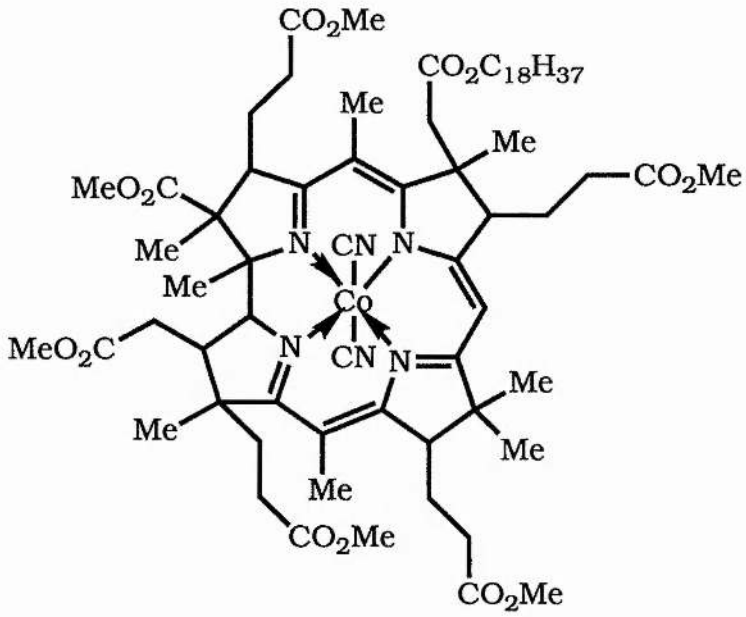

Figure 4-1. The structure of a Cobalt containing anion ionophore.

There has been a lot of work done in the field of anion binding receptors using cryptands like those used for cation transport.[11] Examples of such materials are given in Figure 4-2. These can all be seen to contain multiple amino groups. Some of these are protonated at neutral pH and it is the interaction between the anion and protonated amines that gives rise to the complexation. If there is no positive charge then no complex is formed. The problem with these materials, in the mediation of transport, is that they have more than one positive charge, so the cation/carrier complex has net positive charge. This can be overcome by the incorporation of a large lipophilic anion e.g. dinonylnaphthalene sulphonate ($DNNS^-$) into the membrane.[12] This anion would be expected to remain in the membrane outside the cavity of the carrier. To improve further the lipid solubility of the complex the polyamine was tosylated leaving only the bridgehead sites for protonation. The transport studies were

carried out in a U-tube system and showed that the presence of the DNNS- improved the selectivity of the cryptand type ionophores without altering the selectivity of a linear amine, trioctylamine.

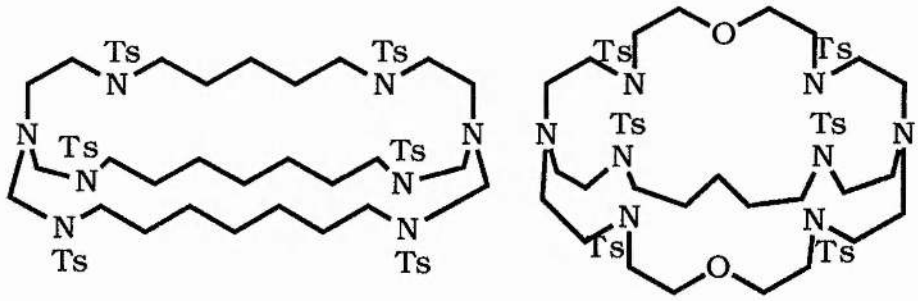

Figure 4-2. Two of the cryptands used as anion ionophores.

This showed that anion receptors can be easily changed into anion carriers to produce selective anionic ionophores. The selectivity observed here arises from the size of the cavity of the ionophore rather than solvation effects. These materials can be applied to biological systems as an aid to understanding the processes of anion transport.[12]

4.2 Cation transport.

The field of synthetic cation ionophores is vast with many different types of material being used. A full survey of all the work done in this field would be out of place here, so, this section of the introduction will be only a brief history of the field of synthetic ionophores. The areas of anionic and proton ionisable ionophores which are the areas of interest to the work described here are described in a little more depth.

Macrocyclic polyethers (crown ethers) were first described by Pedersen in 1967.[13] His pioneering work along with that of

Lehn and Cram led to their receiving the Nobel Prize in Chemistry in 1987. There have been many reviews on the crown ethers[14] and similar materials, such as cryptands[15] and lariat ethers.[16] These have covered everything from synthesis[17] to transport properties.[18]

Synthetic ionophores come in many shapes and sizes[19] designed to complex with different species. One thing they all have in common is that the more strictly controlled the stereochemistry and the more rigid the structure the more stable and selective are the complexes formed. This is clearly shown by some work done on podand ionophores.[20] These are non-macrocyclic ionophores and are often polyethers, this class includes materials such as tetraglyme see Figure 4-3. The materials studied in this work were linear polyethers with well defined stereochemistry Figure 4-3. These were seen to form much more stable complexes with alkali metal ions than the corresponding linear polyethers with undefined stereochemistry. The stabilities of the complexes formed compared favourably with those seen for crown ethers although the selectivities are slightly decreased. The naturally occurring ionophores are also mostly non-macrocyclic species with well defined stereochemistry. Possibly this is a route for further research to take.

It is the organisation of the molecule into its complexing form which is the source of the differences in free energy. In the non-complexed state there is no cavity in cryptand 2,2,2 or organised binding site in [18]-crown-6.[19] It is only when the cation is bound that this arrangement of the molecule is produced. This rearrangement of the molecule is the major energy barrier to

Tetraglyme

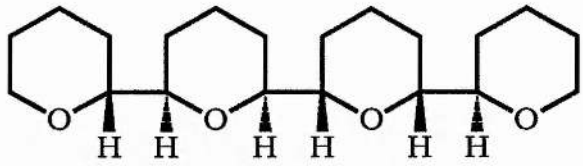

Figure 4-3 Podand ionophores from ref 20.

complex formation. If the structure is synthesised such that the molecule is sterically constrained to adopt a conformation similar to that of the final complex this energy barrier will be minimised. One such class of compounds are the spherands developed by Cram and co-workers.[21] Designing such materials carefully can provide a high selectivity for one cation or molecule.

The preferences are often worked out in terms of host-guest association constant (K_a) values obtained by the extraction of metal picrate solutions into an organic layer.[22] This method relies on the fact that a neutral ionophore must extract an anion into the organic layer to balance the charge on the metal/ionophore complex. The concentration of picrate extracted from aqueous solution into a chloroform layer with and without host present is determined spectrophotometrically, as are the respective concentrations in the aqueous layer. The extraction process can be represented by the equations given in Scheme 4-1.

Thus if the concentration of picrate is determined in the 4 layers, aqueous and organic, with and without host, then K_e, K_d and hence K_a can be calculated.

$$[M^+\ Pic^-]_{org} + [H] \overset{K_a}{\rightleftharpoons} [M^+ . H . Pic^-]_{org}$$

$$[M^+]_{aq} + [Pic^-]_{aq} + [H]_{org} \overset{K_e}{\rightleftharpoons} [M^+ . H . Pic^-]_{org}$$

$$[M^+] + [Pic^-]_{aq} \overset{K_d}{\rightleftharpoons} [M^+\ Pic^-]_{org}$$

where $K_a = \frac{K_e}{K_d}$

Scheme 4-1. The equations governing the picrate extraction experiment.

The preference for ion A^+ over ion B^+ is the ratio of $K_a{}^A/K_a{}^B$ and can be as high as $>10^{10}$ for sodium over potassium in some spherands. Arranging the hosts in order of decreasing selectivity gives a list of:

Spherands > cryptands > coronands > podands.

This listing follows the order of structural preorganisation.

4.2.1 Proton ionisable crown ethers.

Polyether antibiotics a large highly active class of naturally occurring ionophores contain a proton ionisable group, usually a carboxylic acid. This removes the necessity of also transporting an anion to maintain electroneutrality as the anionic function is actually part of the molecule. It is possible to synthesise crown ethers containing an acidic group which also exhibit this

advantage. This should speed up transport for two reasons:

1) The ionised headgroup of the crown ether will project from the membrane facilitating the first approach of a solvated cation, much as is observed in polyether antibiotics.

2) There is no necessity for the crown ether/metal complex to carry a counter ion into solution. The complex formed is electronically neutral.

Therefore the rate of transport and selectivity should be improved by incorporating an acidic group into the crown ether molecule. A review article on these materials has been published recently.[23]

There have been three different approaches to the synthesis of proton-ionisable crown ethers.[23] These are:

1) Attachment of a pendant side arm including or terminating with an ionisable entity
2) Inclusion within the crown ether framework of an ionisable entity such that the proton and the atom to which it is bound project into the cavity
3) Inclusion of a heteroatom bearing an ionisable proton at a ligating position in the framework

An example of each of these types is given in Figure 4-3. The most extensive group are those of type 1, the work in this thesis was on this type of material.

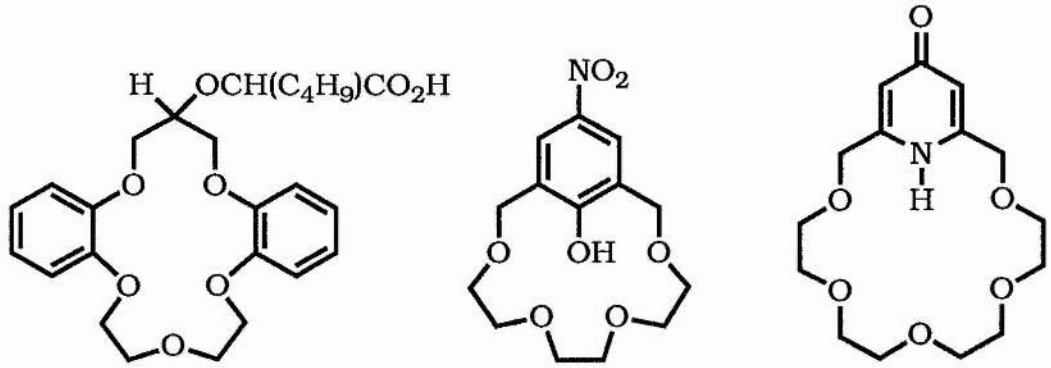

1 2 3

Figure 4-3. Examples of the three major types of proton ionisable crown ethers.

The pK_a's of the pendant side chains have been found to be similar to those of the parent acid, unless there is appreciable hydrogen bonding between the ionisable proton and the oxygen atoms in the macrocyclic cavity. The pK_a is seen to increase with increasing chain length of the pendant side arm as the greater flexibility enables a closer approach of the two groups. This makes such hydrogen bonding stronger.[23]

The complexation of metal cations has been studied for many proton ionisable crown ethers. There are a number of desirable structural features for the formation of stable complexes. These features are[23]:-

1) The cavity must be the correct size to fit the cation
2) The anionic moiety should be sited at the correct distance from the cavity for an ion pair to form
3) The anionic charge should match that of the cation to produce a 1:1 complex.

These are not really surprising neither is the fact that both the anionic and neutral forms of the crown ether can complex. The neutral form always has a lower association constant, K_a, implying that there is competition between the proton and metal ion for the ligand site. It has also been noted that if the ionisable site is remote from the cavity, it, not the cavity may be the dominant binding site.[24] This is more likely if there is poor size matching of the cavity and cation.

Solvent extraction studies on these materials have shown that, except at high pH, the complexes formed had two or more ligand molecules per cation.[25,26] It was also seen that the extraction ability of solvents decreases with increasing polarity, chloroform was the most effective and p-xylene the least.

Transport studies also show a dependence on the pH. These have been mostly carried out in a U-tube type apparatus, see Figure 2-2, with the source phase at high pH and the receiving phase at low pH. This ensures complete complexation with cation in the source phase and complete dissociation of the complex in the receiving phase. Changing the pH gradient sometimes has little effect[27] but in some systems large changes in the transport rates[28] or even changes of selectivity have been observed.[29]

The kinetics of the process also depend on pH, although the metal ion concentration is also important in some cases. The effects seen depend on the type of system being studied. In some cases at high pH the transport is first order in metal ion if the metal ion is at roughly the same concentration as the crown ether. If the metal ion is present at considerably higher concentration

then the process is observed to be zeroth order in metal ion.[27]. This is believed to occur when desorption of the complex from the aqueous organic interface is rate limiting.[23]

The only experiment so far reported for these materials in phospholipid bilayers was a comparison with two naturally occurring ionophores, valinomycin and nigericin.[30]

Thus proton ionisable crown ethers are useful tools for separating both metallic and biological cations. There is however still no predictive model for the best system to be used for a given separation, so a certain amount of trial and error is involved. This class of compounds are still less active and efficient transporters than the naturally occurring ionophores. This means that a synthetic ionophoric antibiotic is not in sight.

4.3 Results and Discussion.

4.3.1 Anion Transport.

Previous work in the group had already demonstrated the unsuitability of the lanthanides and most of the transition metals for use as contrast reagents.[31] The only species which was found to produce sufficient relaxation was the manganous ion, a high spin species with 5 unpaired electrons. Unfortunately however this was also seen to destroy the vesicles far to rapidly for any measurements to be made. A sufficient stabilisation was obtained by the addition of phosphate ions to enable the transport to be studied using this system.[5] It was discovered that the increased stability was probably due to the acidity of the manganese/phosphate solution which was added. This decreased the pH in the external solution to pH4, well outside the biological pH range. The observed stabilisation was thought to be due to the protonation of the lipid headgroups, thereby preventing the Mn^{2+} ions from interacting with the membrane by electrostatic repulsion see Figure 4-4.

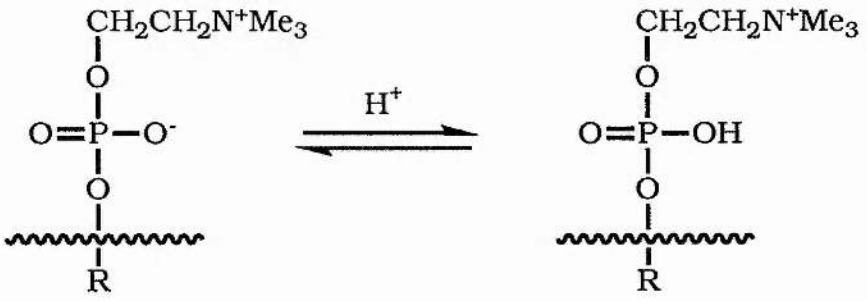

Neutral membrane Positively charged membrane

Figure 4-4. Showing the effect of protonating the membrane.

If this is the case then inducing a positive charge in the

membrane should have a similar effect. To this end a set of vesicles incorporating cetyl pyridinium bromide were produced. This is commonly used to produce positively charged membrane surfaces, but it was also found to be an efficient chloride ion transporter, presumably via the formation of an ion pair, as seen earlier with tetrabutylammonium. To reduce the transport rate the headgroup hydrophilicity was increased. This was attempted by substituting carbinol groups in the 3 and 5 positions of the pyridyl ring (see Figure 4-5). The aim of this was to add hydrogen bonding groups to the pyridinium salt to try to reduce its solubility in the membrane. These materials were, however, also seen to mediate anion transport so this approach was abandoned.

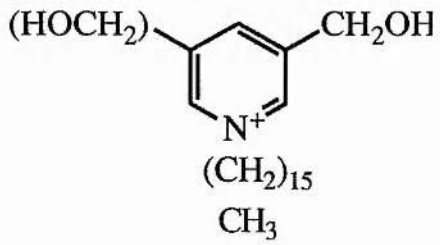

Figure 4-5. The materials used to try to protect the vesicles from destruction by Mn^{2+} ions.

The charge on a membrane surface effects the observed transport processes [32] so an electroneutral method should give better results than the above procedures. To this end two completely different techniques were tried. These used different types of material to do the same job, either shift or relax a halide nmr signal. The first material tried was dextran magnetite.[33] This basically consists of small sugar coated, and therefore water soluble, particles of magnetite. It is formed by the precipitation of magnetite, Fe_3O_4, in a solution of dextran, a polysaccharide with a

Figure 4-6. The combination spectrum showing the shift and relaxation generated by dextran magnetite on the ^{35}Cl signal in aqueous solution.

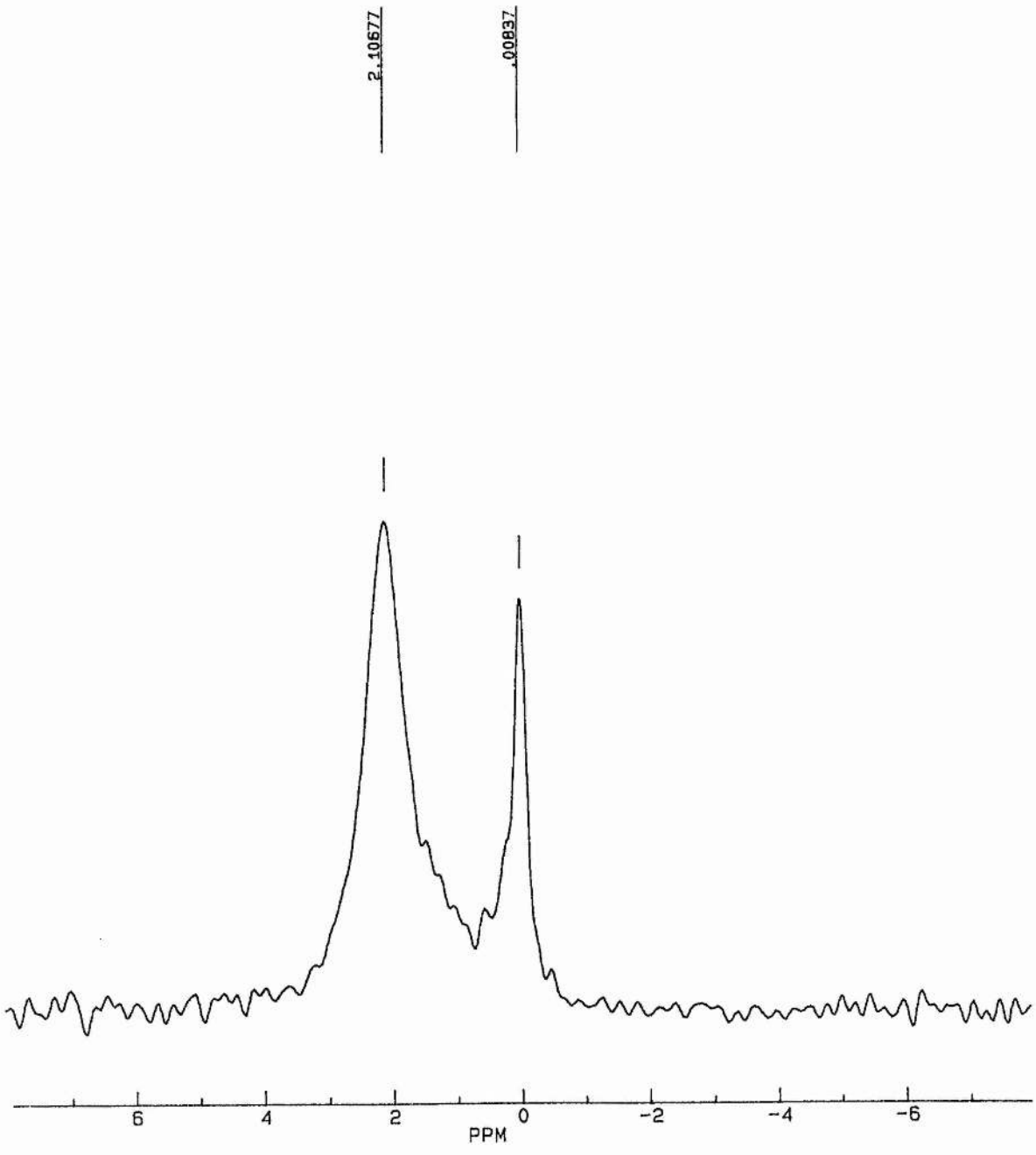

molecular mass of, in this case, about 18000 Daltons. Preliminary tests showed that this both shifted and broadened the ^{35}Cl nmr signal in NaCl solution.[34] That this method would be good enough to produce distinct peaks can be seen by the combination spectrum in Figure 4-6. This spectrum was formed by the superposition of spectra obtained with and without dextran magnetite present. Unfortunately when applied to a set of vesicles no separation of the peaks was seen, which means that dextran magnetite is no use for this system. The reasons for this failure are interesting, the vesicles were not destroyed (this was shown by addition of dysprosium bistripolyphosphate and observation of the ^{23}Na signal) and it would be unusual for a sugar of this size to dissolve through a phospholipid bilayer. The only explanation which we could come up with is that the magnetic field caused by the magnetite operates over a sufficiently large distance to affect ions inside the vesicle without crossing the membrane.

A further type of material tried as a contrast reagent was a stable nitroxide radical. In this case the species used was 4-amino-TEMPO (Figure 4-7) buffered at pH 6.2.

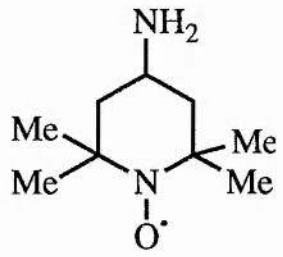

Figure 4-7. The structure of 4-amino-TEMPO.

In the first experiment carried out with 4-amino-TEMPO the solution was not buffered. It was seen that no shift was generated

until the amine was protonated by addition of acetic acid, as the chloride ions would not then be attracted close to the radical centre (Table 4-1). The experiment was repeated with the solution buffered at pH6.2 which gave the data in Table 4-2. It can be seen that this reagent produced a shift but no line broadening in the ^{35}Cl spectrum from potassium chloride solution. This shift was easily sufficient to separate the "in" and "out" signals and was seen to be pH dependent, at alkaline pH the shift was much smaller. The slope of shift vs 4-amino-TEMPO added is almost linear but the pH increased as the buffer was quenched. The addition of 4-amino-TEMPO to the vesicles produced a couple of problems. One was that the buffer used, PIPES, tended to destroy the vesicles but, more importantly, no contrast was seen. This was almost certainly due to penetration of the membrane by the 4-amino-TEMPO. The vesicles were shown to be intact by addition of dysprosium bis-triphosphate and subsequent observation of two signals in the ^{39}K spectrum.

The use of such radicals shows promise for the further future study of anion transport by nmr if the problem of lipid solubility

Table 4-1. The effect of 4-amino TEMPO on the line width and frequency of a ^{35}Cl signal in unbuffered aqueous solution.

TEMPO/Cl^-	Line width/Hz	Frequency/Hz
0	10.98	0
1%	10.98	1.22
4%	10.99	3.05
10%	12.82	6.10
Acetic acid	17.70	37.84

Table 4-2. The effect of 4-amino TEMPO on the line width and frequency of a ^{35}Cl signal in aqueous solution buffered at pH 6.2.

TEMPO/Cl^-	Line width/Hz	Frequency/Hz
0	12.21	18.31
1%	13.42	18.31
4%	13.43	20.75
10%	14.65	23.19
30%	14.03	35.40
60%	15.26	48.83
100%	15.26	58.29

can be overcome. This may be achievable by working at more acidic pH or by quaternising the amine function so the free base is not available to diffuse through the membrane. It is unlikely that such a material would be sufficiently lipophilic to carry a counter ion through a membrane with it.

4.3.2 The preparation and testing of anion carriers.

The other part of this work on anion transport has been to attempt the manufacture of synthetic ionophores. The material which has been used for most of this work has been tetrabutylammonium bromide. It was attempted to manufacture more efficient ionophores with little success. The idea was to incorporate groups which could hydrogen bond to a bound anion thereby stabilising the complex formed. The first species made were hydroxylated trialkyl amines such as (1) in Figure 4-7. It was important to try to test these materials for transport properties, but vesicles are expensive and time consuming to prepare so a more efficient method had to be found. The method used was to add aliquots of a solution of the potential ionophore to a methanol

solution of cæsium chloride and look for any line broadening in the ^{35}Cl spectrum. If the line was broadened then complexation was probably occurring but if no broadening was seen then the material could be ignored as a potential ionophore.

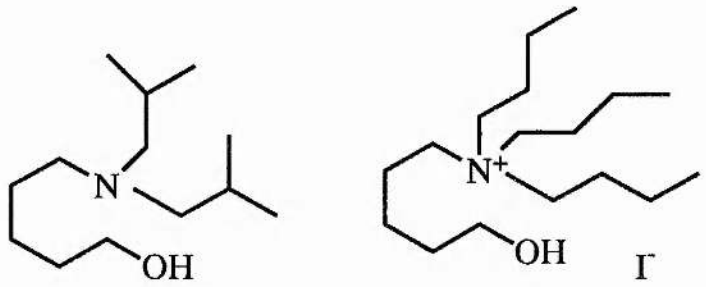

(1) (2)

Figure 4-7. Two anion ionophores tested for transporting ability.

The simple amines used above were all found to be inactive as complexation agents so something was obviously missing. To remedy this defect the amine was quaternised with a further butyl group to give materials such as (2). This was found to broaden the chloride signal so an isotope exchange experiment was set up to measure the transport rate. The method used was $^{35}Cl/^{37}Cl$ exchange with a ^{37}Cl enriched external medium with the reaction being followed by ^{35}Cl nmr. This showed that there was transport but it was at roughly the same rate as that mediated by tetrabutylammonium ions under the same conditions see Table 4-3. These data were obtained with 100µl of a 0.1M solution of ionophore in methanol being added to the vesicle suspension.

Table 4-3. The rates of transport of ^{35}Cl mediated by two anion carriers.

	Tetrabutylammonium	Ionophore (2)
Rate($10^{-4}.s^{-1}$)	2.98	5.88

It was tried to make different potential ionophores such as those in Figure 4-8 but the preparations were all unsuccessful.

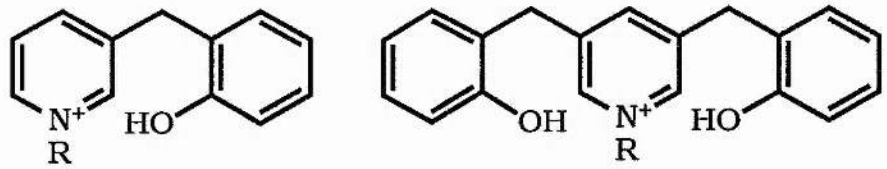

Figure 4-8. Two attempted anion ionophores.

The proposed route for the synthesis of these materials was to use a photo-Fries rearrangement.[35] The projected route is

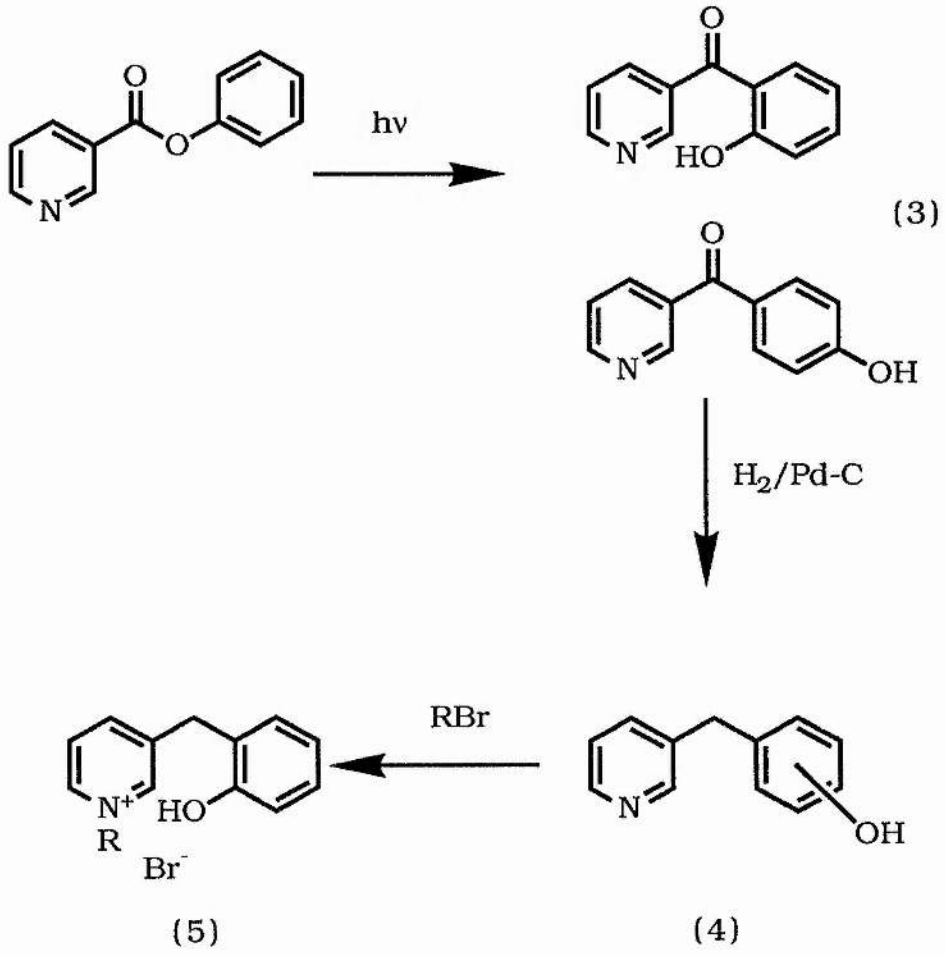

Scheme 4-2. The reaction scheme for the preparation of anion ionophores.

outlined in Scheme 4-2. This would produce the intermediate (3) which could then be hydrogenated to reduce the ketone to an alkyl (3). The final step was to be the quaternisation of this to give the desired product (5). The problems arose in the rearrangement step. The product mixture was too complex to extract the correct material which was only present in miligram quantities.

4.4.1 Cation Ionophores.

A small amount of the work in the thesis was concerned with the preparation of crown ethers incorporating carboxylic acid groups. The parent crown ethers were 15-crown-5 and 16-crown-5 the latter of which first had to be prepared. The general approach was as given in Scheme 4-3 with the carboxylic acid

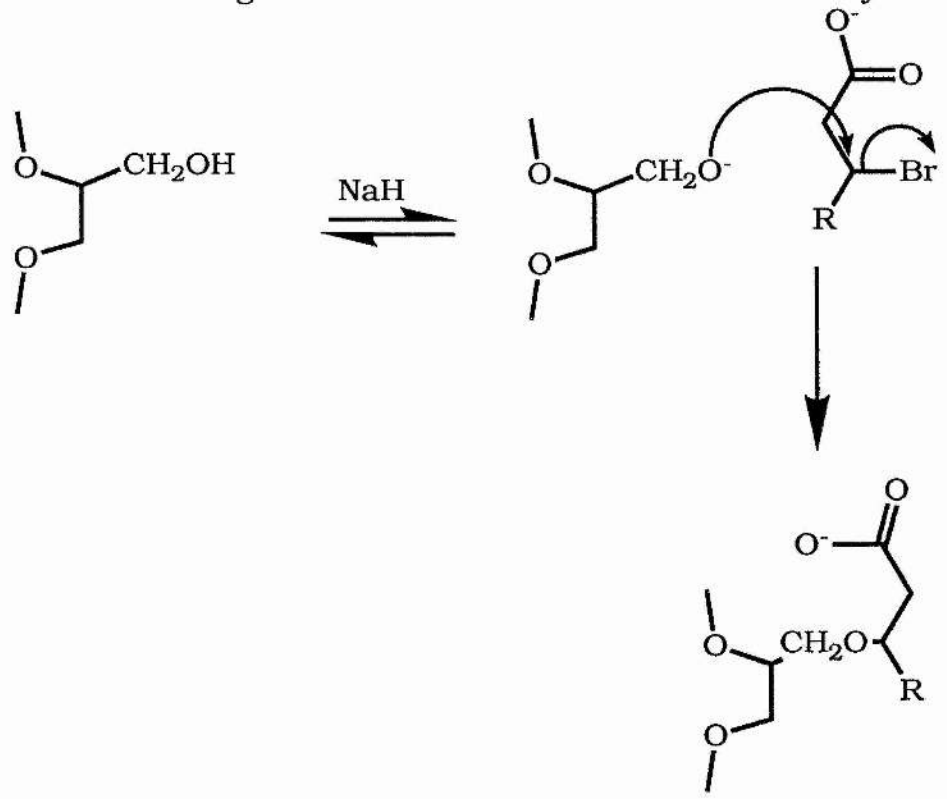

Scheme 4-3. The reaction scheme for the preparation of crown ethers with pendant carboxyl sidearms.

group being added as part of a pendant sidearm. The linkage to the main skeleton of the crown ether was through an ether bridge which was formed by nucleophilic substitution between the crown ether alcohol and bromo acid.

The preparation of methylene-16-crown-5 proceeded smoothly following the literature preparation.[36] The only problems were with the distillation of the final product as this decomposed at around 150°C which meant that a high vacuum was needed for this separation to be successful. The larger problem encountered in this preparation was in the anti-Markownikov hydration of the double bond in (6). This was tried several times using BH_3-THF complex in THF with a complete absence of success. Therefore this area of work was abandoned.

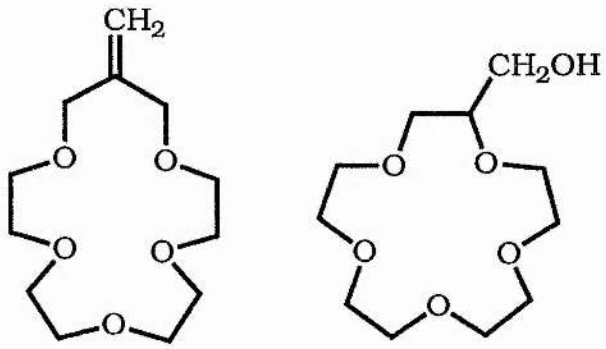

(6) (7)

Figure 4-9. The structures of the two crown ethers used in this work.

In an attempt to identify the preferential chain lengths for transport mediated by proton ionisable crown ethers the synthesis of a number of derivatives of 15-crown-5,methanol, (7), was attempted. These all contained carboxylic acid groups at the

terminus of a pendant sidearm. The bromo acids used in the preparation of these compounds were 2-bromobutanoic acid, 2-bromo octanoic acid, 2-bromohexadecanoic acid and 3-bromopropionic acid. The only one of these which gave an extractable product was the hexadecanoic acid as this was the least water soluble. Purification of this material was difficult as it was a viscous oil. This could be achieved using the unusual feature of this material namely that its sodium salt was no more water soluble than the free acid. Dissolving the product in ether and washing with aqueous base removed the impurities visible in the nmr spectrum.

4.5 Experimental.

Preparation of N-hexadecyl-3-(hydroxymethyl)pyridinium bromide.

3-(Hydroxymethyl)pyridine (3.27g, 30mmol) and hexadecyl bromide (9.15g, 30mmol) were dissolved in isopropanol, ($50cm^3$) and heated under reflux for 16h. The isopropanol was removed by distillation to leave a pale yelow solid. This was recrystallised from isopropanol to give yellow crystals.

Yield 9.5g 76.5% mpt 79-81 °C.

NMR 9.2ppm (1H,s),9.15 (1H,d), 8.56 (1H, d), 8.1 (1H, m), 4.92 (2H, s), 4.8 (2H, tr) 2.05 (2H, br s), 1.34 (28H, m), 0.88 (3H,tr)

Preparation of diethyl pyridine 3,5-dicarboxylate.[37]

Pyridine-3,5-dicarboxylic acid (1.67g, 10mmol) was heated under reflux with thionyl chloride ($15cm^3$) for 7h until no more HCl was evolved. The excess thionyl chloride was removed by distillation at atmospheric pressure. A mixture of 70:30 methylene chloride/pyridine ($100cm^3$) was added and the mixture heated for a further 3h. The reaction mixture was cooled in an ice bath and dried ethanol (1.15g, 25mmol) were added. The mixture was allowed to warm to room temperature and stirred overnight. The solution was washed twice with water ($50cm^3$), twice with base ($50cm^3$) and once more with water. The solution was dried and the solvent removed on a rotary evaporator to leave a yellow oil.

Yield 1.71g 76.0%

NMR 9.15 (2H, tr), 8.65 (1H, q), 4.22 (4H, q), 1.21 (6H, tr).

Preparation of 3,5-bis(hydroxymethyl)pyridinium bromide.

Diethyl pyridine-3,5-dicarboxylate (0.75g, 3.4mmol) was added to Lithium aluminium hydride (LAH) (0.15g, 3.95mmol) suspended in dry THF (50cm^3). The mixture was heated under reflux for 16h. The excess LAH was destroyed with water, 1M NaOH, and water and the mixture filtered. The THF was removed on a rotary evaporator to leave a yellow solid (0.5g, 75.2%)

0.3g (1.5mmol) of this solid was suspended in isopropanol 10 cm^3 and hexadecyl bromide 0.8g (2.6mmol) was added. The mixture was heated under reflux for 36 hours. The unreacted starting material was removed by filtration and the solvent removed by distillation. The resulting yellow solid contained the desired product with unreacted hexadecylbromide. This mixture was not further separated.

NMR. 8.85 (2H, s), 8.48 (1H, s), 3.4 (4H, tr), 1.22 (30H, m), 0.82 (3H, tr)

Preparation of 3(2,hydroxybenzyl)-pyridine.[35]

Pyridine-3-carboxylic acid, (6.15g, 50mmol) was dissolved in thionyl chloride (30cm^3) and heated under reflux for 2h until no more HCl was evolved. The procedure was then the same as that used for diethyl dinicotinate above adding phenol (4.7g, 50mmol) instead of ethanol. The resulting yellow oil solidified on standing and was recrystallised from 40/60 petroleum ether to give white crystals.

Yield 3.2g, 32.2%, mpt 33-35°C

NMR. 9.41 (1H, d), 8.86 (1H, d-d), 8.49 (1H, d-tr), 7.4-7.5 (3H, m), 7.3 (1H, d-tr), 7.23-7.19 (3H, m).

Phenyl nicotinate, (1g, 5mmol) was dissolved in hexane (500cm^3). The solution was illuminated for 72 hours with one, 15W low pressure mercury lamp. The course of the reaction was followed by TLC. The resulting brown precipitate was dissolved in water and extracted with ether. The ether was removed by distillation to leave a mixture of black tar crystals. This mixture was dissolved in aqueous base and washed with ether to remove non-phenolic material. On neutralisation of the aqueous layer an emulsion was formed which was extracted with ether. The mixture was further separated by chromatography on a short silica column eluting with ether. 30mg of the resulting yellow oil was hydrogenated in ethanol over palladium/carbon (20mg) for 41h. in hydrogen. The catalyst was removed by filtration and the ethanol by distillation. TLC showed that there were 4 components in the mixture, no further separation was attempted.

Yield 20mg.

Preparation of diphenyl pyridine 3,5-dicarboxylate.

Diphenyl pyridine 3,5-dicarboxylate was prepared by a similar method to that used for diethylpyridine3,5-carboxylate. The quantities used were: Pyridine 3,5-dicarboxylic acid (6.5g, 39mmol), thionyl chloride (30cm^3), phenol (8.5g, 90mmol). The final product was recrystallised from toluene to give brown crystals.

Yield 10.2g 82%. mpt 121-123°C.

NMR. 9.61 (1H, dd), 9.16 (2H, tr), 7.5-7.4 (4H, m), 7.34-7.23 (6H, m)

Photolysis of this material was attempted under similar conditions but the reaction was unsuccessful producing a complex mixture of products.

Preparation of N,N-di-isobutyl-5-amido pentanoic acid.

Glutaric anhydride (5.7g, 50mmol) and di-isobutylamine, (6.45g, 50 mmol) were stirred overnight at room temperature in dried toluene. The toluene was removed by distillation and the resulting solid residue was dissolved in ether and washed with water. The ether was removed on a rotary evaporator to leave colourless oil.

Yield 8.54g 70.3%.

NMR 3.19 (2H, d), 3.09 (2H, d), 2.42 (4H, dtr), 1.95 (4H, m), 0.9 (6H, d), 0.85 (6H, d)

Preparation of N,N-di-isobutyl-5-hydroxypentylamine.

N,N-di-isobutyl-5-amido pentanoic acid (2.57g, 10.6mmol) was dissolved in dried THF ($30cm^3$). The resulting solution was added dropwise to a suspension of LAH, (0.84g, 22mmol) in dried THF ($20cm^3$). The reaction mixture was heated under reflux for 18 hours until the reaction was complete. The excess LAH was destroyed by addition of water and the resulting suspension extracted several times with ether. The solution was dried over magnesium sulphate and the ether removed by distillation to leave a colourless oil.

Yield 1.42g 62.3%. bpt 100°C 0.5mbar.

NMR 3.6 (2H, tr), 2.5 (1H, br s), 2.31 (2H, tr), 2.06 (4H, d), 1.67 (2H, m), 1.57 (2H, m), 1.39 (4H, m), 0.97 (6H, d).

This method was used as a general procedure for making molecules with hydroxyl and amino functions.

Preparation of N,N,N,N-tributyl 5-hydroxypentylammonium iodide.

Glutaric anhydride (5.7g, 50mmol) was reacted with di-butylamine (6.5g, 50mmol) using the above method. The product was a colourless oil.

Yield 8.7g 71.6%

NMR 3.30 (2H, tr), 3.21 (2H, tr), 2.28 (4H, dtr), 1.95 (2H, quint), 1.50 (4H, m), 1.31 (4H, m), 0.91 (6H, q)

This product 2.57g (10.6mmol) was added to a suspension of LAH 0.8g (mmol) in dry THF and heated under reflux for 16h. The work up was carried out as above to give a yellow oil. This was purified by distillation in vacuo bpt 98°C/0.2mbar.

Yield 1.36g 59.7%.

NMR. 4.0 (1H, br s), 3.57 (2H, tr), 2.4 (6H, tr), 1.62-1.2 (14H, m), 0.92 (6H, tr)

This product (0.54g, 2.5mmol) was added to butyl iodide, (0.46g, 2.5mmol) in ethanol 10cm^3. The reaction was stopped after 4h and a ^{1}H nmr taken. This showed that only partial reaction had occurred, so butyl iodide (0.46g) was added and the mixture was heated under reflux for a further 16h. This gave the desired product.

Yield 0.86g, 86.0%

NMR. 4.11 (1H, br s), 3.64 (2H, tr), 3.42 (8H, m), 1.84-1.24 (18H, m), 1.03 (9H, tr)

Preparation of 15-methylene-1,4,7,10,13-pentaoxacyclohexadecane.

Sodium hydride, (14g, 0.3mol) was suspended in dried THF (150cm^3) and heated to reflux under dry nitrogen. 3-chloro-2-chloromethylprop-1-ene (12.5g, 0.1mol) and tetra-ethyleneglycol 19.4g (0.1mol) were dissolved in dried THF 150cm^3 and added dropwise over the course of 1.5h. The mixture was heated under reflux for a further 30 min and then allowed to cool. The excess hydride was destroyed by addition of methanol. The resulting mixture was filtered and the solvent removed by distillation. The product was redissolved in methylene chloride and washed with water to remove any water soluble impurities. The solution was dried over magnesium sulphate and the solvent removed by distillation. The resulting brown oil was purified by distillation in vacuo. bpt 120-130°C/0.2mbar to give a colourless oil.

Yield 9.2g, 37.4%.

NMR. 5.25 (2H, tr), 4.20 (4H, tr), 3.70 (16H, d)

General method for the preparation of crown ethers with pendant carboxylic sidearms.

Crown ether-methanol (1 equiv) was dissolved in toluene (20cm^3). The mixture was distilled under a Vigreux column to remove water. Sodium hydride (1.2 equiv.) was washed with petroleum ether to remove the oil and suspended in toluene. The crown ether solution and bromo-acid (1 equiv) were added to the sodium hydride suspension and stirred for 4h. Methanol and then water were added to destroy the excess hydride and the the two layers were separated. The toluene was dried over magnesium

sulphate and removed by distillation. The final product was purified by dissolving in chloroform and washing with dilute sodium hydroxide solution. The organic layer was dried over magnesium sulphate.

This was successful with 1,4,7,10,13,pentaoxacyclopentadecane-2-methanol (250mg, 1mmol) and 2-bromohexadecanoic acid (335mg, 1mmol)
Yield 400mg, 79.4%.
NMR. 3.8-3.55 (22H, m), 1.28 (26H, m), 0.88 (3H, tr).

The reaction was also tried without success using 2-bromo-butanoic acid, 2-bromo-octanoic acid and 3-bromo propionic acid.

References to Chapter 4.

[1]Knauf, P.A., (1979), *Curr. Top. Membr. Transp.*, **12**, 249-263.

[2]Liedtke, C.M.(1989), *Annu. Rev. Physiol.*, **51**, 143-160.

[3]Brevard, C. and Granger, P., (1981), *Handbook of High Resolution Multinuclear NMR*, John Wiley & Son, New York.

[4]Brauer, M., Spread, C.Y., Reithmeier, R.A.F. and Sykes, B.D., (1985), *J. Biol. Chem.*, **260**, 11643-11650.

[5]Riddell, F.G., Arumugam, S. and Patel, A., (1990), *J. Chem. Soc. Chem. Commun.*, **1990**, 74-76.

[6]eg. Brandstrom, A. and Kolind-Andersen, H., (1975), *Acta Chem. Scand., Ser. B*, , **29**, 201-205.

[7]Sada, E., Katoh, S., Terashima, M. and Takada, Y. (1985), *AIChE J.*, **31**, 311-316.

[8]Dalgea, L.M., Fyles, T.M. and Robertson, G.D.(1987), *J.Membr. Sci.* **34**, 87-108.

[9] Schulthess, P., Ammann, D., Simon, W., Caderas, C., Stepanek, R. and Krautler, B. (1984), *Helv. Chim. Acta* (1984) **67**, 1026-1032.

[10] Hofmeister, F., (1888), *Arch. Exp. Pathol. Pharmacol.*, **24**, 247.

[11]Graf, E. and Lehn, J.M., (1976), *J. Am. Chem. Soc.*, **98**, 6403-6405.

[12]Dietrich, B., Fyles, T.M., Hosseini, M.W., Lehn, J-M. and Kaye, K.C., (1988) *J. Chem. Soc., Chem. Commun.* **1988**, 691-692

[13]Pedersen, C.J. (1967), *J. Am. Chem. Soc.*, **89**, 2495-2496 & 7017-7036.

[14]Izatt, R.M., Bradshaw, J.S., Nielsen, S.A., Lamb, J.D., Christensen, J.J. and Sen, D., (1985), *Chem. Rev.*, **85**, 271- 339.

[15]Lehn, J.M., (1978), *Pure Appl. Chem.*, **50**, 871-892.

[16]Dishong, D.M., Diamond, C.J., Cinoman, M.I. and Gokel, G.W., (1983), *J. Am. Chem. Soc.*, **105**, 586-593.

[17]Bradshaw, J.S., (1978), In *Synthetic Multidentate Macrocyclic Compounds*, Izatt, R.M. and Christensen, J.J. (Eds), Academic, New York, pp. 53-109.

[18]e.g. Izatt, R.M., Clark, G.A., Bradshaw, J.S., Lamb, J.D. and Christensen, J.J., (1986), *Sep. Purif. Methods*, **15**, 21-72.

19Cram, D.J. (1988), *Angew. Chemie Int. Ed.*, 27, 1009-1022.

20Iimori, T., Still, W.C., Rheingold, A.L. and Staley, D.L., (1989), *J. Am. Chem. Soc.*, **111**, 3439-3440.

[21]Trueblood, K.N., Knobler, C.B., Maverick, E., Helgeson, R.C., Brown, S.B. and Cram, D.J., (1981), *J. Am. Chem. Soc.*, **103**, 5594-5596.

[22]Koenig, K.E., Lein, G.M., Stuckler, P., Kaneda, T. and Cram, D.J. (1979), *J. Am. Chem. Soc.*, **101**, 3553-3566.

[23]Brown, P.R. and Bartsch, R.A. In *Inclusion Aspects of Membrane Chemistry*. Osa, T. and Atwood, J.L. (Eds) (1991) pp 1-57. Kluwer. Dortrecht.

[24]Robison, T.W. and Bartsch, R.A., (1985), *J. Chem. Soc. Chem. Commun.*,**1985**, 990-991.

[25]Nakamura, H., Takagi, M. and Ueno, K. (1980), *Anal. Chem.*, **52**, 1668-1671.

[26]Strzelbicki, J. and Bartsch. R.A., (1981), *Anal. Chem.*, **53**, 1894-1899.

[27]Fyles, T.M., Malik-Diemer, V.A. and Whitfield, D.M. (1981), *Can. J. Chem.* **59**, 1734-1744.

[28]Walkoviak, W., Brown, P.R., Shukla, J.P. and Bartsch, R.A. (1987) *J. Membrane Sci.* **32**, 59-68.

[29]Hriciga, A. an.d Lehn, J.M. (1983), *Proc. Nat. Acad. Sci. USA.*, **80**, 6426-6428.

[30] Thomas, C., Sauterey, C., Castaing, M. Gary-Bobo, C.M., Lehn, J.M. and Plumere, P. (1983), *Biochem. Biophys. Res. Commun.*, **116**, 981-987.

[31]Arumugam, S. unpublished results.

[32]Riddell, F.G. and Arumagam, S. (1988), *Biochim. Biophys. Acta,* **945**, 65-72.

[33]Molday, R.S. and MacKenzie, D., (1982), *J. Immun. Meth.* **52**, 353-367.

[34]M.A. Chippa MSc Thesis. University of St Andrews.

[35]Kanaoka, Y. and Hatanaka, Y. (1974), *Heterocycles*, **2**, 423-426.

[36] Tomoi, M., Abe, A., Ikeda, M., Kihara, K. and Kakiuchi, H., (1978), *Tetrahedron Lett.*, **33**, 3031-3034.

[37]Tsuda, K., Ikekawa, N., Takasaki, R. and Yamakawa, Y., (1953), *Chem. Pharm. Bull. Jap.*, **1**, 142-145.

Chapter 5.

Chapter 5. Conclusions and Further Work.

5.1 Conclusions

The aim of this work was to study the effect of ionophore structure on the transport rates. The transport rates were measured for two ionophores with very similar structures, narasin and salinomycin, to see what effect slight differences in the structure have. This showed that even a small change in the structure, in this case an extra methyl group, had a noticeable effect on both the kinetic and thermodynamic aspects of the transport process. This effect of structural change was also borne out by the preliminary studies carried out on structurally modified forms of salinomycin. These showed that the rates of transport can be decreased by an order of magnitude by hydrogenating the vinylic group in the structure of salinomycin.

The transport studies showed that salinomycin and narasin both transport alkali metal ions as 1:1 metal/ionophore complexes. They are both observed to be potassium selective transporters. The rates observed for salinomycin with potassium were faster than the rates shown by any of the other ionophores tested using this system. Salinomycin showed a thermodynamic as well as kinetic preference for potassium while with narasin there was no large thermodynamic preference. The values for the stability constants of the complexes formed with sodium and potassium were the same, within experimental error.

The gradients of the $1/k'$ vs $[M^+]$ lines for the complexes with a particular cation were seen to be the same for both narasin and salinomycin. The difference in behaviour of the two ionophores is shown in the intercepts. The reasons for this behaviour are a little unclear, the interpretation depends on the diffusion coefficient of the metal/ionophore complex across the membrane. The slopes and intercepts of these graphs can be represented one of three relationships dependent on the relative rates of diffusion and dissociation. If diffusion is rapid then the gradient is $1/k_d$ and intercept $1/k_f$. If dissociation is rapid then the gradient is $1/k_{diff}$ and intercept K_s/k_{diff}. If neither is dominant then there will be a complex relationship for both slope and intercept. The calculations estimating the K_s for the sodium complex, assuming that diffusion was rate limiting, showed that diffusion is an important part of the gradient in these experiments. Therefore this work falls into the third of the categories above, i.e. diffusion and dissociation both occur at similar rates.

Narasin and salinomycin were also tested as lithium ionophores. This showed that they were not particularly efficient lithium carriers, which is as would be expected for potassium ionophores. They were seen, however, to mediate transport at a far higher rate than certain synthetic lithium ionophores.

The finding that small structural differences cause noticeable changes in the transport properties of ionophores led to a study on the conformation of the metal/ionophore complex using nmr. Samples were prepared of the complexes of both salinomycin and narasin with all of the alkali metals. The ^1H and ^{13}C spectra were

taken and assigned using two dimensional nmr techniques. This showed that there were conformational changes in only certain portions of the molecule. Most of the chemical shifts stayed almost constant but there were some which showed a marked dependence on the cation present.

The atoms which showed the greatest variation in chemical shift were seen to be, for the most part, in the areas of the molecule previously described as "hinges". These are areas of conformational flexibility which enable the molecule to "wrap" itself around the complexed cation. The variation in these sites also shows that they are important in the accommodation of different sized cations. There are however also relatively large chemical shift changes in ring C, a rigid area of the molecule. This may be explained by the movement of the hydroxyl group, C(20)-OH, to allow an interaction with the bound cation. This change in chemical shift is accompanied by a change in the coupling constants in this area, demonstrating that there is some flexibility in the molecule at this site.

Thus, the changes in chemical shift show that molecular flexibility is required to accommodate different sized cations. It would be interesting to see how the conformation of the ionophore alters with different cations. This should be able to be determined using nmr and computer modelling techniques.

The final portion of the work was in the field of synthetic ionophores for both cations and anions. The study on proton ionisable crown ethers as cation carriers failed to make any progress due to problems in the synthesis of the materials.

The work on anion transport was however rather more interesting. The problem here was to find a method of generating a contrast between anions inside vesicles and those outside. The only successful method so far published used manganous ions as a relaxation agent. This was found to rely on the use of low pH (~pH4) to stabilise the vesicles. It was tried to find an alternative method at nearer to physiological pH. Dextran magnetite and 4-amino-TEMPO were both found to give rise to a change in chemical shift in aqueous chloride solution. Unfortunately this was not found to be the case in vesicle suspensions. Therefore, in these forms, these are not suitable contrast reagents for chloride ions. If, however, the lipid solubility of the nitroxyl radical were reduced then this could be a good contrast reagent.

5.2 Further Work.

The transport studies of narasin and salinomycin with lithium should be further studied. There is also the possibility of investigating the cæsium transport properties of these materials. There is also a lot more work to do in the investigation of the effect of structure on ion transport properties. Salinomycin and narasin both have extensive ranges of homologues including the 17-epimeric 20-deoxy forms of these materials. Transport studies on a range of these materials may produce some interesting and useful information.

The next step in the ^{1}H nmr studies of these materials would be to elucidate the conformation of the ionophore/metal complexes in solution. Then the conformations of the structurally modified derivatives could also be investigated. Comparing the

conformation to the transport properties could be a very fruitful area for investigation. Once the solution conformation is known the conformation of the complex in a lipid bilayer should be investigated. This would involve the use of deuterated lipids but even so the lines would probably be rather broad. It should, however, be possible to complete such a study.

The work on nitroxyl radicals showed considerable promise but the problem of lipid solubility needs to be overcome. One possible way of achieving this is by the addition of hydroxyl groups to the structure. There is a lot of room for improvement in the area of anion ionphores. These could be made more efficient and more selective by the use of cryptand or coronand type materials.

Appendix **The Transport data for Salinomycin and Narasin with Sodium and Potassium.**

25mM Sodium with Salinomycin.

SL(μl)	SL/PC	LW(Hz)	LB(Hz)	Rate(s^{-1})
0	0	12.204	0	0
2	0.3195	14.647	2.443	7.675
4	0.6390	26.987	14.783	46.442
6	0.9585	16.118	3.914	12.296
8	1.2780	19.366	7.162	22.500
10	1.5975	25.821	13.617	42.779
12	1.9170	24.061	11.857	37.250

50mM Sodium with Salinomycin.

SL(μl)	SL/PC	LW(Hz)	LB(Hz)	Rate(s^{-1})
0	0	9.765	0	0
2	0.3195	11.962	2.197	6.902
4	0.6391	13.671	3.906	12.271
7	1.1184	16.600	6.835	21.473
10	1.5977	20.507	10.742	33.747
13	2.077	23.437	13.672	42.952
16	2.5563	27.587	17.822	55.989

75mM Sodium with Salinomycin.

SL(μl)	SL/PC	LW(Hz)	LB(Hz)	Rate(s^{-1})
0	0	11.718	0	0
2	0.3195	15.380	3.662	11.505
4	0.6390	23.437	11.719	36.816
6	0.9585	20.019	8.301	26.078
8	1.2780	20.995	9.277	29.145
10	1.5975	24.901	13.183	41.416

100mM Sodium with Salinomycin.

SL(µl)	SL/PC	LW(Hz)	LB(Hz)	Rate(s^{-1})
0	0	10.009	0	0
2	0.3195	11.474	1.465	4.602
4	0.6391	12.206	2.197	6.902
7	1.1184	13.915	3.906	12.271
10	1.5977	15.624	5.615	17.640
14	2.2367	18.309	8.300	26.075
18	2.8756	20.751	10.742	33.747
22	3.5149	23.681	13.672	42.952

150mM Sodium with Salinomycin.

SL(µl)	SL/PC	LW(Hz)	LB(Hz)	Rate(s^{-1})
0	0	10.985	0	0
2	0.3195	12.206	1.221	3.836
4	0.6391	13.671	2.688	8.438
7	1.1184	15.624	4.639	14.574
11	1.7574	40.77	29.785	*
15	2.3965	23.925	12.940	40.652
20	3.1953	27.099	16.114	50.424

175 mM Sodium with Salinomycin.

SL(µl)	SL/PC	LW(Hz)	LB(Hz)	Rate(s^{-1})
0	0	10.742	0	0
3	0.4793	12.694	1.952	6.132
6	0.9586	14.649	3.907	12.274
9	1.4379	16.600	5.850	18.403
13	2.0770	18.798	8.056	25.309
17	2.7603	20.751	10.009	31.444
21	3.3551	24.657	13.915	43.715

200mM Sodium with Salinomycin.

SL(µl)	SL/PC	LW(Hz)	LB(Hz)	Rate(s^{-1})
0	0	12.35	0	0
2	0.3195	13.67	1.32	4.147
5	0.7988	15.01	2.66	8.357
8	1.2781	16.85	4.50	14.137
11	1.7574	20.50	8.15	25.604
14	2.2367	18.80	6.45	20.263
17	2.7160	21.73	9.38	29.468
20	3.1953	24.17	11.82	37.134

50mM Potassium with Salinomycin.

SL(µl)	SL/PC	LW(Hz)	LB(Hz)	Rate(s^{-1})
0	0	12.58	0	0
2	0.91	16.73	4.15	13.038
4	1.81	19.53	6.95	21.834
6	2.72	23.68	11.10	34.872
8	3.63	26.12	13.54	42.537

100mM Potassium with Salinomycin.

SL(µl)	SL/PC	LW(Hz)	LB(Hz)	Rate(s^{-1})
0	0	11.48	0	0
2	0.2397	20.18	8.70	27.332
3	0.3595	23.44	11.96	37.573
4	0.4793	26.13	14.65	46.024
5	0.5991	32.96	21.48	67.481

150mM Potassium with Salinomycin.

SL(µl)	SL/PC	LW(Hz)	LB(Hz)	Rate(s^{-1})
0	0	18.07	0	0
1	0.1198	20.02	1.95	6.126
2	0.2397	23.44	5.37	16.870
3	0.3595	23.44	5.37	16.870
4	0.4793	31.74	13.67	42.946
5	1.5991	36.87	18.80	59.062
6	0.7190	34.67	16.60	52.150

175mM Potassium with Salinomycin.

SL(µl)	SL/PC	LW(Hz)	LB(Hz)	Rate(s^{-1})
0	0	23.32	0	0
2	0.91	25.3	1.98	6.22
4	1.81	26.86	3.74	11.75
7	3.17	30.15	6.83	21.46
10	4.53	41.14	17.82	*
13	5.89	33.08	9.76	30.66

200mM Potassium with Salinomycin.

SL(µl)	SL/PC	LW(Hz)	LB(Hz)	Rate(s^{-1})
0	0	23.60	0	0
1	0.453	22.34	-1.26	-4.0
2	0.907	23.20	-0.40	-1.3
4	1.813	24.78	1.18	3.7
6	2.720	28.32	4.72	14.8
8	3.626	26.91	3.31	10.4
11	4.986	29.42	5.82	18.3
14	6.346	36.13	12.53	39.4
17	7.705	36.26	12.66	39.8
20	9.065	37.16	13.56	42.6

50mM Sodium with Narasin.

NS(µl)	NS/PC	LW(Hz)	LB(Hz)	Rate(s^{-1})
0	0	14.65	0	0
1	0.283	20.51	5.86	18.41
2	0.565	29.36	14.71	46.21
3	0.848	27.34	12.69	39.87
5	1.414	35.16	20.51	64.43

100mM Sodium with Narasin.

NS(µl)	NS/PC	LW(Hz)	LB(Hz)	Rate(s^{-1})
0	0	11.2	0	0
1	0.303	15.1	2.9	9.11
2	0.606	17.1	5.9	18.54
3	0.910	20.0	8.8	27.65
4	1.213	21.9	10.7	33.62
6	1.819	29.3	18.1	56.86
7	2.122	28.2	17.0	53.40
8	2.426	32.3	21.1	66.29

150mM Sodium with Narasin.

NS(µl)	NS/PC	LW(Hz)	LB(Hz)	Rate(s^{-1})
0	0	13.6	0	0
1	0.300	14.7	1.1	3.56
2	0.600	16.9	3.3	10.37
3	0.901	17.9	4.3	13.51
4	1.201	23.5	9.9	*
5	1.501	22.0	8.4	26.39
6	1.801	24.6	11.0	34.56
7	2.101	26.0	12.4	38.96

200mM Sodium with Narasin.

NS(µl)	NS/PC	LW(Hz)	LB(Hz)	Rate(s^{-1})
0	0	17.09	0	0
1	0.259	18.06	0.97	3.05
2	0.519	21.00	3.91	12.28
3	0.778	21.97	4.88	15.33
4	1.038	23.92	6.83	21.46
6	1.556	26.86	9.77	30.69

50mM Potassium with Narasin.

NS(µl)	NS/PC	LW(Hz)	LB(Hz)	Rate(s^{-1})
0	0	11.6	0	0
1	0.114	16.47	4.87	15.3
2	0.228	18.80	7.20	22.6
3	0.343	24.41	12.81	40.2
4	0.457	23.08	11.48	36.1
5	0.571	26.49	14.89	46.8
6	0.685	26.37	14.77	46.4
7	0.800	39.80	28.20	88.6

100mM Potassium with Narasin.

NS(µl)	NS/PC	LW(Hz)	LB(Hz)	Rate(s^{-1})
0	0	16.39	0	0
2	0.225	24.44	8.05	25.3
3	0.337	25.47	9.08	28.53
4	0.45	27.67	11.28	35.44
5	0.562	34.47	18.08	56.80
6	0.675	36.45	20.06	63.02

150mM Potassium with Narasin.

NS(µl)	NS/PC	LW(Hz)	LB(Hz)	Rate(s^{-1})
0	0	20.49	0	0
1	0.114	24.15	3.95	11.5
2	0.227	33.22	13.47	36.8
3	0.341	30.88	13.76	32.6
4	0.454	42.01	21.52	*
5	0.568	35.47	14.98	46.9
6	0.681	35.06	15.57	45.8

200mM Potassium with Narasin.

NS(µl)	NS/PC	LW(Hz)	LB(Hz)	Rate(s^{-1})
0	0	27.71	0	0
1	0.113	27.84	0.13	0.41
2	0.226	29.18	1.47	4.62
3	0.338	30.40	2.69	8.45
5	0.564	34.67	6.96	21.87
7	0.790	37.96	10.25	32.20
9	1.015	43.82	16.11	50.61

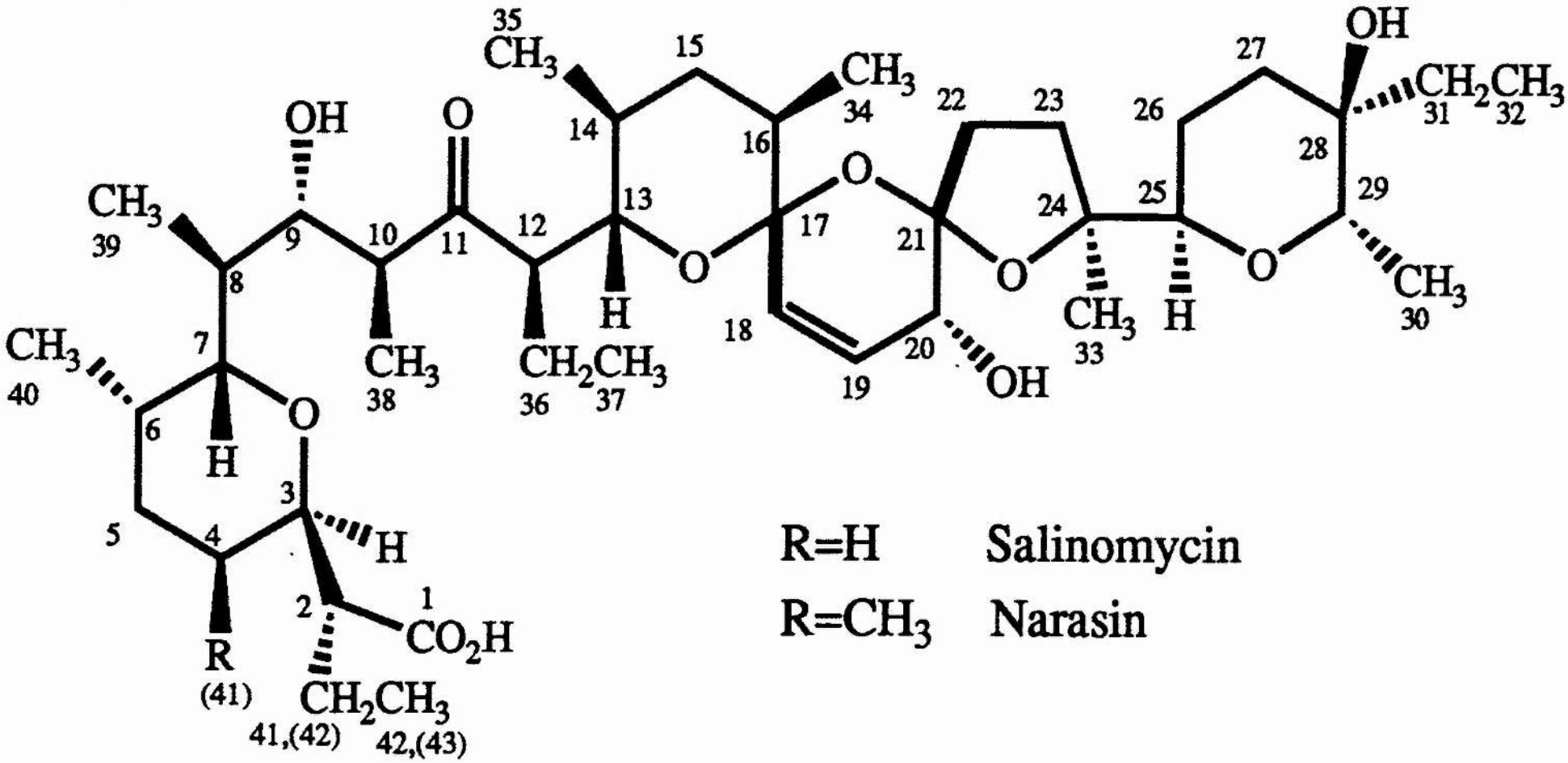
R=H Salinomycin
R=CH3 Narasin